

TARGETING HEAD AND NECK SQUAMOUS CELL CARCINOMA THROUGH NQO1-  
MEDIATED CYTOTOXICITY

BY

JOSHUA MICHAEL FRANCIS

THESIS

Submitted in partial fulfillment of the requirements  
for the degree of Master of Science in Chemistry  
in the Graduate College of the  
University of Illinois at Urbana-Champaign, 2017

Urbana, Illinois

Adviser:

Professor Paul J. Hergenrother

## ABSTRACT

Head and neck squamous cell carcinomas (HNSCC) are a group of anatomically diverse cancers characterized by their resistance to traditional chemotherapy and radiotherapy modalities. Given that as diagnostic and therapeutic strategies in cancer treatment have seen great improvements over the last several decades, it would be only logical that the prognosis of HNSCC should improve. However, this has not been the case as the prognosis for HNSCC has remained unchanged over the last several decades, highlighting a need for new treatment strategies. One potential strategy that has demonstrated potential in a variety of other solid tumors is NQO1-targeted therapy. In this strategy the overexpression of NQO1 can be taken advantage of by the DNQ derivative IB-DNQ which is a futile substrate for NQO1 that generates high levels of cytotoxic ROS selectively inside the cancer cell. Given the high prevalence of NQO1 in HNSCC tumors this appears to be a promising strategy for treating this disease.

Described in Chapter 2 is the evaluation of IB-DNQ in HNSCC cell lines as well as in feline oral squamous cell carcinoma cell lines (FOSCC). The effectiveness of IB-DNQ was found to be directly correlated with the expression of NQO1 in these cell lines. The pharmacokinetic profile and tolerability of IB-DNQ was determined in healthy research cats and parameters from these analyses were used to conduct *in vitro* experiments to mimic these conditions. These experiments showed that tumors expressing NQO1 should respond to treatment with IB-DNQ. Preliminary treatments of cats with FOSCC with IB-DNQ as a single agent, as well as in combination with ionizing radiation have yielded positive/promising responses in several cats.

Described in Chapter 3 is the investigation into enhancing the current therapeutic window of NQO1-targeted therapy. A prodrug approach to IB-DNQ was attempted to increase solubility and/or reduce off-target toxicity. A secondary approach involving the synthesis of novel

derivatives of IB-DNQ containing modifications at a site not previously explored in the SAR of the molecule was also conducted. While the few derivatives synthesized to date all have experienced loss in potency, this site is primed for further investigation and derivatization. Finally, an approach revisiting previously synthesized derivatives of DNQ was implemented in attempts to find a derivative with a greater maximum tolerated dose (MTD) or more favorable pharmacokinetics.

Future studies involving NQO1-independent ROS generation, methemoglobin formations and tumor penetrations are currently being investigated to differentiate DNQ derivatives and identify a lead compound. Ongoing clinical evaluation of NQO1-targeted therapy in feline OSCC aims to establish IB-DNQ as an effective treatment modality as well as strengthen its case for translation into humans.

## TABLE OF CONTENTS

<b>CHAPTER 1. Assessing the potential of NQO1 therapy for head and neck cancer .....</b>	<b>1</b>
1.1 Addressing the lack of prognostic improvement in head and neck cancer.....	1
1.1.1. Treatment of HNSCC .....	1
1.1.2. Stratification of HNSCC status.....	2
1.2. Potential of NQO1 therapy in HNSCC.....	3
1.2.1. Localization of NAD(P)H:quinone oxidoreductase 1.....	3
1.2.2. Genetic regulation of NQO1 .....	4
1.2.3. Overexpression of NQO1 in cancer .....	5
1.2.4. Mechanism of NQO1 .....	5
1.2.5. Prognostic implications of NQO1 expression.....	6
1.3. NQO1 bioactivatable compounds .....	7
1.3.1. Mechanism of NQO1 bioactivatable compounds.....	7
1.3.2. Comparison of NQO1 bioactivatable compounds .....	8
1.4. References.....	9
<b>CHAPTER 2. IB-DNQ for head and neck cancer .....</b>	<b>26</b>
2.1. FOSCC as model of HNSCC.....	26
2.1.1. NQO1 expressions by OSCC cell lines and spontaneous tumors.....	27
2.1.2. In vitro cytotoxicity.....	29
2.1.2.1. In vitro IB-DNQ cytotoxicity in FOSCC cell lines .....	29
2.1.2.2. Sequential exposure to in vitro IB-DNQ induces cumulative cytotoxicity.....	31
2.1.3. Pharmacokinetics of IB-DNQ in healthy cats.....	36

2.1.4. Tolerability of IB-DNQ in healthy cats .....	38
2.1.5. Assessment of off-target systemic oxidative injury .....	39
2.2. Summary of pre-clinical work .....	39
2.3. Clinical evaluations of IB-DNQ in OSCC patients .....	42
2.3.1. Single agent efficacy in patient cats with OSCC .....	42
2.3.2. Combination therapy in patient cats with OSCC .....	44
2.3.2.1. In vitro responses of NQO1 expression to ionizing radiation.....	44
2.3.2.2. Combination efficacy in patient cats with OSCC .....	45
2.4. In vitro cytotoxicity in HNSCC cell lines.....	46
2.5. Summary .....	49
2.6. Materials .....	49
2.7. References.....	57
<b>CHAPTER 3. Enhancing the therapeutic window of IB-DNQ .....</b>	<b>63</b>
3.1. The prodrug approach .....	63
3.1.1. Phosphate prodrug .....	65
3.1.2. Developing a suitable model system.....	68
3.1.2.1. Synthesis of quinolonedione model system.....	68
3.1.2.2. In vitro cytotoxicity of model compounds.....	73
3.1.2.3. Esterification of model compound quinone.....	74
3.1.3. Ester prodrug.....	75
3.2. DNQ derivatives .....	78
3.2.1. Novel DNQ derivatives.....	78
3.2.1.1. SAR of DNQ.....	78

3.2.1.2. Modeling evidence.....	79
3.2.1.3. Synthesis .....	80
3.2.1.4. Cytotoxicity of Halo-IB-DNQ derivatives.....	82
3.2.2. Revisiting previously synthesized derivatives .....	84
3.2.2.1. Synthetic scheme .....	85
3.2.2.2. Pharmacokinetics of derivatives .....	90
3.2.2.3. Tolerability of derivatives.....	92
3.2.2.4. NQO1-independent ROS generation .....	93
3.3. Summary .....	98
3.4. Materials and methods .....	100
3.5. References.....	119

## **Chapter 1. Assessing the potential of NQO1 therapy for head and neck cancer**

### **1.1. Addressing the lack of prognostic improvement in head and neck cancer**

Head and neck cancers describe a collection of cancers arising in diverse anatomical locations in the head and neck. These include cancers of the pharynx (hypo, oro and naso), larynx, oral cavity, paranasal sinuses as well as the nasal cavity and salivary glands,<sup>1,2</sup> the majority which are of squamous cell differentiation.<sup>1,3</sup> Worldwide head and neck squamous cell carcinomas (HNSCC) comprise the sixth most diagnosed malignancy and account for nearly 300,000 deaths annually.<sup>4-8</sup> When diagnosed early, these cancers are very treatable, evidenced by the 80% 5-year survival rate in this group of individuals.<sup>5</sup> Unfortunately early diagnosis describes less than a third of all such malignancies and much more frequently the tumor is diagnosed in the later stages of the disease, where it has become locally advanced, and the 5-year survival rate plummets below 50%.<sup>5</sup> Despite improvements in both diagnostic and treatment modalities over the last several decades,<sup>9-12</sup> there has not been a significant change in prognosis for those with head and neck cancers.<sup>2,13</sup>

#### **1.1.1. Treatment of HNSCC**

The current standard of care for HNSCC is surgical resection of the tumor; however, surgery is only effective when used in treating early stage tumors.<sup>2,14,15</sup> Radiotherapy, showing comparable outcomes to that of surgery,<sup>16,17</sup> has also seen clinical use for early stage tumors. In advanced or late stage malignancies it becomes necessary to use a radiotherapy-surgery combined modality treatment for improvement in outcome.<sup>15,18-21</sup> Unfortunately, approximately 40% of these advanced HNSCCs are unresectable<sup>22,23</sup> due to either (1) the inability to medically

operate on the tumor region, (2) the potential adverse effects of resection on the patient's functional faculties including speech and swallowing or (3) the potential adverse effects of resection on the patient's cosmetic appearance. In these cases, concomitant chemoradiation using ionizing radiation (IR) and a platinum-based antineoplastic agent (most commonly cisplatin) is used.<sup>24-26</sup> However, given the lack of prognostic change seen in HNSCC for several decades with these treatment modalities, there is an urgent need for new treatment modalities for HNSCC, especially for late stage disease.

### **1.1.2. Stratification of HNSCC status**

Currently many cancer treatment strategies utilize a genomic or proteomic component to stratify patients based on their genetic markers to approach treatment in a targeted-manner rather than using more general cytotoxic agents. For example breast cancer can be stratified based on HER2 expression, with HER2 positive tumors responding favorably to treatment with trastuzumab.<sup>27</sup> In melanoma the presence of the V600E *BRAF* mutation is a predictive marker of BRAF inhibitor treatment with the majority of patients receiving such therapy experiencing a dramatic initial response and can therefore be used to stratify individuals possessing this mutation for treatment with vemurafinib and dasatinib.<sup>28,29</sup> Finally, for non-small cell lung cancer (NSCLC), treatment is informed based on the mutational status of EGFR, with gefitinib and erlotinib being used for either exon19del deletion or an L848R missense mutation and the drug osimertinib being used for individuals possessing a T790M EGFR mutation, a mutation that confers resistance to gefitinib and erlotinib.<sup>30</sup>

The only stratification made in HNSCC to date is that of Human Papillomavirus (HPV) status with approximately 25% of HNSCC specimens containing HPV genomic DNA.<sup>31</sup>



Generally those cancers that are HPV positive respond more favorably to radiotherapy and see a significantly better 5-year survival rate than HPV negative individuals (80% vs. 20%).<sup>32-35</sup> In the last decade, EGFR has been explored as a potential target in head and neck cancer. Overexpressed in up to 90% of cases,<sup>36-38</sup> EGFR targeted therapy has seen the approval of cetuximab for HNSCC, the first new drug approved for use in HNSCC cancer in 45 years.<sup>39,40</sup> However, oncogenic signaling pathways still persist after use of cetuximab, which allow for the incidence of distant metastases and local-regional failure. Also despite its nearly ubiquitous expression in HNSCC, there is no evidence to date that EGFR expression levels can predict an individual patient's response to EGFR targeted therapy making it less useful for prioritizing patient treatment.<sup>39,41</sup> Being able to stratify these HPV-negative HNSCC tumors according to a genetic biomarker that could be used to predict individual's response to treatment in a reliable way remains an important step on the path to informing treatment strategy and improving on a grave prognosis that has remained stagnant over the last several decades.

## **1.2. Potential of NQO1 therapy in HNSCC**

### **1.2.1. Localization of NAD(P)H:quinone oxidoreductase 1**

NAD(P)H:quinone oxidoreductase 1 (NQO1) is a dimeric flavoprotein involved in the detoxification of xenobiotics and associated with protection against mutagenesis and carcinogenesis.<sup>42,43</sup> NQO1 is a predominantly cytosolic protein with ~90% being found in the cytoplasm,<sup>44</sup> but can also be found in the endoplasmic reticulum,<sup>45</sup> mitochondria,<sup>46</sup> Golgi body<sup>47</sup> and nucleus of cells.<sup>48</sup> This enzyme is expressed in low levels in normal tissue; however, in certain epithelial cells expression is elevated.<sup>49</sup> This includes respiratory, breast duct, and thyroid

follicle epithelium, the epithelial lining of the colon, and corneal and lens epithelia. Detectable expression is also seen in vascular endothelium, such as the lining of the aorta and capillary endothelium. Adipocytes from the lung, breast, ovary and colon, parasympathetic ganglion in the gastrointestinal tract, and the optic nerve and nerve fibers also stain positively for NQO1. There is minimal expression in hepatic tissues with only trace levels being detected via immunoblot analysis.<sup>49</sup>

### **1.2.2. Genetic regulation of NQO1**

The NQO1 gene itself is 20 kb and consists of 6 exons and 5 introns and contains several cis-activating transcriptional activators including an antioxidant response element (ARE) and a xenobiotic response element (XRE).<sup>50-54</sup> As their names imply, these elements regulate gene expression in response to antioxidants or xenobiotics to protect cells against free radical damage, oxidative stress and neoplasia. NQO1 expression is under the control of the transcription factor Nrf2, which with its repressor KEAP1 comprise one of the major signaling cascades for stress response. Under normal conditions KEAP1 is complexed with Nrf2 in the cytoplasm but upon exposure to antioxidants, Nrf2 is released from Keap1, translocates to the nucleus, and binds ARE to activate gene expression of NQO1.<sup>55-60</sup>

NQO1 has two characterized polymorphisms, NQO1\*2 and NQO1\*3. The NQO1\*2 polymorphism is more commonly present in ~4% of Caucasians and ~20% of Asian populations.<sup>42,43,61-63</sup> The single point nucleotide polymorphism consists of a base substitution of cytosine to thymidine at position 609 of the cDNA sequence. This results in a proline to serine substitution in the protein that appears to cause a change in the enzyme conformation leading to a decrease in FAD binding affinity, loss of enzyme activity and an overall less stable protein that is

broken down in 1.2 h by the ubiquitin proteasomal pathway (UPP). Some studies suggest that individuals expressing this polymorphism have a higher risk of developing cancer while others suggest that this risk is small if present at all.<sup>61,62</sup> The second NQO1 polymorphism, NQO1\*3, is less common and less well studied.<sup>64,65</sup> It results in a cytosine to thymidine base substitution at position 465 in the cDNA which effectively increases alternative splicing of the NQO1 gene leading to a decreased expression of the full protein. Any individuals expressing either of these NQO1 variants would not be expected to derive any benefit from an NQO1 targeted therapy.

### **1.2.3. Overexpression of NQO1 in cancer**

NQO1 is expressed in a variety of solid human tumor types, predominantly those of epithelial origin.<sup>66</sup> NQO1 levels in these solid tumors tend to be 5- to 20 –fold higher than associated normal tissue and the reason for this vast overexpression of NQO1 in solid tumors is still not clear. This overexpression phenomenon has been observed for a wide variety of solid tumors<sup>49,67-90</sup> including those in the breast,<sup>49,67-69</sup> lung,<sup>49,68-76</sup> pancreas,<sup>77-80</sup> prostate<sup>81</sup> and head and neck.<sup>71,82</sup> Furthermore, this enzyme has been implicated for its importance in maintaining oxidative homeostasis in the tumor microenvironment<sup>56</sup> and depletion of NQO1 in these cells resulted in suppressed cell proliferation and tumor growth.<sup>91</sup>

### **1.2.4. Mechanism of NQO1**

NQO1 is an obligatory two electron reductase. Able to catalyze the two electron reduction of a variety of quinone, quinoneimines, azoaromatic and nitro aromatic compounds,<sup>42,92,93</sup> this normal function of NQO1 helps to detoxify these compounds through formation of a stable hydroquinone which can be conjugated (to glutathione, sulfate or glucose),

excreted from the cell and eliminated (Fig. 1.1). This detoxification process prevents one-electron mediated reduction processes from acting on these molecules, which would cause formation of a highly reactive semiquinone that in turn would undergo reduction-oxidation (redox) cycling producing high levels of toxic reactive oxygen species (ROS).<sup>92,93</sup> It also serves as a detoxification enzyme through its ability to scavenge ROS through generation of antioxidant forms of alpha tocopherol<sup>94</sup> and other endogenous quinones (Fig. 1.1).<sup>95</sup>

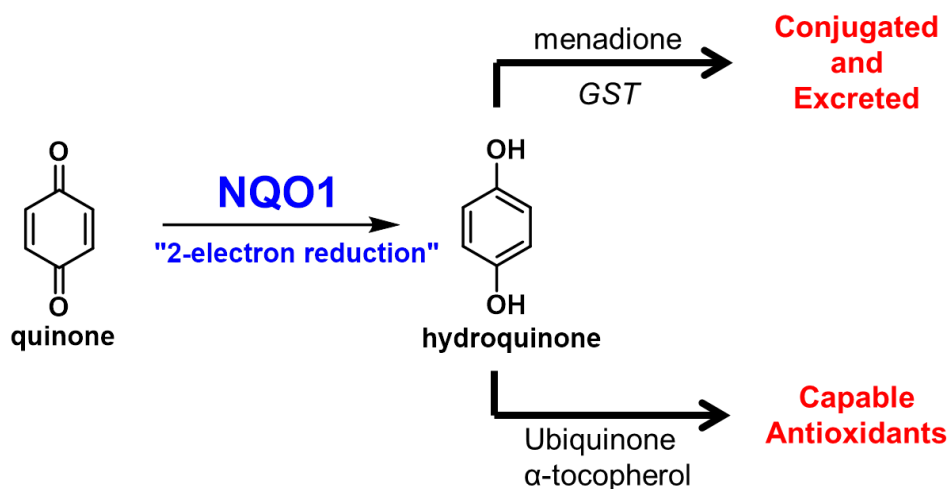


**Figure 1.1.** Normal detoxification and antioxidant mechanisms of NQO1.

### 1.2.5. Prognostic implications of NQO1 expression

NQO1 expression is typically higher in those with advanced stage tumors than early stage and in tumors that have metastasized to the lymph nodes. Tumors expressing high levels of NQO1 typically have a graver prognosis than their low NQO1 expressing counterparts.<sup>67,75,83-85</sup> Due to the increased NQO1 expression in larger, late stage tumors it is likely that either NQO1 overexpression may confer a drive to grow, invade and metastasize or that the increased NQO1 expression is simply due to the increased oxidative cellular environment which induces upregulation of the enzyme that maintains homeostasis.

### 1.3. NQO1 bioactivatable compounds

While there have been many reports of anticancer agents that mediate their effects through NQO1-bioactivation,<sup>96-101</sup> there are currently only two true compounds that exert their cytotoxic effects through NQO1-dependent means,<sup>102,117</sup>  $\beta$ -lapachone ( $\beta$ -lap) and deoxyxyboquinone (DNQ) (Fig 1.2).  $\beta$ -lap has demonstrated significant cytotoxicity in lung<sup>103-105</sup> and breast<sup>102,105-110</sup> cancer cell lines, as well as in vivo mouse models.<sup>103,111</sup> Currently  $\beta$ -lap (ARQ761) is in clinical trials (NCT01502800 and NCT02514031).

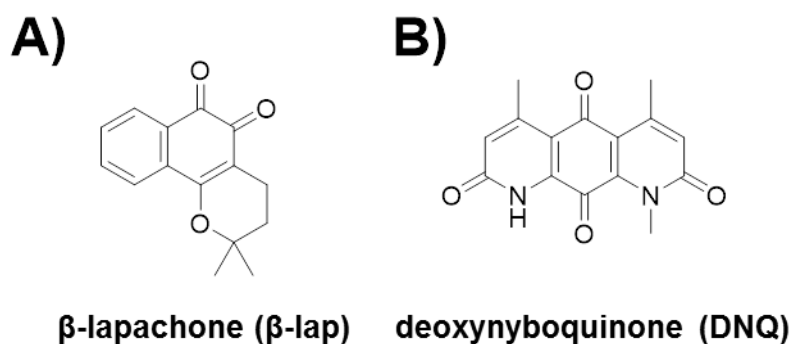


**Figure 1.2.** Structures of NQO1 bioactivatable compounds (a)  $\beta$ -lapachone and (b) deoxyxyboquinone.

#### 1.3.1. Mechanism of NQO1 bioactivatable compounds

The classical mode of an anticancer agent and enzyme is for the anticancer molecule to bind in some form to the enzyme and inhibit its activity.  $\beta$ -lapachone and DNQ are unique in that instead of inhibiting the activity of NQO1 they are actually substrates for the enzyme.<sup>104,112</sup> They are able to hijack the natural function of NQO1 in order to induce their cytotoxic effects. These molecules undergo the two electron reduction mediated by NQO1; however, unlike other quinones these two compounds do not form a stable hydroquinone. Instead these hydroquinones rapidly react with molecular oxygen present in the cell to generate a semiquinone intermediate

through release of ROS that can then react with another molecule of oxygen to form a second molecule of ROS and regenerate the parent quinone, ready to be processed again (Fig. 1.3). It is through this redox cycle and ROS generation that  $\beta$ -lap and DNQ exert their cytotoxic mechanism. This process is catalytic and generates  $\geq 60$  mol of ROS within one minute.<sup>106,108</sup>

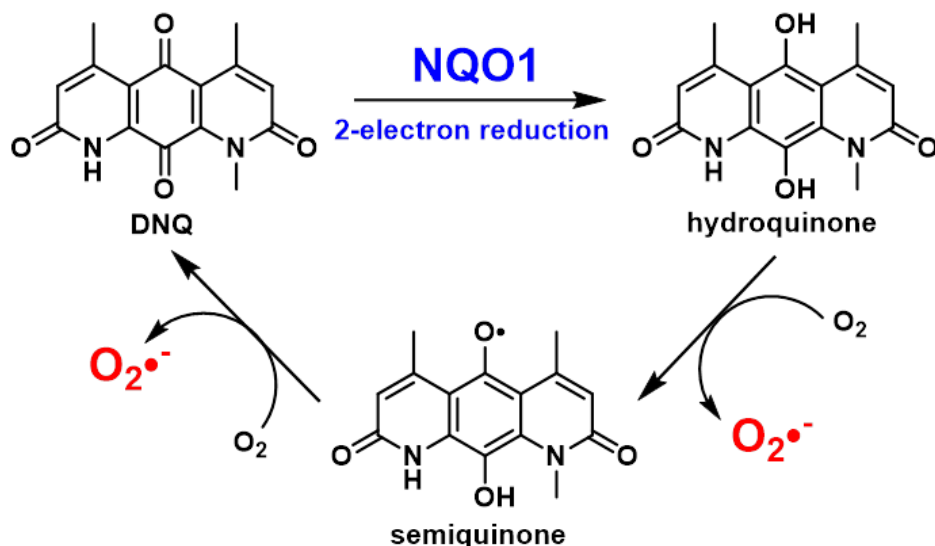


**Figure 1.3.** DNQ exerts cytotoxic mechanism of action through NQO1-mediated redox cycling.

The rapid generation and large quantities of superoxide leads to DNA base damage and single strand breaks. This leads in turn to significant PAR formation and drastic reduction in NAD<sup>+</sup> and ATP levels due to hyperactivation of PARP-1, which is recruited to the damage site and attempts to repair those breaks. Hyperactivation of PARP-1 leads to a PARP-1-dependent mode of cell death known as parthanatos.<sup>108,113-116</sup>

### 1.3.2. Comparison of NQO1 bioactivatable compounds

In head to head experiments comparing putative NQO1-activated anticancer agents, DNQ demonstrated superiority over mitomycin C and RH1 (both of which were shown not to be

substrates for NQO1), streptonigrin and  $\beta$ -lapachone.<sup>117</sup> DNQ as an in vitro substrate for NQO1 was processed 9 times faster than  $\beta$ -lap which was the next best substrate.<sup>117</sup> The ability NQO1 to process DNQ was highly efficient and approached the diffusion controlled limit.<sup>117</sup> Similarly in head-to-head cell culture experiments DNQ was 10-100 fold more potent in two different cell lines (A549, a lung adenocarcinoma cell line, and MiaPaCa2, a pancreatic cancer cell line). Additionally DNQ has a larger therapeutic window, extended hepatic stability and dramatically longer half-life in mice than  $\beta$ -lap<sup>112</sup> making it the current gold standard for NQO1-mediated anticancer therapy. Recently studies have shifted from DNQ to a derivative isobutyl-deoxyxyboquinone (IB-DNQ), which possesses similar catalytic and cytotoxic profiles to DNQ,<sup>117</sup> but is more water soluble,<sup>117,118</sup> and more tolerated in vivo.<sup>119,120</sup> Therefore IB-DNQ provides an optimal candidate for evaluating the effectiveness of NQO1-targeted therapy in HNSCC.

#### **1.4. References**

- (1) Vigneswaran, N.; Williams, M.D. Epidemiological Trends in Head and Neck Cancer and Aids in Diagnosis. *Oral Maxillofac. Surg. Clin. North Am.* **2014**, *26*(2), 123-141.
- (2) Cognetti, D.M.; Weber, R.S.; Lai, S.Y. Head and Neck Cancer: An Evolving Treatment Paradigm. *Cancer* **2008**, *113*(70), 1911-1932.
- (3) Sanderson, R.J.; Ironside, J.A.D. Squamous cell carcinomas of the head and neck. *BMJ* **2002**, *325*(7368), 822-827.
- (4) Parkin, D.M.; Bray, F.; Ferlay, J.; Pisani, P. Global cancer statistics. *CA Cancer J. Clin.* **2002**, *55*(2), 74-108.

- (5) Leemans, C.R.; Boudewijn, J.M.B.; Brakenhoff, R.H. The molecular biology of head and neck cancer. *Nat. Rev. Cancer* **2011**, *11*, 9-22.
- (6) Shibuya, K.; Mathers, C.D.; Boschi-Pinto, C.; Lopez, A.D.; Murray, C.J.L. Global and regional estimates of cancer mortality and incidence by site: II. Results for the global burden of disease 2000. *BMC Cancer* **2002**, *2*, 37.
- (7) Jemal, A.; Siegal, R.; Ward, E. Hao, Y.; Xu, J.; Murray, T.; Thun, M.J. Cancer statistics, 2008. *CA Cancer J. Clin.* **2008**, *58*, 71-96.
- (8) Siegel, R.L.; Miller, K.D.; Jemal, A. Cancer statistics, 2016. *CA Cancer J. Clin.* **2016**, *66*, 7-30.
- (9) Vikram, B. Adjuvant therapy in head and neck cancer. *CA Cancer J. Clin.* **1998**, *48*, 199-209.
- (10) Shah, J.P.; Lydiatt, W. Treatment of cancer of the head and neck. *CA Cancer J. Clin.* **1995**, *45*, 352-368.
- (11) Pignon, J.P.; Bourhis, J.; Domenge, C.; Designe, L. Chemotherapy added to locoregional treatment for head and neck squamous-cell carcinoma: three meta-analyses of updated individual data. *Lancet* **2000**, *355*, 949-955.
- (12) Forastiere, A.A.; Koch, W.M.; Trotti, A.; Sidransky, D. Head and Neck Cancer. *N. Engl. J. Med.* **2001**, *345*, 1891-1900.
- (13) Carvalho, A.L.; Nishimoto, I.N.; Califano, J.A.; Kowalski, L.P. Trends in incidence and prognosis for head and neck cancer in the United States: a site-specific analysis of the SEER database. *Int. J. Cancer* **2005**, *114*(5), 806-816.



- (14) Gregoire, V. Lefebvre, J.L.; Licitra, L.; Felip, E. Squamous cell carcinoma of the head and neck: EHNS-ESMO-ESTRO Clinical Practice Guidelines for diagnosis, treatment and follow-up. *Ann. Oncol.* **2010**, *21*(Suppl. 5), v184-v186.
- (15) Epstein, J.B.; Thariat, J.T.1 Bensadoun, R.; Barasch, A.; Murphy, B.A.; Kolnick, L.; Popplewell, L.; Maghami, E. Oral Complications of Cancer and Cancer Therapy. *CA Cancer J. Clin.* **2012**, *62*, 400-422.
- (16) Hinerman, R.W.; Mendenhall, W.M.; Amdur, R.J.; Stringer, S.P.; Villaret, D.B.; Robbins, K.T. Carcinoma of the supraglottic larynx: treatment results with radiotherapy alone or with planned neck dissection. *Head Neck* **2002**, *24*(5), 456-467.
- (17) Garden, S.S.; Morrison, W.H.; Clayman, G.L.; Ang, K.K.; Peters, L.J. Early squamous carcinoma of the hypopharynx: outcomes of treatment with radiation alone to the primary disease. *Head Neck* **1996**, *18*, 317-322.
- (18) Adelstein, D.J.; Li, Y.; Adams, G.L.; Wagner, H.; Kish, J.A.; Ensley, J.F.; Schuller, D.E.; Forastiere, A.A. An intergroup phase III comparison of standard radiation therapy and two schedules of concurrent chemoradiotherapy in patients with unresectable squamous cell head and neck cancer. *J. Clin. Oncol.* **2003**, *21*(1), 92-98.
- (19) Kokal, W.A.; Neifeld, J.P.; Eisert, D.; Lipsett, J.A.; Lawrence, W.; Beatty, J.D.; Parker, G.A.; Pezner, R.D.; Riihimaki, D.U.; Terz, J.J. Postoperative radiation as adjuvant treatment of the carcinoma of the oral cavity, larynx, and pharynx: preliminary report of a prospective randomized trial. *J. Surg. Oncol.* **1988**, *38*, 71-76.
- (20) Frank, J.L.; Garb, J.L.; Kay, S.; McClish, D.K.; Bethke, K.P.; Lind, D.S.; Mellis, M.; Slomka, W.; Sismanis, A.; Neifeld, J.P. Postoperative radiotherapy improves survival in squamous cell carcinoma of the hypopharynx. *Am. J. Surg.* **1994**, *168*, 476-480.

- (21) DeStefani, A.; Magnano, M.; Cavalot, A.; Usai, A.; Lerda, W.; Mola, P.; Albera, R.; Ragona, R.; Gabriele, P.; Bussi, M.; Cortesina, G. Adjuvant radiotherapy influences the survival of patients with squamous cell carcinoma of the head and neck who have poor prognoses. *Otolaryngol. Head Neck Surg.* **2000**, *123*, 630-636.
- (22) Seiwert, T.Y.; Salama, J.K.; Vokes, E.E. The chemoradiation paradigm in head and neck cancer. *Nat. Clin. Pract. Oncol.* **2007**, *4*(3), 156-171.
- (23) Dinshaw, K.A.; Agarwal, J.P.; Ghosh-Laskar, S.; Gupta, T.; Shrivastava, S.K. Radical radiotherapy in head and neck squamous cell carcinoma: an analysis of prognostic and therapeutic factors. *Clin. Oncol.* **2006**, *18*, 383-389.
- (24) Jemal, A.; Bray F.; Center, M.M.; Ferlay, J.; Ward, E.; Forman, D. Global cancer statistics. *CA Cancer J. Clin.* **2011**, *61*(2), 69-90.
- (25) Calais, G.; Alfonsi, M.; Bardet, E.; Sire, C.; Germain, T.; Bergerot, P.; Rhein, E.; Tortochaux, J.; Oudinot, P.; Bertrand, P. Randomized trial of radiation therapy versus concomitant chemotherapy and radiation therapy for advanced-stage oropharynx carcinoma. *J. Natl. Cancer Inst.* **1999**, *91*(24), 2081-2086.
- (26) Forastiere, A.A.; Goepfert, H.; Maor, M.; Pajak, T.F.; Weber, R.; Morrison, W.; Glisson, B.; Trotti, A.; Ridge, J.A.; Chao, C.; Peters G.; Lee, D.J.; Leaf, A.; Ensley, J.; Cooper, J. Concurrent chemotherapy and radiotherapy for organ preservation in advanced laryngeal cancer. *N. Engl. J. Med.* **2003**, *349*(22), 2091-2098.
- (27) Vogel, C.L.; Cobleigh, M.A.; Tripathy, D.; Gutheil, J.C.; Harris, L.N.; Fehrenbacher, L.; Slamon, D.J.; Murphy, M.; Novotny, W.F.; Burchmore, M.; Shak, S.; Stewart, S.J.; Press, M. Efficacy and safety of trastuzumab as a single agent in first-line treatment of HER2-overexpressing metastatic breast cancer. *J. Clin. Oncol.* **2002**, *20*(3), 719-726.

- (28) Cirenajwis, H.; Ekedahl, H.; Lauss, M.; Harbst, K.; Carneiro, A.; Enoksson, J.; Rosengren, F.; Werner-Hartman, L.; Tornngren, T.; Kvist, A.; Fredlund, E.; Bendahl, P.; Jirstrom, K.; Lundgren, L.; Howlin, J.; Borg, A.; Gruvberger-Saal, S.K.; Saal, L.H.; Nielsen, K.; Ringner, M.; Tsao, H.; Olsson, H.; Ingvar, C.; Staaf, J.; Jonsson, G. Molecular stratification of metastatic melanoma using gene expression profiling: Prediction of survival outcome and benefit from molecular targeted therapy. *Oncotarget* **2015**, *6*(14), 12297-12309.
- (29) Chapman, P.B.; Hauschild, A.; Robert, C.; Haanen, J.B.; Ascierto, P.; Larkin, J.; Dummer, R.; Garbe, C.; Testori, A.; Maio, M.; Hogg, D.; Lorigan, P.; Lebbe, C.; Jouary, T.; Schadendorf, D.; Ribas, A.; O'Day, S.J.; Sosman, J.A.; Kirkwood, J.M.; Eggermont, A.M.M.; Dreno, B.; Nolop, K.; Li, J.; Nelson, B.; Hou, J.; Lee, R.J.; Flaherty, K.T.; McArthur, G.A. Improved survival with vemurafenib in melanoma with BRAF V600E mutation. *N. Engl. J. Med.* **2011**, *364*, 2507-2516.
- (30) Chan, B.A.; Hughes, B.G.M. Targeted therapy for non-small cell lung cancer: current standards and the promise of the future. *Transl. Lung Cancer Res.* **2015**, *4*(1), 36-54.
- (31) Kreimer, A.R.; Clifford, G.M.; Boyle, P.; Franceschi, S. Human papillomavirus types in head and neck squamous cell carcinomas worldwide: a systemic review. *Cancer Epidemiol. Biomarkers Prev.* **2005**, *14*, 467-475.
- (32) Suh, Y.; Amelio, I.; Guerrero Urbano, T.; Tavassoli, M. Clinical update on cancer: molecular oncology of head and neck cancer. *Cell Death and Disease* **2014**, *5*, e1018.
- (33) Ang, K.K.; Harris, J.; Wheeler, R.; Weber, R.; Rosenthal, D.I.; Nguyen-Tan, P.F.; Westra, W.H.; Chung, C.H.; Jordan, R.C.; Lu, C.; Kim, H.; Axelrod, R.; Silverman, C.C.; Redmond, K.P.; Gillison, M.L. Human papillomavirus and survival of patients with oropharyngeal cancer. *N. Engl. J. Med.* **2010**, *363*(1), 24-35.

- (34) Licitra, L.; Perrone, F.; Bossi, P.; Suardi, S.; Mariani, L.; Artusi, R.; Oggionni, M.; Rossini, C.; Cantu, G.; Squadrelli, M.; Quattrone, P.; Locati, L.D.; Bergamini, C.; Olmi, P.; Pierotti, M.A.; Pilotti, S. High-risk human papillomavirus affects prognosis in patients with surgically treated oropharyngeal squamous cell carcinoma. *J. Clin. Oncol.* **2006**, *24*, 5630-5636.
- (35) Lindel, K.; Beer, K.T.; Laissue, J.; Greiner, R.H.; Aebbersold, D.M. Human papillomavirus positive squamous cell carcinoma of the oropharynx: a radiosensitive subgroup of head and neck carcinoma. *Cancer* **2001**, *92* 805-813.
- (36) Zimmermann, M.; Zouhair, A.; Azira, D.; Ozsahin, M. The epidermal growth factor receptor (EGFR) in head and neck cancer: its role and treatment implications. *Radiat. Oncol.* **2006**, *1*, 11.
- (37) Rubin Grandis, J.; Melhem, M.F.; Gooding, W.E.; Day, R.; Holst, V.A.; Wagener, M.M.; Drenning, S.D.; Twardy, D.J. Levels of TGF- $\alpha$  and EGFR protein in head and neck squamous cell carcinoma and patient survival. *J. Natl. Cancer Inst.* **1998**, *90*(11), 824-832.
- (38) Rubin Grandis, J.; Melhem, M.F.; Barnes, E.L.; Twardy, D.J. Quantitative immunohistochemical analysis of transforming growth factor- $\alpha$  and epidermal growth factor receptor in patients with squamous cell carcinoma of the head and neck. *Cancer* **1996**, *78*(6), 1284-1292.
- (39) Harari, P.M.; Wheeler, D.L.; Grandis, J.R. Molecular Target Approaches in Head and Neck Cancer: EGFR and Beyond. *Semin. Radiat. Oncol.* **2009**, *19*(1), 63-68.
- (40) Fung, C.; Grandis, JR. Emerging drugs to treat squamous cell carcinomas of the head and neck. *Expert Opin. Emerg. Drugs* **2010**, *15*(3), 355-373.
- (41) Hansen, A.R.; Siu, L.L. Epidermal Growth Factor Receptor Targeting in Head and Neck Cancer: Have We Been Just Skimming the Surface? *J. Clin. Oncol.* **2013**, *31*(11), 1381-1383.

- (42) Siegel D.; Yan, C.; Ross, D. NAD(P)H:quinone oxidoreductase 1 (NQO1) in the sensitivity and resistance to antitumor quinones. *Biochem. Pharmacol.* **2012**, *83*, 1033-1040.
- (43) Danson, S.; Ward, T.H.; Butler, J.; Ranson, M. DT-diaphorase: a target for new anticancer drugs. *Cancer Treat. Rev.* **2004**, *30*, 437-449.
- (44) Eliasson, M.; Bostrom, M.; Depierre, J.W. Levels and subcellular distributions of detoxifying enzymes in the ovarian corpus luteum of the pregnant and non-pregnant pig. *Biochem. Pharmacol.* **1999**, *58* 1287-1292.
- (45) Danielson, L.; Ernster, L.; Ljunggren, M. Selective extraction of DT-diaphorase from mitochondria and microsomes. *Acta Chem. Scand.* **1960**, *14*, 1837-1838.
- (46) Conover, T.E.; Ernster, L. DT diaphorase IV. Coupling of exxtramitochondrial reduced pyridine nucleotide oxidation to mitochondrial respiratory chain. *Biochem. Biophys. Acta* **1968**, *67*, 268-280.
- (47) Edlund, C.; Elhrmammer, A.; Dallner, G. Distribution of newly synthesized DT-diaphorase in rat liver. *Biosci. Rep.* **1982**, *2*, 861-865.
- (48) Winski, S.L.; Koutalos, Y.; Bentley, D.L.; Ross, D. Subcellular localization of NAD(P)H:quinone oxidoreductase 1 in human cancer cells. *Cancer Res.* **2002**, *62*, 1420-1424.
- (49) Siegel, D.; Ross, D. Immunodetection of NAD(P)H:quinone oxidoreductase 1 (NQO1) in human tissues. *Free Radic. Biol. Med.* **2000**, *29*, 246-253.
- (50) Jaiswal, A.K. Human NAD(P)H:quinone oxidoreductase (NQO1) gene structure and induction by dioxin. *Biochemistry* **1991**, *30*, 10647-10653.
- (51) Joseph, P.; Xie, T.; Xu, Y.; Jaiswal, A.K. NAD(P)H:quinone oxidoreductase 1 (DT-diaphorase): expression, regulation and role in cancer. *Oncol. Res.* **1994**, *6*, 525-532.

- (52) Yao, K.; O'Dwyer, P.J. Involvement of NF- $\kappa$ B in the induction of NAD(P)H:quinone oxidoreductase (DT-diaphorase) by hypoxia, oltipraz and mitomycin C. *Biochem. Pharmacol.* **1995**, *49*, 275-282.
- (53) Dhakshinamoorthy, S.; Long, D.J.; Jaiswal, A.K. Antioxidant regulation of genes encoding enzymes that detoxify xenobiotics and carcinogens. *Curr. Top. Cell. Reg.* **2000**, *36*, 201-216.
- (54) Jaiswal, A.K. Nrf2 signaling in coordinated activation of antioxidant gene expression. *Free Radic. Biol. Med.* **2004**, *36*(10), 1199-1207.
- (55) Dhakshinamoorthy, S.; Jain, A.K.; Bloom, D.A.; Jaiswal, A.K. Bach1 competes with Nrf2 leading to negative regulation of the antioxidant response element (ARE)-mediated NAD(P)H:quinone oxidoreductase 1 gene expression and induction in response to antioxidants. *J. Biol. Chem.* **2005**, *290*(17), 16891-16900.
- (56) Leinonen, H.M.; Kansanen, E.; Polonen, P.; Heinaniemi, M.; Levonen, A.L. Role of the Keap1-Nrf2 pathway in cancer. *Adv. Cancer Res.* **2014**, *122*, 281-320.
- (57) Hayes, J.D.; McMahon, M. NRF2 and KEAP1 mutations: permanent activation of an adaptive response in cancer. *Trends Biochem. Sci.* **2009**, *34*, 176-188.
- (58) Solis, L.M.; Behrens, C.; Dong, W.; Suraokar, M. Ozburn, N.C.; Moran, C.A.; Corvalan, A.H.; Biswal, S.; Swisher, S.G.; Bekele, B.N.; Minna, J.D.; Stewart, D.J.; Wistuba, I.I. Nrf2 and Keap1 abnormalities in non-small cell lung carcinoma and association with clinicopathologic features. *Clin. Cancer Res.* **2010**, *16*, 3743-3753.
- (59) Itoh, K.; Wakabayashi, N.; Katoh, Y.; Ishii, T.; Igarashi, K.; Engel, J.D.; Yamamoto, M. Keap1 represses nuclear activation of antioxidant responsive elements by Nrf2 through binding to the amino-terminal Neh2 domain. *Genes Dev.* **1999**, *13*(1), 76-86.

- (60) Dhakshinamoorthy, S.; Jaiswal, A.K. Functional characterization and role of INrf2 in antioxidant response element-mediated expression and antioxidant induction of NAD(P)H:quinone oxidoreductase 1 gene. *Oncogene* **2001**, *20*(29), 3906-3917.
- (61) Lou, Y.; Li, R.; Xiong, L.; Gu, A.; Shi, C.; Chu, T.; Zhang, X.; Gu, P.; Zhong, H.; Wen, S.; Han, B. NAD(P)H:quinone oxidoreductase 1 (NQO1) C609T polymorphism and lung cancer risk: a meta-analysis. *Tumour Biol.* **2013**, *34*, 3967-6979.
- (62) Peng, Q.; Lu, Y.; Lao, X.; Chen, Z.; Li, R.; Sui, J.; Qin, X.; Li, S. The NQO1 Pro187Ser polymorphism and breast cancer susceptibility: evidence from an updated meta-analysis. *Diagn. Pathol.* **2014**, *9*, 100.
- (63) Kelsey, K.T.; Ross, D.; Traver, R.D.; Christiani, D.C.; Zuo, Z.F.; Spitz, M.R.; Wang, M.; Xu, X.; Lee, B.K.; Schwartz, B.S.; Wienck, J.K. Ethnic variation in the prevalence of a common NAD(P)H:quinone oxidoreductase polymorphism and its implications for anti-cancer chemotherapy. *Br. J. Cancer* **1997**, *76*, 852-854.
- (64) Gaedigk, A.; Tyndale, R.F.; Jurima-Romet, M.; Sellers, E.M.; Grant, D.M.; Leeder, L.S. NAD(P)H:quinone oxidoreductase: polymorphisms and allele frequencies in Caucasian, Chinese and Canadian Native Indian and Inuit populations. *Pharmacogenetics* **1998**, *8*, 305-313.
- (65) Pan, S.S.; Han, Y.; Farabaugh, P.; Xia, H. Implication of alternative splicing for expression of a variant NAD(P)H:quinone oxidoreductase-1 with a single nucleotide polymorphism at 465C>T. *Pharmacogenetics* **2002**, *12*, 479-488.
- (66) Cresteil, T.; Jaiswal, A.K. High levels of expression of the NAD(P)H:quinone oxidoreductase (NQO1) gene in tumor cells compared to normal cells of the same origin. *Biochem. Pharmacol.* **1991**, *42*, 1021-1027.

- (67) Yang, Y.; Zhang, Y.; Wu, Q.; Cui, X.; Lin, Z.; Liu, S.; Chen, L. Clinical implications of high NQO1 expression in breast cancers. *J. Exp. Clin. Cancer Res.* **2004**, *33*, 14.
- (68) Marin, A.; Lopez de Cerain, A.; Hamilton, E.; Lewis, A.D.; Martinez-Penuela, J.M.; Idoate, M.A.; Bello, J. DT-diaphorase and cytochrome B5 reductase in human lung and breast tumours. *Br. J. Cancer* **1997**, *76*, 923-929.
- (69) Schlager, J.J.; Powis, G. Cytosolic NAD(P)H:(quinone-acceptor) oxidoreductase in human normal and tumor tissue: effects of cigarette smoking and alcohol. *Int. J. Cancer* **1990**, *45*, 403-409.
- (70) Malkinson, A.M.; Siegel, D.; Forrest, G.L.; Gazdar, A.F.; Oie, H.K.; Chan, D.C.; Bunn, P.A.; Mabry, M.; Dykes, D.J.; Harrison, S.D.; Ross, D. Elevated DT-diaphorase activity and messenger RNA content in human non-small cell lung carcinoma: relationship to the response of lung tumor xenografts to mitomycin C. *Cancer Res.* **1992**, *52*, 4752-4757.
- (71) Smitskamp-Wilms, E.; Giaccone, G.; Pinedo, H.M.; van der Laan, B.F.; Peters, G.J. DT-diaphorase activity in normal and neoplastic tissues: an indicator for sensitivity to bioreductive agents? *Br. J. Cancer* **1995**, *72*, 917-921.
- (72) Kolesar, J.M.; Pritchard, S.C.; Kerr, K.M.; Kim, K.; Nicolson, M.C.; McLeod, H. Evaluation of NQO1 gene expression and variant allele in human NSCLC tumors and matched normal lung tissue. *Int. J. Oncol.* **2002**, *21*, 1119-1124.
- (73) Bey, E.A.; Bentle, M.S.; Reinicke, K.E.; Dong, Y.; Yang, C.R.; Girard, L.; Minna, J.D.; Bornmann, W.G.; Gao, J.; Boothman, D.A. An NQO1- and PARP-1-mediated cell death pathway induced in non-small-cell lung cancer cells by beta-lapachone. *Proc. Natl. Acad. Sci. U.S.A.* **2007**, *104*, 11832-11837.



- (74) Yilmaz, A.; Mohamed, N.; Patterson, K.A.; Tang, Y.; Shilo, K.; Villalona-Calero, M.A.; Davis, M.E.; Zhou, X.; Frankel, W.; Otterson, G.A.; Beall, H.D.; Zhao, W. Increased NQO1 but not c-MET and surviving expression in non-small cell lung carcinoma with KRAS mutations. *Int. J. Environ. Res. Public Health* **2014**, *11*, 9491-9502.
- (75) Li, Z.; Zhang, Y.; Jin, T.; Men, J.; Lin, Z.; Qi, P.; Piao, Y.; Yan, G. NQO1 protein expression predicts poor prognosis of non-small cell lung cancers. *BMC Cancer* **2015**, *15*, 207.
- (76) Kim, H.; Song, J.S.; Lee, J.C.; Lee, D.H.; Kim, S.; Lee, J.; Kim, W.S.; Rho, J.K.; Kim, S.Y.; Choi, C. Clinical significance of NQO1 polymorphism and expression of p53, SOD2, PARP1 in limited-stage small cell lung cancer. *Int. J. Clin. Exp. Pathol.* **2014**, *7*(10), 6743-6751.
- (77) Logsdon, C.D.; Simeone, D.M.; Binkley, C.; Arumugam, T.; Greenson, J.K.; Giordano, T.J.; Misek, D.E.; Kuick, R.; Hanash, S. Molecular profiling of pancreatic adenocarcinoma and chronic pancreatitis identifies multiple genes differentially regulated in pancreatic cancer. *Cancer Res.* **2003**, *63*, 2649-2657.
- (78) Lewis, A.M.; Ough, M.; Hinkhouse, M.M.; Tsao, M.S.; Oberley, L.W.; Cullen, J.J. Targeting NAD(P)H:quinone oxidoreductase (1) in pancreatic cancer. *Mol. Carcinog.* **2005**, *43*, 215-224.
- (79) Lyn-Cook, B.D.; Yan-Sanders, Y.; Moore, S.; Taylor, S.; Word, B.; Hammons, G.J. Increased levels of NAD(P)H:quinone oxidoreductase 1 (NQO1) in pancreatic tissues from smokers and pancreatic adenocarcinomas: a potential biomarker of early damage in the pancreas. *Cell Biol. Toxicol.* **2006**, *22*, 73-80.
- (80) Awadallah, N.S.; Dehn, D.; Shah, R.J.; Russell-Nash, S.; Chen, Y.K.; Ross, D.; Bentz, J.S.; Shroyer, K.R. NQO1 expression in pancreatic cancer and its potential use as a biomarker. *Appl. Immunohistochem. Mol. Morphol.* **2008**, *16*, 24-31.

- (81) Dong, Y.; Bey E.A.; Li, L.S.; Kabbani, W.; Yan, J.; Xie, X.J.; Hsieh, J.T.; Gao, J.; Boothman, D.A. Prostate cancer radiosensitization through PARP-1 hyperactivation. *Cancer Res.* **2010**, *70*(20), 8088-8096.
- (82) Li, L.S.; Reddy, S.; Lin, Z.H.; Liu, S.; Park, H.; Chun, S.G.; Bornmann, W.G.; Thibodeaux, J.; Yan, J.; Chakrabarti, G.; Xie, X.J.; Sumer, B.D.; Boothman, D.A.; Yordy, J.S. NQO1-mediated tumor-selective lethality and radiosensitization for head and neck cancer. *Mol. Cancer Ther.* **2016**, *15*(7), 1757-1767.
- (83) Cui, X.; Li, L.; Yan, G.; Meng, K.; Lin, Z.; Nan, Y.; Jin, G.; Li, C. High expression of NQO1 is associated with poor prognosis in serous ovarian carcinoma. *BMC Cancer* **2015**, *15*, 244.
- (84) Lin, L.; Qin, Y.; Jin, T.; Liu, S.; Zhang, S.; Shen X.; Lin, Z. Significance of NQO1 overexpression for prognostic evaluation of gastric adenocarcinoma. *Exp. Mol. Pathol.* **2014**, *96*, 200-205.
- (85) Ma, Y.; Kong, J.; Yan, G.; Ren, X.; Jin, D.; Jin, T.; Lin, L.; Lin, Z. NQO1 overexpression is associated with poor prognosis in squamous cell carcinoma of the uterine cervix. *BMC Cancer* **2014**, *14*, 414.
- (86) Cheng, Y.; Li, J.; Martinka, M.; Li, G. The expression of NAD(P)H:quinone oxidoreductase 1 is increased along with NF-kappaB p105/p50 in human cutaneous melanomas. *Oncol. Rep.* **2010**, *23*, 973-979.
- (87) Mikami, K.; Naito, M.; Ishiguro, T.; Yano, H.; Tomida, A.; Yamada, T.; Tanaka, N.; Shirakusa, T.; Tsuruo, T. Immunological quantitation of DT-diaphorase in carcinoma cell lines and clinical colon cancers: advanced tumors express greater levels of DT-diaphorase. *Jpn. J. Cancer Res.* **1998**, *89*, 910-915.

- (88) Ji, L.; Wei, Y.; Jiang, T.; Wang, S. Correlation of Nrf2, NQO1, MRP1, cmyc and p53 in colorectal cancer and their relationships to clinicopathologic features and survival. *Int. J. Clin. Exp. Pathol.* **2014**, 7(3), 1124-1131.
- (89) Oh, E.T.; Kim, J.W.; Kim, J.M.; Kim, S.J.; Lee, J.S.; Hong, S.S.; Goodwin, J.; Ruthenborg, R.J.; Jung, M.G.; Lee, H.J.; Lee, C.H.; Park, E.S.; Kim, C.; Park, H.J. NQO1 inhibits proteasome-mediated degradation of HIP-1alpha. *Nat. Comm.* **2016**, 7, 13593.
- (90) Buranrat, B.; Chau-in, S.; Prawan, A.; Puapairoj, A.; Zeekpudsa, P.; Kukongviriyapan, V. NQO1 expression correlates with cholangiocarcinoma prognosis. *Asian Pacific J. Cancer Prev.* **2012**, 13, 131-136.
- (91) Madajewski, B.; Moatman, M.A.; Chakrabarti, G.; Boothman, D.A.; Bey, E.A. Depleting tumor-NQO1 potentiates anoikis and inhibits growth of NSCLC. *Mol. Cancer Res.* **2016**, 14(1), 14-25.
- (92) Dinkova-Kostova, A.T.; Talalay, P. NAD(P)H:quinone acceptor oxidoreductase 1 (NQO1) a multifunctional antioxidant enzyme and exceptionally versatile cytoprotector. *Arch. Biochem. Biophys.* **2010**, 501, 116-123.
- (93) Ross, D.; Kepa, J.K.; Winski, S.L.; Beall, H.D.; Anwar, A.; Siegel, D.; NAD(P)H:quinone oxidoreductase 1 (NQO1): chemoprotection, bioactivation, gene regulation and genetic polymorphisms. *Chem. Biol. Interact.* **2000**, 129, 77-97.
- (94) Siegel, D.; Bolton, E.M.; Burr, J.A.; Liebler, D.C.; Ross, D. The reduction of alpha-tocopherolquinone by human NAD(P)H:quinone oxidoreductase: the role of alpha-tocopherolhydroquinone as a cellular antioxidant. *Mol. Pharmacol.* **1997**, 52, 300-305.
- (95) Beyer, R.E.; Segura-Aguilar, J.; Di Bernardo, S.; Cavazzoni, M.; Fato, R.; Fiorentini, D.; Cristina Galli, M.; Setti, M.; Landi, L.; Lenaz, G. The role of DT-diaphorase in the maintenance

of the reduced antioxidant form of coenzyme Q in membrane systems. *Proc. Natl. Acad. Sci. U.S.A.* **1996**, *93*, 2528-2532.

(96) Beall, H.D.; Mulcahy, R.T.; Siegel, D.; Traver, R.D.; Gibson, N.W.; Ross, D. Metabolism of bioreductive antitumor compounds by purified rat and human DT-diaphorases. *Cancer Res.* **1994**, *54*, 3196-3201.

(97) Siegel, D.; Beall, H.; Senekowitsch, C.; Kasai, M.; Arai, H.; Gibson, N.W.; Ross, D. Bioreductive activation of mitomycin C by DT-diaphorase. *Biochemistry* **1992**, *31*, 7879-7885.

(98) Fitzsimmons, S.A.; Workman, P.; Grever, M.; Paull, L.; Gamalier R.; Lewis, A.D. Reductase enzyme expression across the National Cancer Institute Tumor cell line panel: correlation with sensitivity to mitomycin C and EO9. *J. Natl. Cancer Inst.* **1996**, *88*, 259-269.

(99) Nemeikaite-Ceniene, A.; Sarlauskas, J.; Anusevicius, Z.; Nivinskas, H.; Cenas, N. Cytotoxicity of RH1 and related aziridinybenzoquinones: involvement of activation by NAD(P)H:quinone oxidoreductase (NQO1) and oxidative stress. *Arch. Biochem. Biophys.* **2003**, *416*, 110-118.

(100) Ross, D.; Beall, H.D.; Siegel, D.; Traver, R.D.; Gustafson, D.L. Enzymology of bioreductive drug activation. *Br. J. Cancer* **1996**, *27*(Suppl.), S1-S8.

(101) Colucci, M.A.; Moody, C.J.; Couch, G.D. Natural and synthetic quinones and their reduction by the quinone reductase enzyme NQO1: from synthetic organic chemistry to compounds with anticancer potential. *Org. Biomol. Chem.* **2008**, *6*, 637-656.

(102) Cao, L.; Li, L.S.; Spruell, C.; Xiao, L.; Chakrabarti, G.; Bey, E.A.; Reinicke, K.E.; Srougi, M.C.; Moore, Z.; Dong, Y.; Vo, P.; Kabbani, W.; Yang, C.R.; Wang, X.; Fattah, F.; Morales, J.C.; Motea, E.A.; Bornmann, W.G.; Yordy, J.S.; Boothman, D.A. Tumor-selective,

futile redox cycle-induced bystander effects elicited by NQO1 bioactivatable radiosensitizing drugs in triple-negative breast cancers. *Antiox. Redox Signal.* **2014**, *21*(2), 237-250.

(103) Blanco, E.; Bey, E.A.; Khemtong, C.; Yang, S.G.; Setti-Guthi, J. Chen, H. Kessinger, C.W.; Carnevale, K.A.; Bornmann, W.G.; Boothman, D.A.; Gao, J. Beta-lapachone micellar nanotherapeutics for non-small cell lung cancer therapy. *Cancer Res.* **2010**, *70*, 3896-3904.

(104) Bey, E.A.; Bentle, M.S.; Reinicke, K.E.; Dong, Y.; Yang, C.R.; Girard, L.; Minna, J.D.; Bornmann, W.G.; Gao, J.; Boothman, D.A. An NQO1- and PARP-1-mediated cell death pathway induced in non-small-cell lung cancer cells by beta-lapachone. *Proc. Natl. Acad. Sci. U.S.A.* **2007**, *104*, 11832-11837.

(105) Blaco, E.; Bey, E.A.; Dong, Y.; Weinberg, B.D.; Sutton, D.M.; Boothman, D.A.; Gao, J. Beta-lapachone-containing PEG-PLA polymer micelles as novel nanotherapeutics against NQO1-overexpressing tumor cells. *J. Control. Release* **2007**, *122*, 365-374.

(106) Pink, J.J.; Wuerzberger-Davis, S.; Tagliarino, C.; Planchon, S.M.; Yang, X.; Froelich, C.J.; Boothman, D.A. Activation of cysteine protease in MCF-7 and T47D breast cancer cells during beta-lapachone-mediated apoptosis. *Exp. Cell Res.* **2000**, *255*, 144-155.

(107) Wuerzberger, S.M.; Pink, J.J.; Planchon, S.M.; Byers, K.L.; Bornmann, W.G.; Boothman, D.A. Induction of apoptosis in MCF-7:WS8 breast cancer cells by beta-lapachone. *Cancer Res.* **1998**, *58*, 1876-1885.

(108) Bey, E.A.; Reinicke, K.E.; Srougi, M.C.; Varnes, M.; Anderson, V.E.; Pink, J.J.; Li, L.S.; Patel, M.; Cao, L.; Moore, Z.; Rommel A.; Boatman, M.; Lewis, C.; Euhus, D.M.; Bornmann, W.G.; Buchsbaum, D.J.; Spitz, D.R.; Gao, J.; Boothman, D.A. Catalase abrogates beta-lapachone-induced PARP1 hyperactivation-directed programmed necrosis in NQO1-positive breast cancers. *Mol. Cancer Ther.* **2013**, *12*, 2110-2120.

- (109) Bentle, M.S.; Reinicke, K.E.; Bey, E.A.; Spitz, D.R.; Boothman, D.A. Calcium-dependent modulation of poly(ADPribose) polymerase-1 alters cellular metabolism and DNA repair. *J. Biol. Chem.* **2006**, *281*, 33684-33696.
- (110) Pink, J.J.; Planchon, S.M.; Tagliarino, C.; Varnes, M.E.; Siegel, D.; Boothman, D.A. NAD(P)H:quinone oxidoreductase activity is the principal determinant of beta-lapachone cytotoxicity. *J. Biol. Chem.* **2000**, *275*, 5416-5424.
- (111) Li, L.S.; Bey, E.A.; Dong, Y.; Meng, J.; Patra, B.; Yan, J.; Xie, X.J.; Brekken, R.A.; Barnett, C.C.; Bornmann, W.G.; Gao, J.; Boothman, D.A. Modulating endogenous NQO1 levels identifies key regulatory mechanisms of action of beta-lapachone for pancreatic cancer therapy. *Clin. Cancer Res.* **2011**, *17*, 275-285.
- (112) Huang, X.; Dong, Y.; Bey, E.A.; Kilgore, J.A.; Bair, J.S.; Li, L.S.; Patel, M.; Parkinson, E.I.; Wang, Y.; Williams, N.S.; Gao, J.; Hergenrother, P.J.; Boothman, D.A. An NQO1 substrate with potent anticancer activity that selectively kills by PARP1-induced programmed necrosis. *Cancer Res.* **2012**, *72*, 3038-3047.
- (113) Bentle, M.S.; Bey, E.A.; Dong, Y.; Reinicke, K.E.; Boothman, D.A. New tricks for old drugs: the anticarcinogenic potential of DNA repair inhibitors. *J. Mol. Histol.* **2006**, *37*, 203-218.
- (114) Bentle, M.S.; Reinicke, K.E.; Dong, Y.; Bey, E.A.; Boothman, D.A. Nonhomologous end joining is essential for cellular resistance to the novel antitumor agent, beta-lapachone. *Cancer Res.* **2007**, *67*, 6936-6945.
- (115) Boothman, D.A.; Greer, S.; Pardee, A.B. Potentiation of halogenated pyrimidine radiosensitizers in human carcinoma cells by beta-lapachone (3,4-dihydro-2,2-dimethyl-2H-naphtho[1,2-b]pyran-5,6-dione), a novel DNA repair inhibitor. *Cancer Res.* **1987**, *47*, 5361-5366.

- (116) Boothman, D.A.; Trask, D.K.; Pardee, A.B. Inhibition of potentially lethal DNA damage repair in human tumor cells by beta-lapachone, an activator of topoisomerase I. *Cancer Res.* **1989**, *49*, 605-612.
- (117) Parkinson, E.I.; Bair, J.S.; Cismesia, M.; Hergenrother, P.J. Efficient NQO1 substrates are potent and selective anticancer agents. *ACS Chem. Biol.* **2013**, *8*, 2173-2183.
- (118) Bair, J.S. The Development of Deoxynyboquinone as a Personalized Anticancer Compound, University of Illinois at Urbana-Champaign, 2012.
- (119) Parkinson, E.I. Deoxynyboquinones as NQO1-targeted Anticancer Compounds and Deoxynybomycins as Potent and Selective Antibiotics, University of Illinois at Urbana-Champaign, 2015.
- (120) Parkinson, E.I.; Hergenrother, P.J. Deoxynyboquinones as NQO1-activated cancer therapeutics. *Acc. Chem. Res.* **2015**, *48*, 2715-2723.

## Chapter 2. IB-DNQ for head and neck cancer

Portions of this Chapter are reprinted with permission from Lundberg, A.P.; Francis, J.M; Pajak, M.; Parkinson, E.I.; Wycislo, K.L.; Rosol, T.J.; Brown, M.E.; London, C.A.; Dirikolu, L.; Hergenrother, P.J.; Fan, T.M. *Invest. New Drugs* **2017**, *35*, 134-144.

### 2.1. FOSCC as model of HNSCC

Experimental model systems used for testing novel anticancer compounds have relied on murine tumor models, yet greater than 90% of oncology agents demonstrating robust activity in mouse models fail to become approved drugs for humans.<sup>1</sup> This low translational success rate of novel drugs can be partially ascribed to the limitations of murine tumor models to accurately predict drug efficacy in human patients.<sup>2-5</sup> The inclusion of pets with naturally occurring cancers has recently emerged as a potential complementary development strategy for improving the prediction of a drug's potential for clinical success or failure.<sup>6-8</sup>

Many cancers arising naturally in companion animals share genetic, molecular and clinical similarities to the human disease.<sup>9-11</sup> Specifically, feline oral squamous cell carcinoma (OSCC) might serve as an appropriate epithelial malignancy for the advancement of NQO1 bioactivatable drugs, such as IB-DNQ, based on shared cancer biology between domestic felids and humans diagnosed with HNSCC.<sup>12,13</sup>

Feline OSCC is the most common oral tumor in cats and despite medical advances in cancer treatment remains associated with a grave prognosis with cats succumbing to local disease progression within 2-4 months of diagnosis, regardless of therapy.<sup>14,15</sup> Therefore there is



a need to identify novel and effective treatments for OSCC,<sup>16</sup> and advances made with NQO1-mediated therapy in these patients should be directly translatable to their human counterparts.

### **2.1.1. NQO1 expressions by OSCC cell lines and spontaneous tumors**

NQO1 expression in feline cell lines has not been investigated previously and as there are no NQO1 antibodies designed specifically for feline NQO1, thus other NQO1 antibodies must be used. Feline cross-reactivity of anti-NQO1 antibody was confirmed by Western blot analysis (Fig 2.1). The 3 immortalized feline OSCC cell lines variably expressed NQO1 protein confirmed by Western blot analysis and immunohistochemistry (Fig. 2.2a & b). The expression of NQO1 was robust in the SCCF1 and SCCF2 cell lines, while the SCCF3 cell line had the lowest expression. NQO1 expressions correlated with enzymatic activities with SCCF1 and SCCF2 exerting comparable functional activities of  $1719.7 \pm 462.6$  nmol/min/ $\mu$ g and  $1685.0 \pm 967.4$  nmol/min/ $\mu$ g, respectively. Concordant with reduced NQO1 expression, the SCCF3 cell line possessed approximately 1-log order less NQO1 activity compared to either SCCF1 or SCCF2, measuring  $126.3 \pm 53.8$  nmol/min/ $\mu$ g ( $p < 0.05$ , Fig 2.2c). In naturally occurring feline OSCC samples, 46 out of 50 tumors were evaluable for NQO1 staining. The majority of tumors (40/46) demonstrated some degree of NQO1 expression, with categorical staining intensities being 26.1% (+++), 32.6% (++) and 28.3% (+). Six tumors, accounting for 13% of samples, were completely devoid of any NQO1 staining (Fig. 2.3). Analogous to feline OSCC tumors, the majority of human OSCC tissues (43/60) expressed NQO1 with categorical staining intensities being 21.7% (+++), 23.3% (++) , 25% (+) and 30% negative (Fig 2.3).

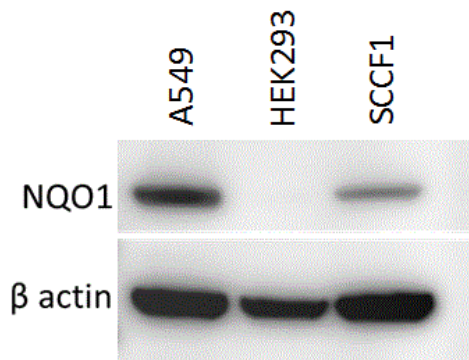


**Figure 2.1.** Confirmatory Western blot for feline cross reactivity of anti-NQO1 antibody. A549, a lung cancer cell line, and HEK293, a BLANK cell line, were used as positive and negative controls respectively.  $\beta$ -actin levels were used as loading controls.

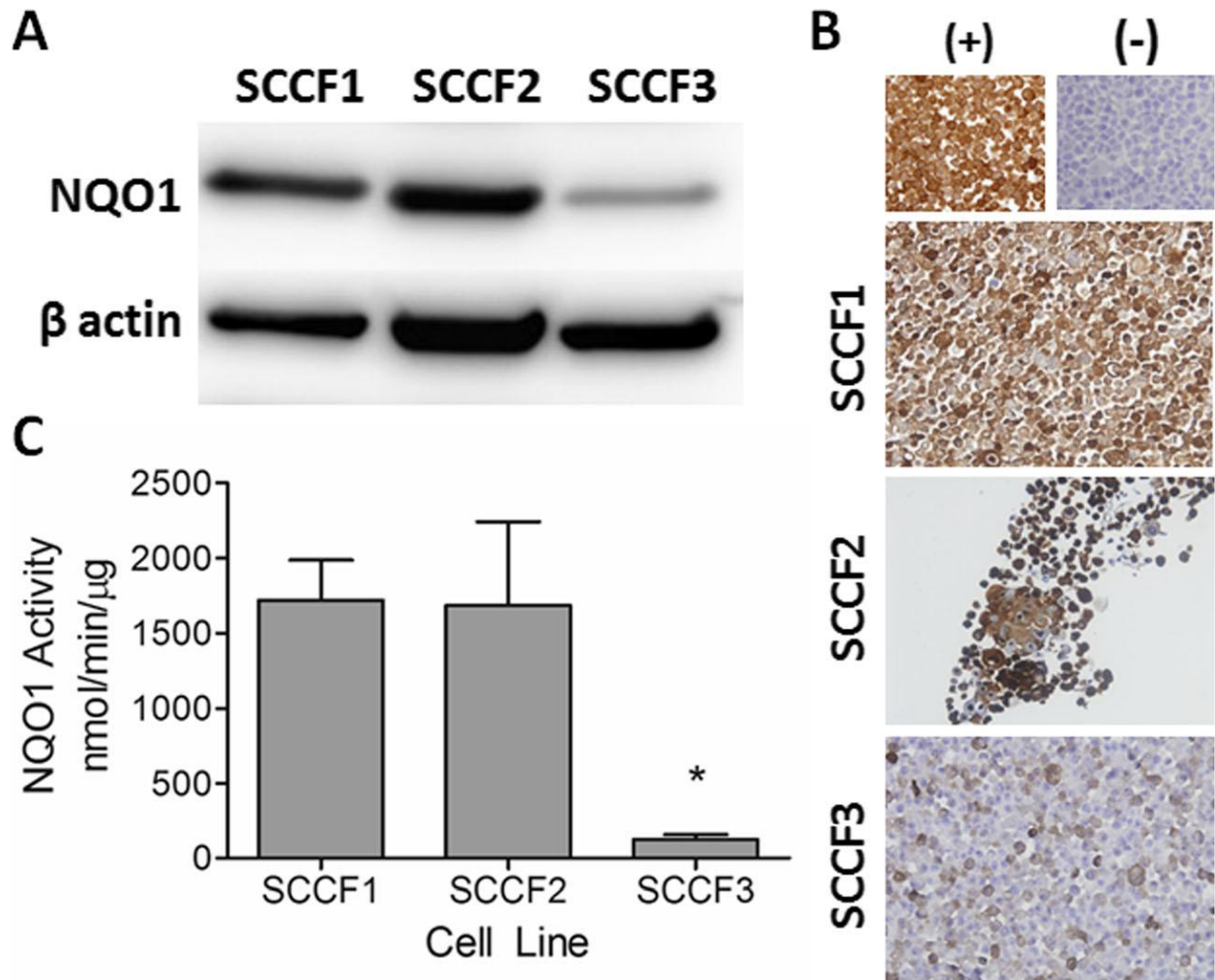


**Figure 2.2.** In 3 feline OSCC immortalized cell line, variable NQO1 protein expression detected by (a) Western blot and (b) immunohistochemistry; human positive (A549) and negative

**Figure 2.2. (cont.)** (HEK293) control cells. Confirmation of (c) variable NQO1 enzymatic activities correlate with protein expressions. Data presented as average  $\pm$ SD; \*denotes  $p < 0.05$ .

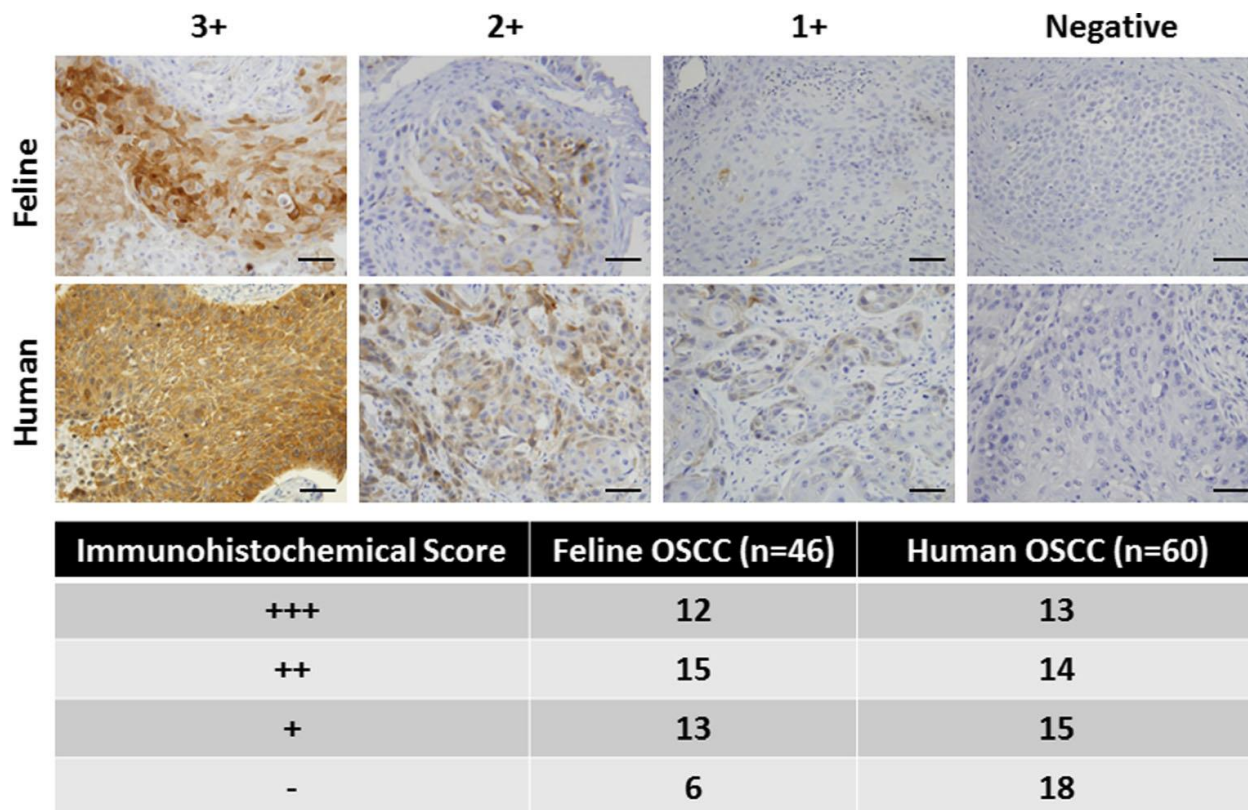


**Figure 2.3.** Forty-six and sixty spontaneous feline- and human-derived OSCC samples, respectively, evaluated for NQO1 protein expression by immunohistochemistry. Representative images and tabulated summary of categorical NQO1 intensity grading relative to positive control (A549). Scale bar = 100  $\mu$ m.

## 2.1.2. In vitro cytotoxicity

### 2.1.2.1. In vitro IB-DNQ cytotoxicity in FOSCC cell lines

Based upon the established mechanism of NQO1-mediated bioactivatable drugs to induce cancer cell death,<sup>17-20</sup> the potency of IB-DNQ against the 3 feline OSCC cell lines was explored. Dose response curves of SCCF1, SCCF2 and SCCF3 to IB-DNQ mediated cytotoxicity correlated with enzymatic activities (Fig 2.4), with IB-DNQ demonstrating greater cytotoxic

potency against SCCF1 and SCCF2 cell lines ( $IC_{50}$   $0.37 \pm 0.14 \mu\text{M}$  and  $0.12 \pm 0.10 \mu\text{M}$ , respectively), and less against the SCCF3 cell line ( $IC_{50}$   $2.11 \pm 0.51 \mu\text{M}$ ). Induction of cytotoxicity by NQO1-mediated activity was confirmed by a reduction in cell death and right shifting of the dose response curve when cells were co-incubated with IB-DNQ and the NQO1 inhibitor dicoumarol. Consistent with previous results,<sup>18</sup> in comparison with  $\beta$ -lapachone, IB-DNQ demonstrates a 5-10 fold increase in cytotoxic potency against SCCF1 and SCCF2 cell lines and approximately a 2-fold increase in potency against the SCCF3 cell line. The  $IC_{50}$  values for  $\beta$ -lapachone against SCCF1, SCCF2 and SCCF3 were  $2.87 \pm 0.51 \mu\text{M}$ ,  $1.39 \pm 0.28 \mu\text{M}$ , and  $3.11 \pm 0.49 \mu\text{M}$ , respectively.

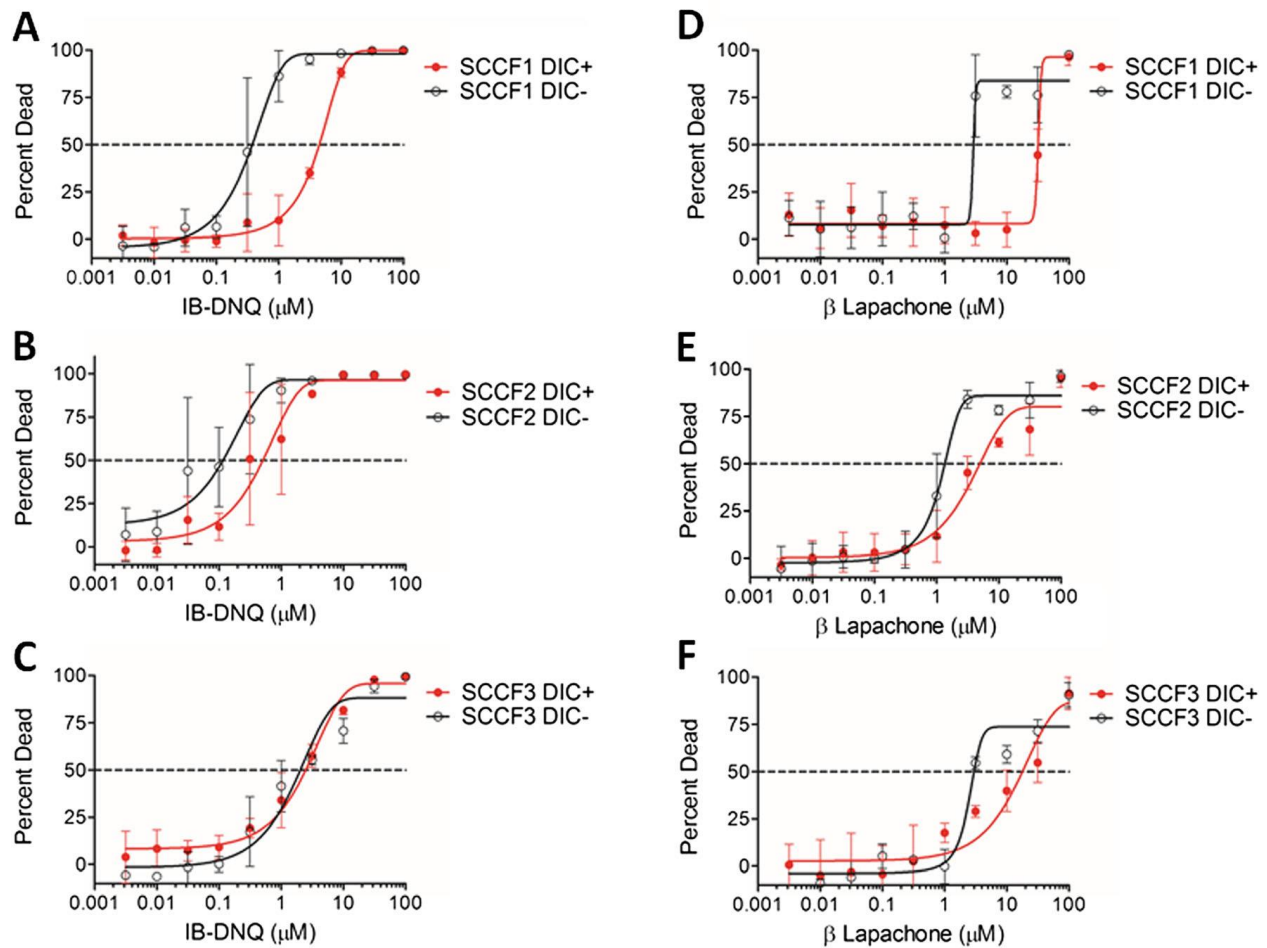


**Figure 2.4.** Dose-dependent cytotoxic effects of IB-DNQ (a-c) and  $\beta$ -lapachone (d-f) in 3 immortalized feline OSCC cell lines, in the presence or absence of dicoumarol (25  $\mu\text{M}$ ).

**Figure 2.4. (cont.)** Increased susceptibility of (a/d) SCCF1 and (b/e) SCCF2 cell lines to NQO1 mediated cytotoxicity predicted by correlative NQO1 enzyme activity levels. Attenuated NQO1 mediated cytotoxicity in (c/f) SCCF3 cell line based upon reduced NQO1 expression and activity.

#### **2.1.2.2. Sequential exposure to in vitro IB-DNQ induces cumulative cytotoxicity**

Often in the drug development process, a disconnect exists between a compound's potency in cell culture and its potency *in vivo* which can lead to failure of the compound. Relevant compound concentrations and duration of compound exposure are two variables that influence cell culture potency and that can be different *in vivo*. Additionally, the majority of cell culture experiments involve a single exposure to compound, a contrast from the multiple administrations typically encountered in a clinical setting. Therefore a set of cell culture experiments were designed in which cells would be exposed to, in repeated, short bursts, compound based on preliminary pharmacokinetic data from Section 2.1.3. These experiments would mimic *in vivo* conditions and potentially be a more accurate predictor of compound potency *in vivo*.

Sequential and repeated exposure to IB-DNQ for time durations (1h) and at concentrations ( $\leq 3.0 \mu\text{M}$ ) likely to be achievable *in vivo* were assessed in the SCCF1 cell line. At the lowest concentration of IB-DNQ ( $0.1 \mu\text{M}$ ), no significant loss in cell viability was identified regardless of the number of sequential 1-h daily pulse exposures (Fig 2.5). On the contrary, substantive increases in cytotoxicity were documented following exposure to IB-DNQ at  $0.4 \mu\text{M}$ , with approximately 60-65% death occurring after 1 or 2 sequential, treatments and greater than 90% loss of viability following 5 consecutive daily exposures to IB-DNQ (Fig X). At the highest concentration of IB-DNQ ( $3.0 \mu\text{M}$ ), near quantitative cytotoxicity was achieved following  $\geq 2$  consecutive treatments, with 96% cell death being induced following sequential



IB-DNQ exposure (Fig 2.5). The induction of cytotoxicity as a function of IB-DNQ concentration and sequential exposure is summarized in Table 2.1.

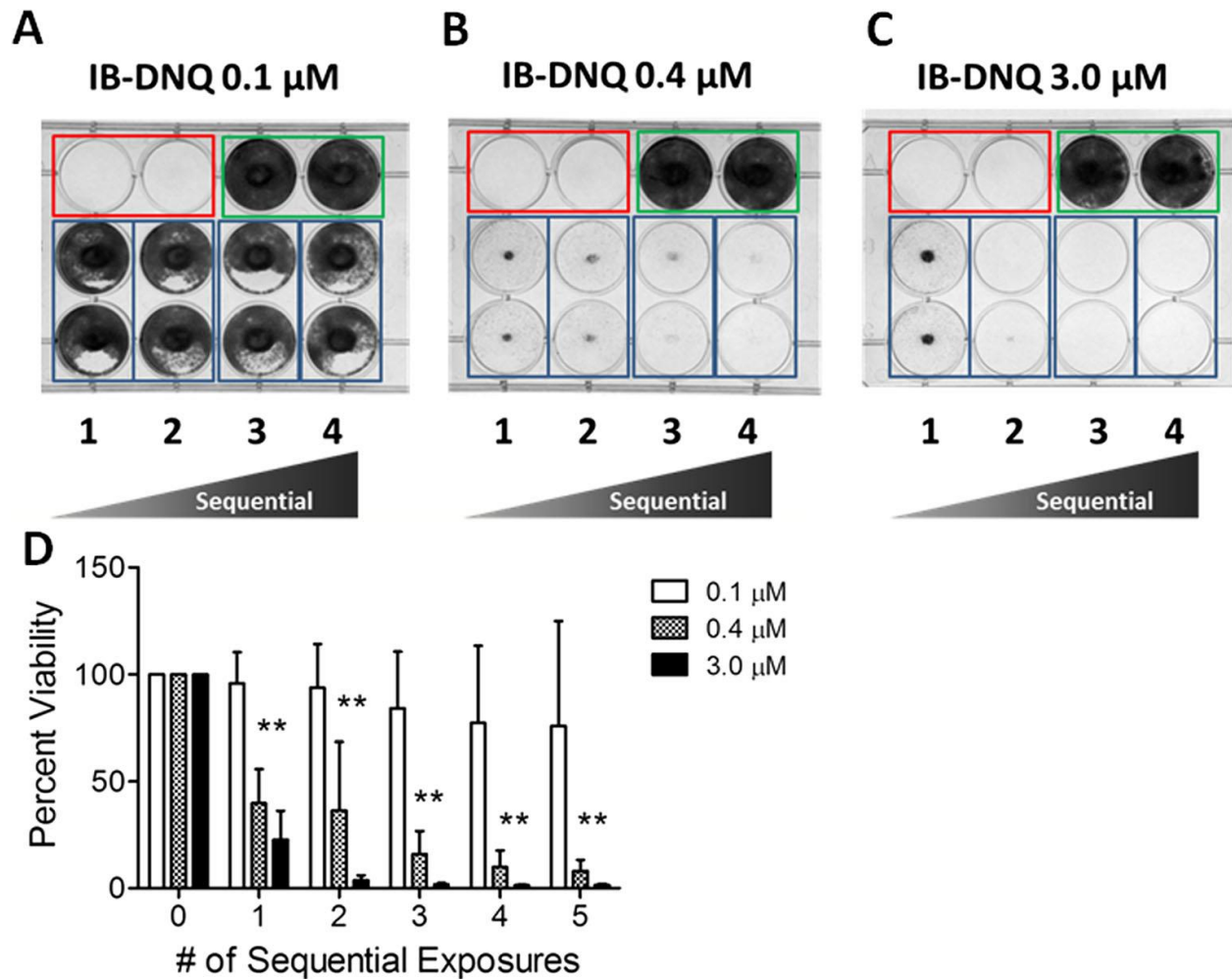


**Figure 2.5.** Repeated exposure of SCCF1 cells to IB-DNQ for biologically-achievable time durations (60 min) induces cytotoxicity in a dose dependent manner with SRB viability assay. (a/d) No observed cumulative cytotoxicity observed with the lowest concentration of IB-DNQ, however, concentrations of 0.4  $\mu\text{M}$  (b/d) and 3.0  $\mu\text{M}$  (c/d) exert substantive to profound cytotoxicity after  $\geq 2$  sequential IB-DNQ exposures. Negative control wells (red outline) with no cells, positive control wells (green outline) with untreated cells, and sequential treated wells (blue outline) with IB-DNQ exposed cells. Data represented as average  $\pm$  SD; \*\* $p < 0.01$ .

**Table 2.1.** Cytotoxicity following sequential exposure to IB-DNQ

IB-DNQ Number of Treatments	0.1 $\mu$ M % Viable	0.4 $\mu$ M % Viable	3.0 $\mu$ M % Viable
0	100 $\pm$ 0	100 $\pm$ 0	100 $\pm$ 0
1	96.0 $\pm$ 14.4	39.8 $\pm$ 16.0**	22.9 $\pm$ 13.5**
2	93.9 $\pm$ 20.4	36.4 $\pm$ 32.2**	3.7 $\pm$ 2.5**
3	84.2 $\pm$ 26.5	15.9 $\pm$ 10.9**	1.9 $\pm$ 0.5**
4	77.3 $\pm$ 36.2	9.9 $\pm$ 7.8**	1.4 $\pm$ 0.4**
5	75.8 $\pm$ 49.3	8.0 $\pm$ 5.4**	1.5 $\pm$ 0.6**

Data expressed as average  $\pm$  SD

Sequential and repeated exposure to IB-DNQ for time durations (1h) and at concentrations ( $\leq$  3.0  $\mu$ M) likely to be achievable *in vivo* were next assessed in the SCCF3 cell line (Fig 2.6). Due to the decreased expression of NQO1 in this cell line it was expected that the effect of sequential exposure to IB-DNQ would be attenuated. At the lowest concentrations of IB-DNQ, neither 0.1  $\mu$ M nor 0.4  $\mu$ M showed any significant loss in cell viability regardless of the number of sequential 1-h daily pulse exposures. At the highest concentration of IB-DNQ (3.0  $\mu$ M), initially there appeared to be no response to IB-DNQ, but upon subsequent exposures to IB-DNQ, an incremental loss in cell viability was identified with approximately 50% cell death occurring at the end of 4 sequential exposures. Additional studies that incorporate a higher number of exposures to determine whether this trend continues or if after a certain number of exposures the cells would develop resistance to IB-DNQ would help inform treatment protocols in the clinic. The induction of cytotoxicity as a function of IB-DNQ concentration and sequential exposure in SCCF3 cells is summarized in Table 2.2.

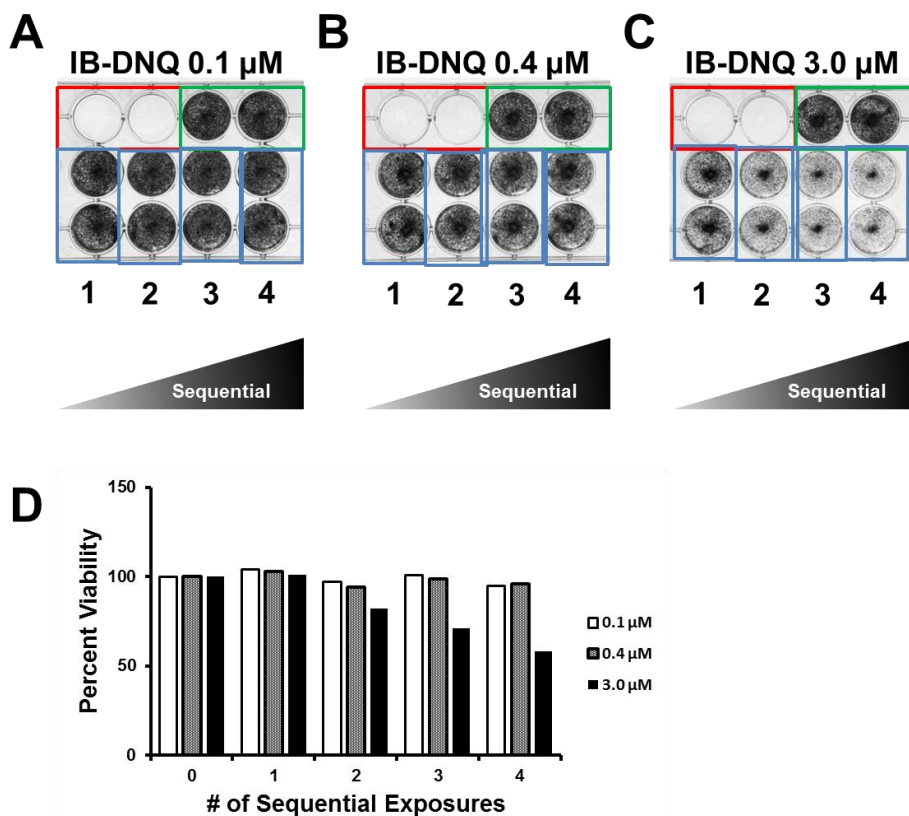


**Figure 2.6.** Repeated exposure of SCCF3 cells to IB-DNQ for biologically-achievable time durations (60 min) induces cytotoxicity in a dose dependent manner with SRB viability assay. (a,b,d) No observed cumulative cytotoxicity observed with the lowest concentrations of IB-DNQ, however, concentrations of 3.0  $\mu\text{M}$  (c/d) exert incremental cytotoxicity after  $\geq 2$  sequential IB-DNQ exposures. Negative control wells (red outline) with no cells, positive control wells (green outline) with untreated cells, and sequential treated wells (blue outline) with IB-DNQ exposed cells. N=1.

**Table 2.2.** Cytotoxicity following sequential exposure to IB-DNQ in SCCF3 cells

IB-DNQ	0.1 $\mu\text{M}$	0.4 $\mu\text{M}$	3.0 $\mu\text{M}$
Number of Treatments	% Viable	% Viable	% Viable
0	100	100	100
1	104	103	101
2	97	94	82
3	101	99	71
4	95	96	58

N=1



From preliminary pharmacokinetic studies in healthy felines it became apparent that, in contrast to mice, IB-DNQ was short lived *in vivo*. Therefore a similar sequential exposure experiment was performed in NQO1 expressing SCCF1 cells in order to target the minimum incubation time for IB-DNQ to exert cytotoxicity (Fig. 2.7). SCCF1 cells were incubated with a concentration of 3.0  $\mu\text{M}$  IB-DNQ for a 15 minute window every 24 h for up to four exposures. Given this minimal time frame, it was surprising to see drastic loss in cell viability within two exposures up to 60% cell death similar to that seen with the longer 1-h incubation time. At the end of 4 IB-DNQ exposures less than 15% of cell were still viable. The induction of cytotoxicity upon 15 min of exposure as a function of IB-DNQ concentration and sequential exposure is summarized in Table 2.3

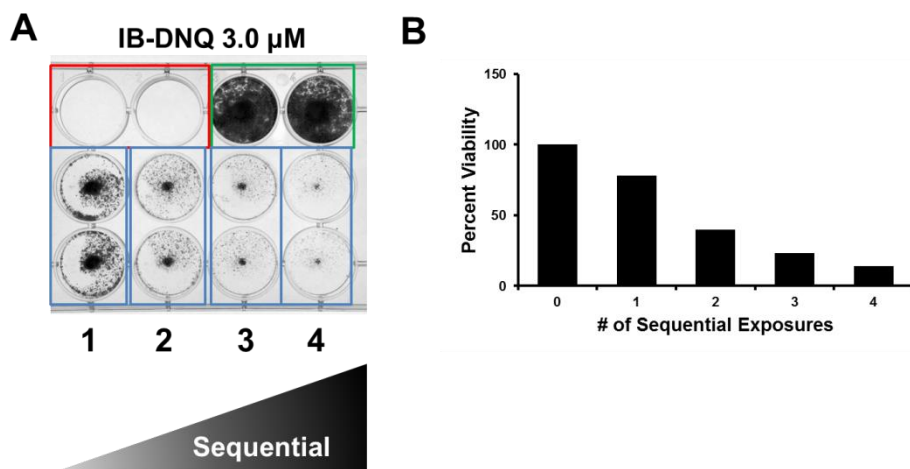


**Figure 2.7.** Repeated exposure of SCCF1 cells to IB-DNQ for extremely short time durations (15 min) induces cytotoxicity in a dose dependent manner with SRB viability assay. (a/b) a concentration of 3.0  $\mu\text{M}$  exerts substantive to profound cytotoxicity after  $\geq 2$  sequential IB-DNQ exposures. Negative control wells (red outline) with no cells, positive control wells (green outline) with untreated cells, and sequential treated wells (blue outline) with IB-DNQ exposed cells. N=1.

**Table 2.3.** Cytotoxicity following 15 min sequential exposure to IB-DNQ

IB-DNQ Number of Treatments	3.0 $\mu$ M % Viable
0	100
1	78
2	40
3	23
4	14

N=1

### 2.1.3. Pharmacokinetics of IB-DNQ in healthy cats

Pharmacokinetics were derived from 4 healthy research cats, following single-dose, IV administration at 0.5 mg/kg, 1.0 mg/kg, and 2.0 mg/kg; average peak plasma concentration levels were  $1227.4 \pm 273.3$  ng/mL ( $3.8 \pm 0.8$   $\mu$ M),  $1731.3 \pm 163.5$  ng/mL ( $5.3 \pm 0.5$   $\mu$ M), and  $3426.3$  ng/mL  $\pm 1249.7$  ( $10.5 \pm 3.8$   $\mu$ M), respectively (Fig 2.8a). Terminal elimination half-life at 0.5 mg/kg, 1.0 mg/kg and 2.0 mg/kg IV was  $19.5 \pm 2.2$  min,  $30.0 \pm 17.4$  min, and  $115.8 \pm 90.7$  min, respectively. Orally dosed IB-DNQ at 1.0 mg/kg achieved peak plasma concentrations and oral bioavailability of  $94.7 \pm 52.1$  ng/mL and 13.8%, respectively (Fig 2.8b). Full pharmacokinetic parameters for IB-DNQ administered IV and PO are detailed in Tables 2.4 and 2.5.

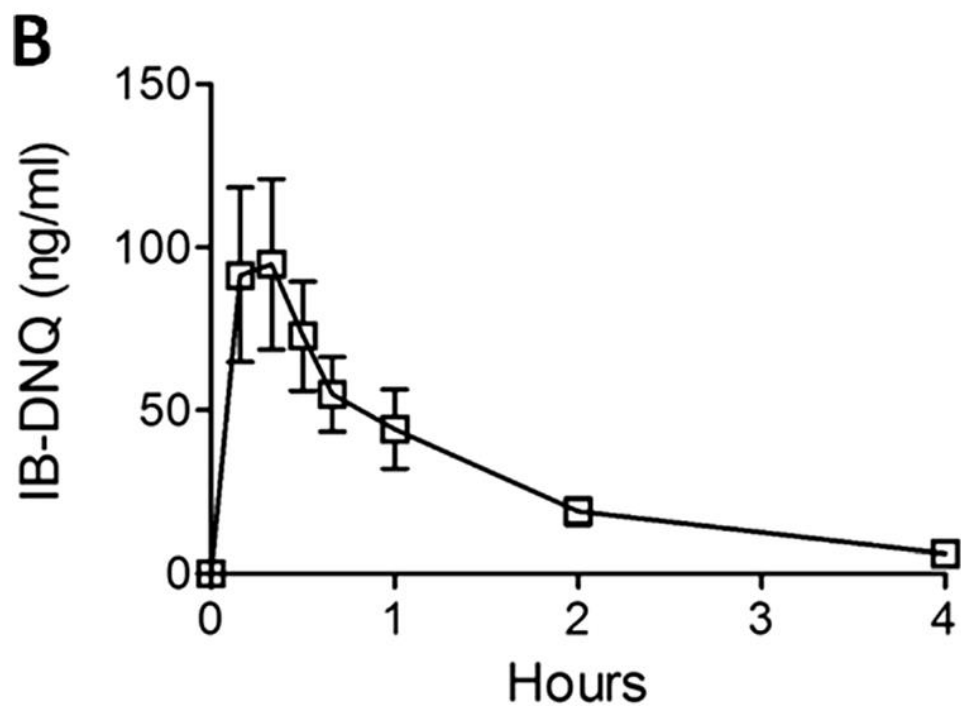
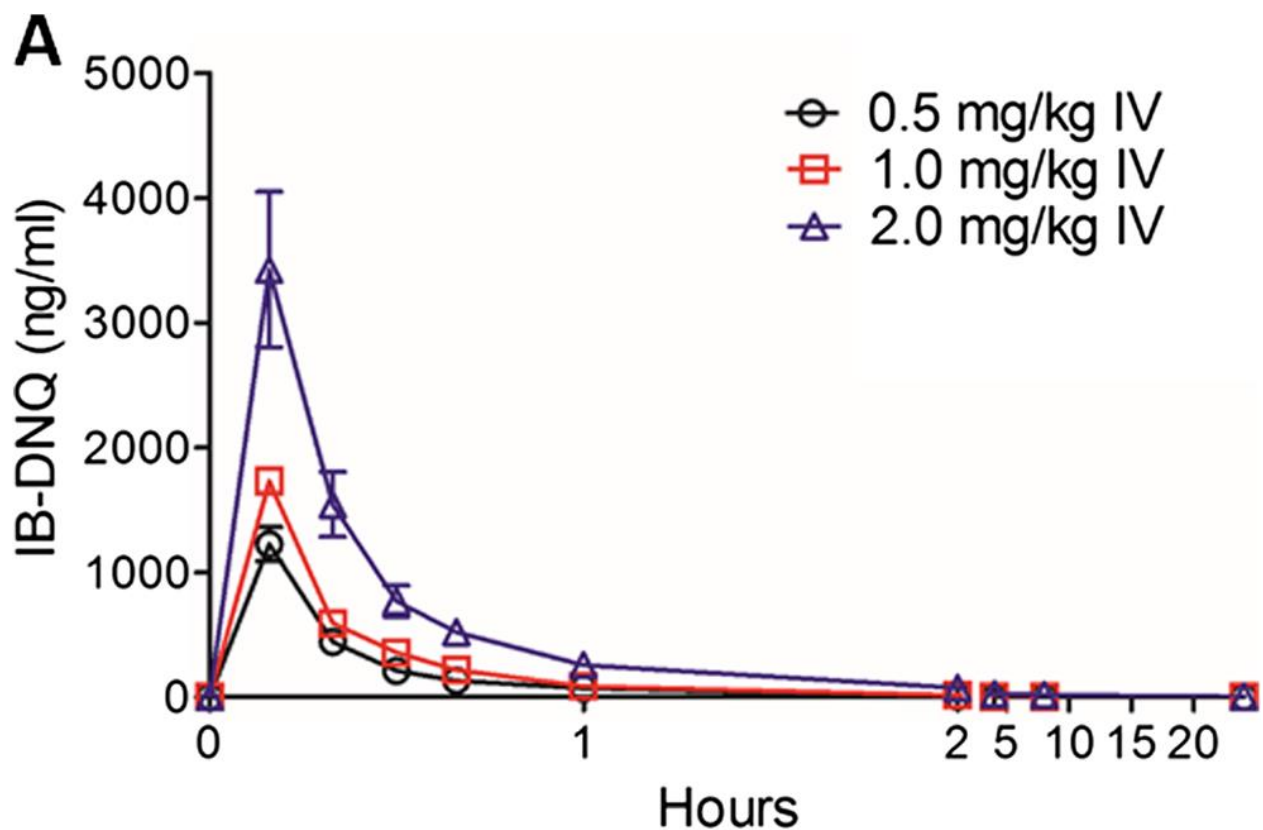


**Figure 2.8.** Pharmacokinetic profile of (a) intravenous IB-DNQ dosed at 0.5 mg/kg, 1.0 mg/kg, and 2.0 mg/kg as an aqueous solution in HP $\beta$ CD, and (b) oral IB-DNQ dosed at 1.0 mg/kg via gavage as an oral slurry in HP $\beta$ CD. Data represented as average  $\pm$  SD.

**Table 2.4.** Pharmacokinetic parameters of IB-DNQ following IV administration

	0.5 mg/kg IV	1.0 mg/kg IV	2.0 mg/kg IV
AUC <sub>0-inf</sub> (ng x min/mL)	44,223.5 ± 6969.2	55,732.6 ± 6043.8	113,064.4 ± 46844.1
K10-HL (min)	5.7 ± 0.4	8.2 ± 3.7	13.7 ± 1.5
α (1/min)	0.2 ± 0.0	0.1 ± 0.1	0.1 ± 0.0
β (1/min)	0.0 ± 0.0	0.0 ± 0.0	0.0 ± 0.0
t <sub>1/2</sub> α (min)	4.3 ± 0.1	6.2 ± 4.1	10.9 ± 1.5
t <sub>1/2</sub> β (min)	19.5 ± 2.2	30.0 ± 17.4	115.8 ± 90.7
A (ng/mL)	483.4 ± 1068.6	4659.9 ± 1628.0	5582.9 ± 2395.2
B (ng/mL)	507.3 ± 202.0	813.8 ± 838.2	198.5 ± 162.5
C <sub>max</sub> (ng/mL)	1227.4 ± 273.3	1731.3 ± 163.5	3426.3 ± 1249.7
Cl (mL/min)	40.3 ± 6.8	63.4 ± 7.0	73.9 ± 39.8
AUMC <sub>0-inf</sub> (ng x min x min/mL)	577,057.8 ± 109,204.2	1,017,022.9 ± 266,567.0	7,697,841.3 ± 8,839,491.6
MRT (min)	13.0 ± 1.3	18.5 ± 5.6	57.7 ± 50.8
V <sub>ss</sub> (mL)	524.5 ± 91.5	1189.9 ± 438.1	3409.0 ± 1857.8
V2 (mL)	191.6 ± 34.3	430.5 ± 164.6	1956.2 ± 2043.2
Cl <sub>D2</sub> (mL/min)	9.4 ± 3.1	18.0 ± 9.4	13.5 ± 5.0

Parameters derived from 4 research cats and expressed as average ± SD

**Table 2.5.** Pharmacokinetic parameters of IB-DNQ following 1.0 mg/kg PO administration

	1.0 mg/kg PO
AUC (min*ng/mL)	7718.1 ± 3311.3
K01_HL (min)	4.3 ± 2.4
K10_HL (min)	54.5 ± 26.1
CL_F (mL/min)	588.0 ± 424.4
Tmax (min)	15.1 ± 8.7
Cmax (ng/mL)	97.5 ± 51.8

Parameters derived from 4 research cats and expressed as average ± SD

#### 2.1.4. Tolerability of IB-DNQ in healthy cats

To assess the tolerability of IB-DNQ, we evaluated hematologic, non-hematologic, and clinical observational toxicities associated with each administration. Prior to IB-DNQ administration, baseline CBCs and chemistry panels were performed and then repeated at 1, 3, 7 and 14 days post-treatment. No clinically meaningful hematologic or non-hematologic toxicities were documented throughout the duration of study. Additionally, each feline subject was monitored for the development of acute clinical side effects peri-infusion and post-infusion (30 min). The most notable observed clinical abnormalities were ptyalism and tachypnea in all cats

following 2.0 mg/kg IV, with clinical symptoms resolving within 30 min of infusion completion. At 1.0 mg/kg, cats exhibited transient tachypnea in the absence of ptyalism. Administration at 0.5 mg/kg IV and 1.0 mg/kg PO did not elicit any observable symptoms. Long-term follow-up for an additional 9 months confirmed the absence of delayed-onset clinical, hematologic, and non-hematologic toxicity, further supporting an acceptable safety profile.

### **2.1.5. Assessment of off-target systemic oxidative injury**

The potential for non-specific systemic oxidative injury as a consequence of IB-DNQ exposure was assessed by quantifying changes in serum 8-OHdG. At 0.5 mg/kg IV, pre-treatment and post-treatment concentrations of serum 8-OHdG were  $9.0 \pm 2.1$  ng/mL and  $8.1 \pm 1.7$  ng/mL, respectively ( $p = 0.3$ ). At the highest dosage of IB-DNQ (2.0 mg/kg IV), a reduction in serum 8-OHdG concentrations were detected between pre-treatment ( $9.2 \pm 2.2$  ng/mL) and post-treatment ( $7.8 \pm 2.0$  ng/mL) sampling ( $p = 0.02$ )

## **2.2. Summary of pre-clinical work**

Given the mechanism of NQO1 bioactivatable agents, solid tumor histologies overexpressing NQO1 would be expected to be most responsive to IB-DNQ. Overexpression of NQO1 has been documented across a multitude of epithelial cancers arising from tissues of the gastrointestinal, reproductive and respiratory systems.<sup>21-23</sup> Relevant to the current investigation, NQO1 is shown to be overexpressed by malignantly transformed squamous cell epithelium arising from the uterine cervix and oral cavity.<sup>24,25</sup> Specific to OSCC, overexpression of NQO1 has been identified in 45% of primary tumor samples, and demonstrated the feasibility of targeting NQO1 with  $\beta$ -lapachone in combination with ionizing radiation.<sup>24</sup> Complementing

these findings, results from our study further confirms the suitability of OSCC as a tumor histology that might benefit from NQO1 bioactivatable therapies as 45% (27/60) of human-derived tissue microarray samples demonstrated robust (++ or +++) NQO1 expression. Importantly, we provide new information that supports the inclusion of feline OSCC as a relevant comparative tumor model for exploring NQO1-mediated therapies based upon the identification of intense (++ or +++) NQO1 expression on 59% (27/46) of naturally-occurring feline OSCC tumor samples.

Multiple studies have demonstrated that quinone-containing compounds, such as  $\beta$ -lapachone and DNQ, have the capacity to serve as NQO1 substrates that generate ROS thereby inducing cancer cell death.<sup>6,18,26,27</sup> Despite the exertion of selective anticancer cytotoxicity, the clinical translation of these agents has been hindered by their modest activity, unfavorable pharmacokinetics or narrow biologic tolerability.<sup>20</sup> As such, impetus exists for the rational development of newer NQO1 substrates with improved potency, pharmacokinetics, and biocompatibility. Regarding potency, IB-DNQ exerted 5- to 10-fold increase in cytotoxicity in robust NQO1 expressing OSCC cell lines in comparison to  $\beta$ -lapachone. Importantly, IB-DNQ exerted substantive cytotoxicity in OSCC cell lines at biologically relevant durations of drug exposure (1h) and concentrations (0.4  $\mu$ M, or equivalent 130 ng/mL) readily and safely achievable in healthy research cats receiving IB-DNQ dosages  $\geq 1.0$  mg/kg IV. The melding of classical in vitro cell-based experiments with necessary in vivo modeling justifies continued development of IB-DNQ for translational applications.

Biocompatibility of investigational agents is essential for successful translational applications, and in the context of NQO1 bioactivatable molecules, excessive or systemic production of reactive oxygen species has potential to induce global endothelial cell injury,

inflammation, and consequent end-organ failure. Prior research with DNQ, the parent compound of IB-DNQ, demonstrated that one mole of DNQ in the presence of NQO1-expressing cancer cells can generate greater than 60 mol of superoxide per minute.<sup>20</sup> When administered to mice, both DNQ and  $\beta$ -lapachone possess narrow ranges for biologic compatibility and drug exposures predicted to exert anticancer activities closely approximate similar concentrations that induce the formation of methemoglobinemia,<sup>20</sup> a biomarker of red blood cell oxidative stress. Given the potential for off-target oxidative injury, it is scientifically judicious to evaluate NQO1 bioactivatable molecules in model systems that are sufficiently sensitive for the detection of oxidative stress. In the current study, we employed the inclusion of healthy felines as a model system to test the biocompatibility of IB-DNQ. The felid species is uniquely vulnerable to global oxidative injury given the high number of free sulfhydryl groups on their hemoglobin allowing for identification of oxidative stress through the detection of Heinz bodies and resultant hemolytic anemia.<sup>28</sup> Our findings suggest that IB-DNQ is highly biocompatible in the felid species, with clinically negligible hematologic (Heinz body anemia) and non-hematologic toxicities following repeated systemic exposures to IB-DNQ predicted to exert anticancer activities. Further confirmation of IB-DNQ's oxidative tolerability in healthy felines was supported by the serial quantification of hydroxydeoxyguanosine (8-OHdG), a specific biomarker for DNA oxidation. In all research felines, no increases in serum 8-OHdG concentrations were identified 24-h following 0.5 mg/kg and 2.0 mg/kg IV IB-DNQ administration.

Collectively, the cell-based and live animal data derived from a uniquely sensitive species presented in this study strongly supports continued development of IB-DNQ as a novel and biocompatible drug for the treatment of NQO1 expressing cancers, such as OSCC in both

felids and human cancer patients. The future purposeful inclusion of companion animals as a naturally-occurring tumor model holds promise for expediting the drug development pathway for NQO1 bioactivatable molecules, and might provide intriguing and relevant findings to support the tractability of IB-DNQ, as a single agent or in combination with other cytotoxic modalities, for continued drug development and clinical translation.

### **2.3. Clinical evaluations of IB-DNQ in OSCC patients**

#### **2.3.1. Single agent efficacy in patient cats with OSCC**

Three felines with histologically-confirmed FOSCC were recruited for a small pilot study to evaluate the tolerability and anticancer activities of IB-DNQ administered IV at a dosage of 1.0 mg/kg for 3-4 consecutive treatments over a 4-6 week period. Originally the pilot study was designed to for patients to receive 3 consecutive treatments of 1.0 mg/kg IV IB-DNQ over a six week period with two weeks in between treatment times, however, it was determined that research cats were able to tolerate dosing every week and even up to five consecutive days. Therefore, since OSCC rapidly progresses in felines and a more accelerated dosing regimen was well tolerated, after completion of the first cat in the study, the design was modified to administration once a week for up to four treatments. Prior to treatment, computed tomography (CT) scans were performed in all cats to establish the initial tumor burden (Fig. 2.9). Tumor samples were collected from each cat and stained for NQO1 expression by IHC and scored similar to HNSCC and FOSCC microarray scoring (Fig. 2.9). One week after the culmination of treatments, CT scans were repeated in the patient cats to assess the effectiveness of IB-DNQ treatment. The result of 1.0 mg/kg IV IB-DNQ in the small cohort of cats was 1 partial response



(43% reduction in tumor cross sectional area), 1 stable disease (5% increased) and 1 progressive disease (82% increases). The clinical responses to IB-DNQ correlate well with the expression of NQO1 in the tumor biopsies (Fig 2.9).

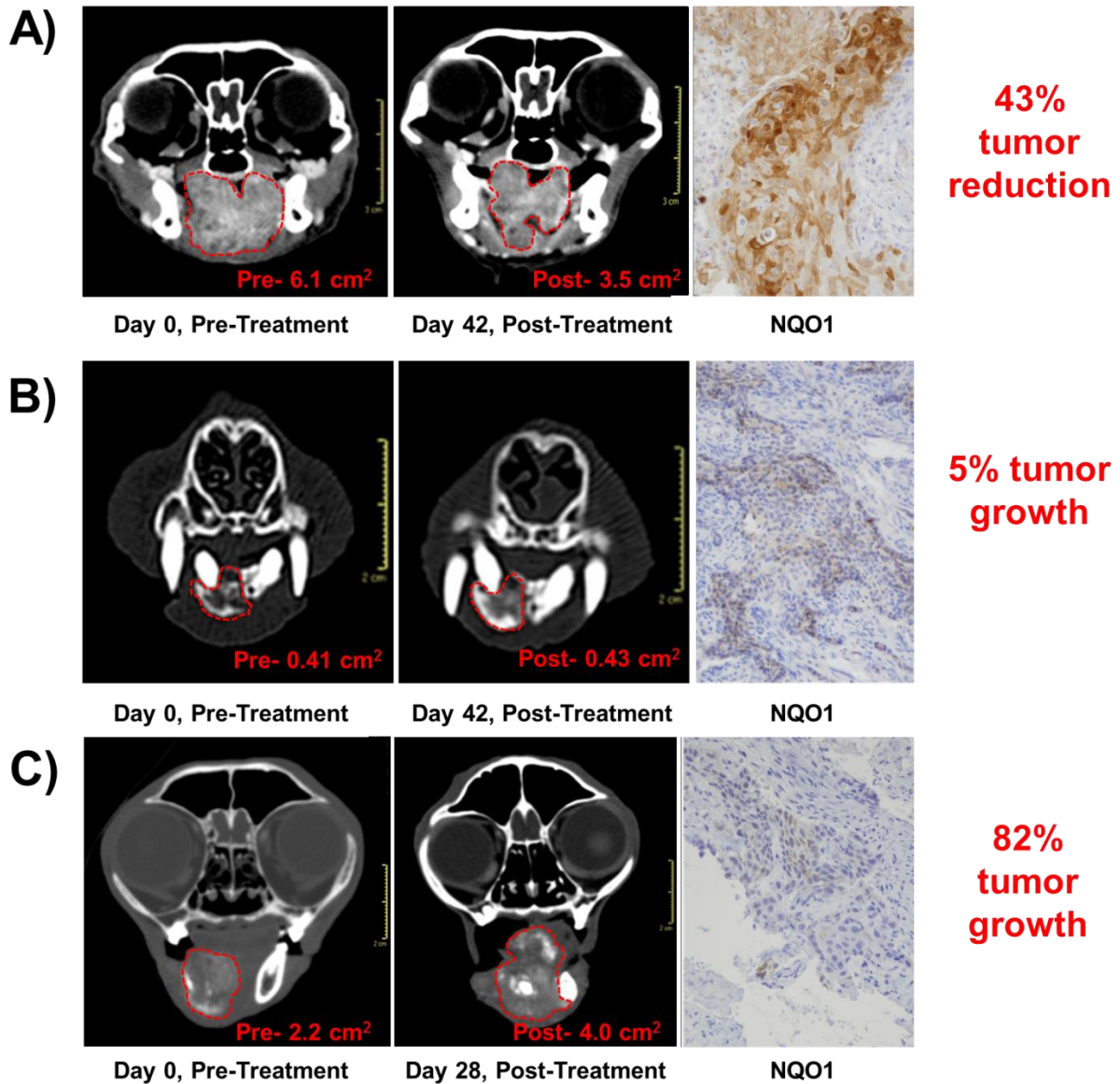


**Figure 2.9.** Clinical responses to single agent IB-DNQ. For (a-c) the pre-treatment CT scan (far left), the post-treatment CT scan upon the completion of 3-4 doses 1 mg/kg IV IB-DNQ (middle) and the IHC tumor biopsy evaluated for NQO1 expression. Patients' responses to treatment correlate well to tumor expression NQO1 (a) High expression; partial response (b) medium expression; stable disease (c) low expression; progressive disease.

## **2.3.2. Combination therapy in patient cats with OSCC**

### **2.3.2.1. In vitro responses of NQO1 expression to ionizing radiation**

IHC staining of HNSCC and FOSCC tumors showed that roughly 25% of head and neck tumors express NQO1, albeit at low levels that should not respond to single agent IB-DNQ. Recent studies have shown that NQO1 expression can be induced in response to ionizing radiation<sup>29-31</sup> and other methods.<sup>32-35</sup> As combined treatment modalities involving radiation are commonly used in HNSCC, a combined IR + IB-DNQ therapy may allow for greater response in the 50% of tumors expressing medium to high levels of NQO1 as well allowing therapeutic access to the other 25% of tumors that express NQO1, but not at levels required for single agent IB-DNQ efficacy. SCCF3 (low NQO1 expressing feline OSCC, Fig. 2.2) cells were exposed to IR at doses of 2, 4, 6 or 8 Gy and monitored for NQO1 expression (Fig 2.10a) and activity (Fig 2.10b) for up to 24 h post radiation exposure. The levels of NQO1 expression appear elevated 4-h post-radiation and remains elevated 24-h post-radiation. NQO1 activity shows a similar upregulation, showing maximal peak increase in response to 8 Gy radiation roughly 2-4 h post-exposure. Systemic administration of IB-DNQ 2-4 h after exposure to 8 Gy IR should be the optimal window for administration in order to maximize the potential cytotoxic response in medium and low NQO1 expressing tumors.

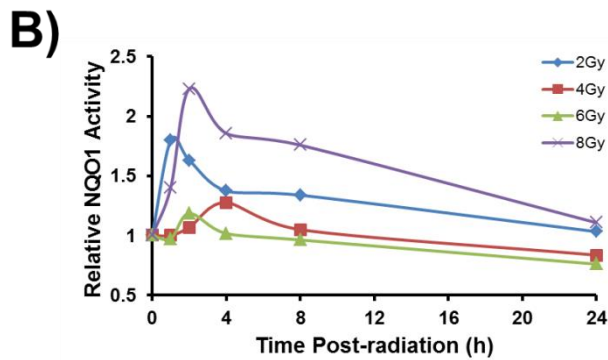
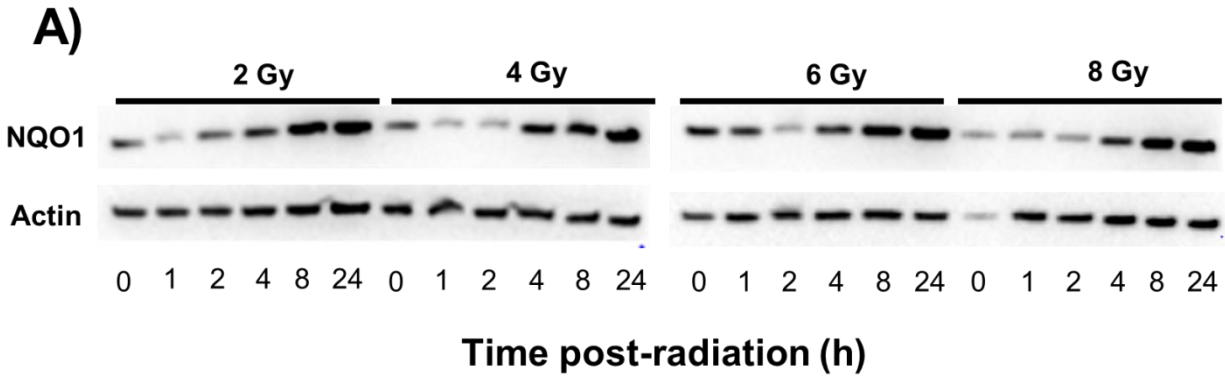


**Figure 2.10.** IR induced NQO1 expression as determined by (a) Western blot analysis and confirmed by (b) enzyme activity for 2-8 Gy over a 24-h period post-radiation.

### 2.3.2.2. Combination efficacy in patient cats with OSCC

Two felines with histologically-confirmed FOSCC were enrolled in a small pilot study to evaluate the tolerability and anticancer activities of IR and IB-DNQ combination therapy. Felines were exposed to 8 Gy IR and treated systemically with 1 mg/kg IV IB-DNQ 4 hours after radiation weekly for 4 consecutive treatments. Initial tumor CTs and tumor biopsies were taken prior to treatment (Fig 2.11). At the culmination of 4 treatments, follow-up CTs were taken to examine the effectiveness of the combination treatment (Fig 2.11). Both patients had observable reduction in tumor size with 42% reduction observed in the medium NQO1 expressing tumor and 45% reduction in the low NQO1 expressing patient. The results in this small cohort of patients demonstrate that combination of IR and subsequent systemic IB-DNQ administration

can be applied clinically and is a potentially promising treatment modality for FOSCC, especially in those expressing low levels of IB-DNQ which are not expected to respond strongly to single agent IB-DNQ.

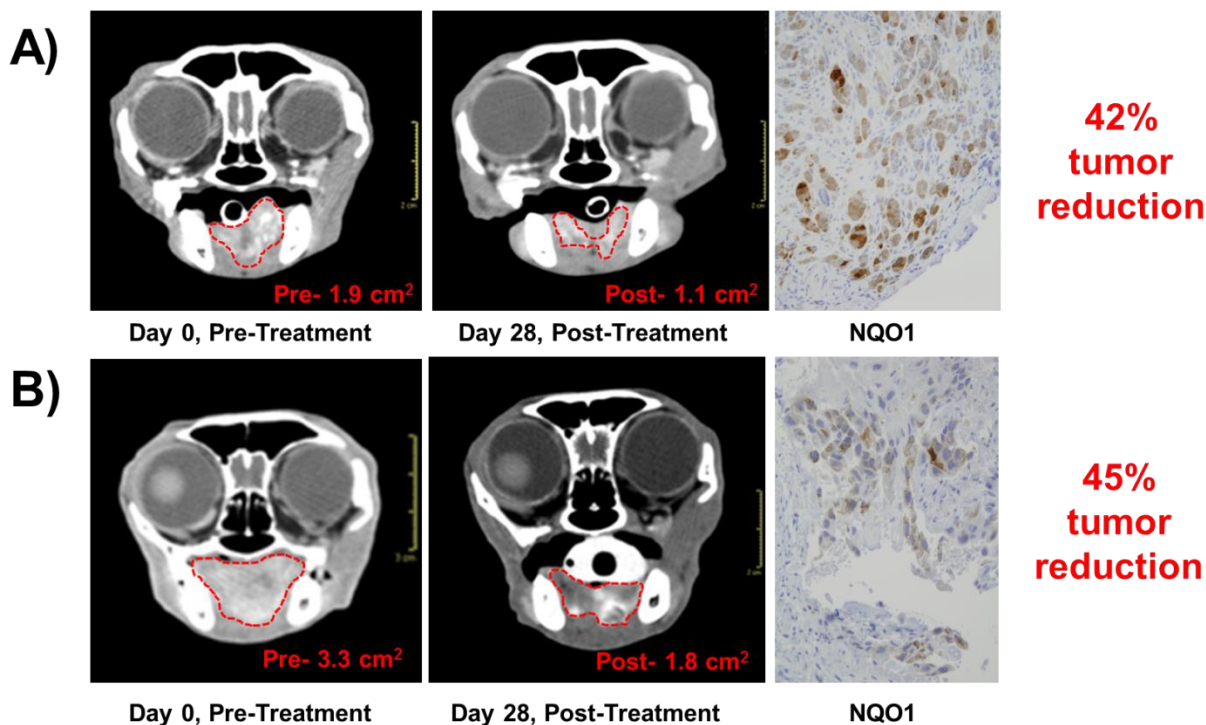


**Figure 2.11.** Clinical responses to combination IR and IB-DNQ. For (a & b) the pre-treatment CT scan (far left), the post-treatment CT scan upon the completion of 4 doses 1 mg/kg IV IB-DNQ (middle) and the IHC tumor biopsy evaluated for NQO1 expression. While both patients would be predicted to not respond favorably to single agent IB-DNQ based on tumor NQO1 expression, both saw regression with combination IR and IB-DNQ.

#### 2.4. In vitro cytotoxicity in HNSCC cell lines

As discussed previously, sample primary tumors from human patients with HNSCC demonstrated a high prevalence of NQO1 expression. The expression of NQO1 was further evaluated in a panel of five HNSCC cell lines received from Dr. David A. Boothman (UT Southwestern) that had previously been reported to widely range in NQO1 expression levels. Western blot analysis of these cell lines were examined in relation to A549, a high NQO1-

expressing non-small cell lung carcinoma cell line, and MDA-MB-231, a breast cancer cell line possessing a NQO1\*2 polymorphism which results in the production of nonfunctional NQO1 that is quickly degraded by the cell, as positive and negative controls respectively (Fig 2.12). NQO1 expression was highest in Detroit562 and FaDu cells. Intermediate expression levels were observed in MDA686LN cells and low levels were observed with the HN30 cell line. The JHU029 cell lines possessed no observable NQO1 expression.

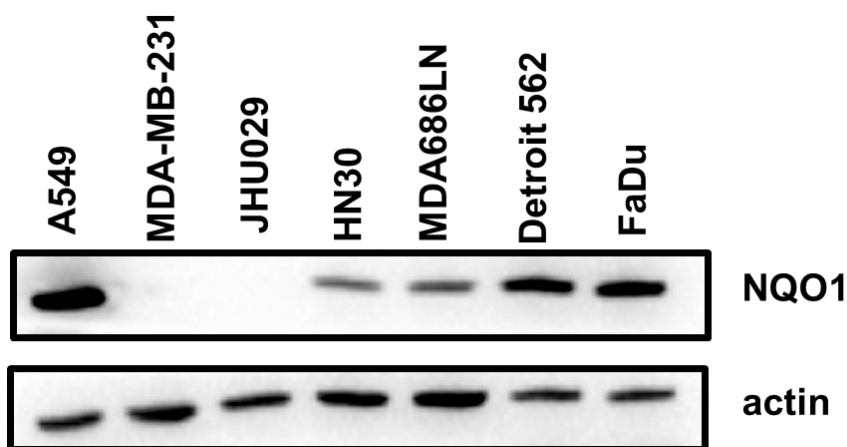


**Figure 2.12.** In 5 HNSCC immortalized cell lines, variable NQO1 protein expression detected by western blot; positive (A549) and negative (HEK293) control cells.  $\beta$ -actin used as loading control.

The potency of IB-DNQ was evaluated in JHU209, HN30, MDA686LN and FaDu in the presence or absence of 100 nM ES936, a mechanistic inhibitor of NQO1 (Fig. 2.13). Cells were exposed to IB-DNQ for a 2-h pulse in the presence or absence of a 1-h pretreatment with ES936. The cytotoxicity of IB-DNQ in the non-NQO1 expressing JHU029 cell line remained unchanged in the presence or absence of this specific inhibitor,  $5.14 \pm 0.02 \mu\text{M}$  and  $4.57 \pm 2.88 \mu\text{M}$  respectively. In HN30 cells with low NQO1 expression and MDA686LN cells with intermediate NQO1 expression, a three-fold protection from IB-DNQ cytotoxicity was observed in the presence of ES936 ( $3.7 \pm 0.5 \mu\text{M}$  vs.  $11.5 \pm 1.1 \mu\text{M}$  for HN30 and  $2.8 \pm 0.3 \mu\text{M}$  vs.  $7.7 \pm 2.4 \mu\text{M}$

for MDA686LN). IB-DNQ was most potent in FaDu cells ( $0.27 \pm 0.03 \mu\text{M}$ ), the cell line with the most robust NQO1 expression, and experienced a 35-fold protect by pre-incubation with ES936 ( $9.4 \pm 1.2 \mu\text{M}$ ).

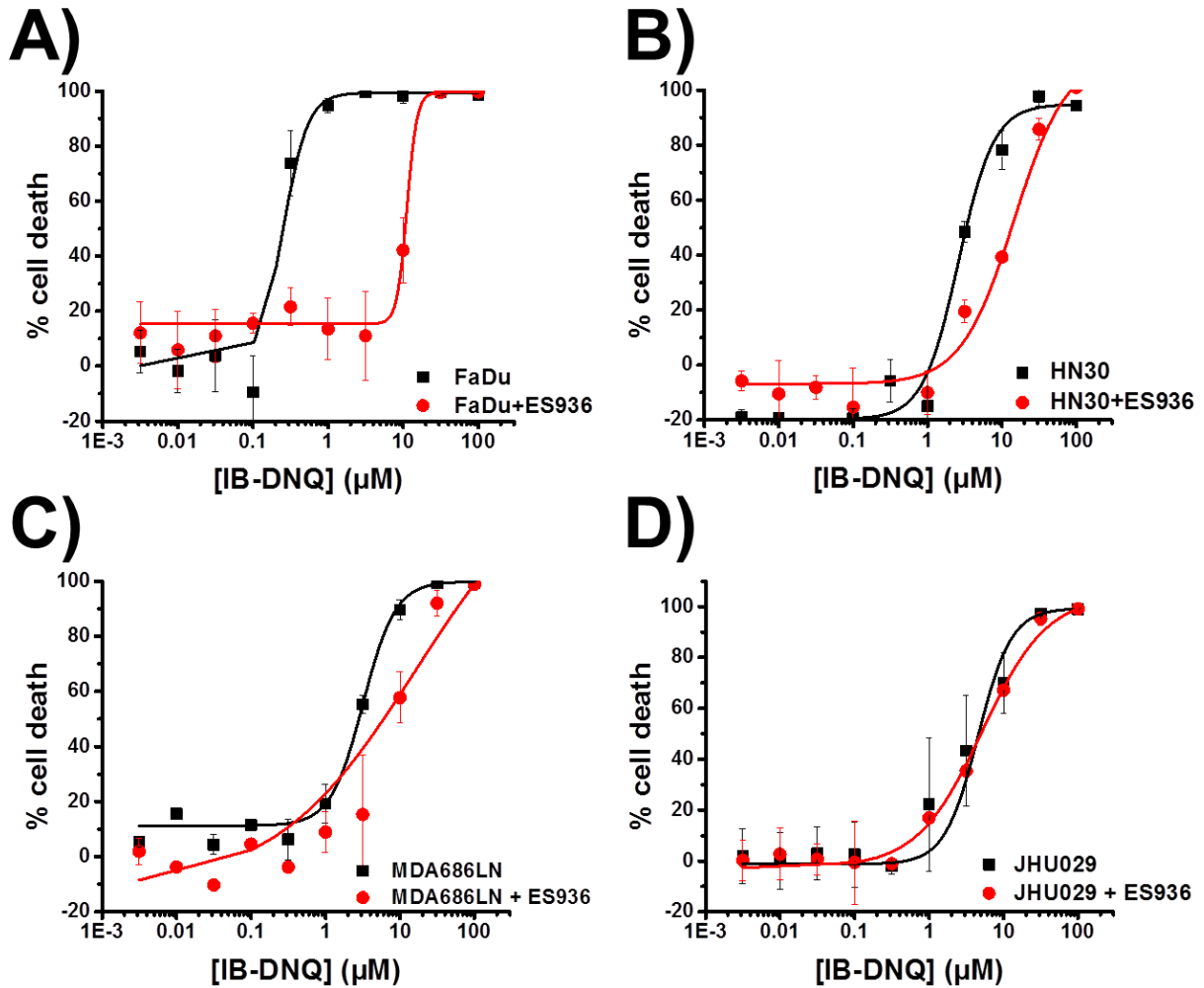


**Figure 2.13.** Dose-dependent cytotoxic effects of IB-DNQ in 4 immortalized HNSCC cell lines, in the presence or absence of ES935 (100 nM). Increased susceptibility of (a) FaDu, (b) HN30, (c) MDA686LN cell lines to NQO1 mediated cytotoxicity predicted by correlative NQO1 enzyme expression levels. Attenuated NQO1 mediated cytotoxicity in (d) JHU029 cell line based upon reduced NQO1 expression.

## **2.5. Summary**

The identification of molecular aberrations specific to tumors provides the opportunity to develop selective and effective anti-cancer strategies. As such, efforts in cancer therapeutic research have focused intensely either on the discovery of new druggable targets or the development of better drugs that act upon known targets. In the current investigation, we generate data to advance therapeutic development through novel experimental therapeutics that act upon existing druggable targets. Specifically, the findings reported herein substantiate the continued development of IB-DNQ, a novel NQO1 bioactivatable molecule, for the treatment of OSCC, a NQO1 expressing tumor histology. To expedite the advancement of IB-DNQ towards translational applications in human oncology patients, we characterized the *in vitro* anticancer activities, and *in vivo* tolerability and pharmacokinetics of IB-DNQ in domestic felids, a species highly sensitive to oxidative injury and stress.<sup>28,36,37</sup> Given that unacceptable drug toxicity and lack of activity remain major barriers along the road to successful new drug development, the promising cell-based cytoreductive activities in conjunction with the confirmed tolerability and predictable pharmacokinetics of IB-DNQ in a highly sensitive species and relevant comparative tumor model, improves confidence in the tractability of IB-DNQ as a novel anticancer agent for the treatment of human oncology patients.

## **2.6. Materials**

### **Cell lines and reagents**

Three feline OSCC cell lines (SCCF1, SCCF2, SCCF3; provided by Thomas J. Rosol, the Ohio State University) were used in this study. Cell lines were cultured in Dulbecco's Modified Eagle's Medium (DMEM) with 10% fetal bovine serum (FBS) and 1% penicillin/streptomycin

(100 IU/mL each). Cells were maintained at 37°C in 5% CO<sub>2</sub>. IB-DNQ was synthesized as previously described.<sup>18</sup> For all in vitro experiments, IB-DNQ or  $\beta$ -lapachone (Sigma-Aldrich, St. Louis, MO) was reconstituted with 99.5% DMSO (Sigma-Aldrich, St. Louis, MO) to produce 10 mM stock solution which was kept frozen at -80°C until needed. For in vivo experiments, IB-DNQ was reconstituted to 1.0 mg/mL in 2-hydroxypropyl- $\beta$ -cyclodextrin (HP $\beta$ CD) (Sigma-Aldrich, St. Louis, MO) and sterile water at a pH of 8.0-8.5 prior to administration.

### **Antibodies**

Anti-NQO1 antibody (goat polyclonal; ab2346), anti- $\beta$  actin antibody (mouse monoclonal; ab6276) and horseradish peroxidase (HRP) conjugated anti-mouse secondary antibody (ab6814) were purchased from Abcam (Abcam, Cambridge, MA) and anti-goat secondary antibody (SC-2020) was purchased from Santa Cruz Biotechnology (Santa Cruz Biotechnology, Dallas, TX). StrepTactin-HRP conjugate was purchased from Bio-Rad (Bio-Rad, Hercules, CA). Cross-reactivity of the anti-NQO1 antibody against feline tissues was validated by Western blot analysis and immunohistochemistry with the inclusion of known human positive (A549) and negative (HEK293) control cell lines purchased from American Tissue Culture Collection (Manassas, VA).

### **Western Blot Analysis**

Cell lysate proteins were collected using a commercial reagent and provided protocol (M-PER Assay, Thermo Scientific, Rockford, IL). For each cell line, 30  $\mu$ g of protein were electrophoresed on a 4-20% SDS-PAGE gel and transferred to a nitrocellulose membrane. Membranes were blocked with Tris-Buffered Saline with Tween 20 (TBST) in 5% milk for 1 h



at room temperature. Western blot analysis was performed using the anti-NQO1 antibody at a concentration of 1:1000 in TBST with 5% milk. The membrane was washed 3 times with TBST and probed with the secondary antibody diluted (1:5000) in TBST with 5% milk. For anti- $\beta$ -actin, antibody dilution of 1:2000 and secondary antibody was used at a dilution of 1:5000. Blots were developed using a standard chemiluminescence detection kit (GE Healthcare Life Sciences, Pittsburgh, PA) and ChemiDoc XRS+ molecular imager system (Bio-Rad, Hercules, CA) with Image Lab Software (Bio-Rad, Hercules, CA). Relative protein expressions were adjusted against  $\beta$ -actin serving as a loading control. At least 2 independent experiments were performed.

### **Immunohistochemistry**

*Cell lines:* Adherent cell cultures of OSCC and the human positive (A549) and negative (HEK293) control cell lines were collected, pelleted, and formalin fixed followed by resuspension in agarose gel to create an agarose-embedded cell pellet. Cell pellets were trimmed, processed and cut onto slides. Slides were treated and stained with the NQO1 antibody according to manufacturer recommendations, and counter stained with hematoxylin. Staining intensity for each OSCC cell line was compared with that of the positive control (A549). NQO1 staining intensity was scored categorically: (-) no staining; (+) light staining; (++) moderate staining; and (+++) intense staining.

*Tissue blocks and microarrays:* Thirteen feline OSCC tissue blocks from the University of Illinois Veterinary Diagnostic Laboratory, a tissue microarray of 37 feline OSCC samples provided by Cheryl A. London and Megan E. Brown, the Ohio State University, and a commercially-available tissue microarray of 60 human OSCC samples (US Biomax) were assessed by immunohistochemistry for NQO1 expression. The staining intensity for each sample

was compared with the staining of the positive (A549) control using the previously described scoring system.

### **NQO1 enzymatic activity assay**

NQO1 enzymatic activity was quantified with an activity assay (Abcam, Cambridge, MA, ab184867). Varying concentrations of OSCC protein from each cell line, in the presence or absence of an NQO1 inhibitor, (25  $\mu$ M dicoumarol) were added to reagents provided according to the assay protocol. Rate of change of absorbance ( $\Delta$ 550 nm) was read on a SpectraMax Plus 384 microplate reader (Molecular Devices, Sunnyvale, CA). Three experimental replicates were performed for all cell lines.

### **Dose-dependent in vitro IB-DNQ cytotoxicity assay**

Cells were seeded at 5000 cells per well in 96 well plates and allowed to attach. Media containing varying concentrations (0.003-100 $\mu$ M) of  $\beta$ -lapachone or IB-DNQ was made and cells were exposed for 2-h. Treatment media was removed and replaced with drug-free media and cells were allowed to grow for 48 h. To investigate the inhibitory effects of dicoumarol on NQO1 activity, cells were treated with vehicle (DMSO) or with a combination of 25  $\mu$ M dicoumarol with  $\beta$ -lapachone or IB-DNQ for 2-h. Viability was assessed using the sulforhodamine B (SRB) assay.<sup>38</sup> Percent death was plotted against concentration and fitted to a logistic dose response curve.

### **Repeated exposure in vitro IB-DNQ cytotoxicity assay**

The SCCF1 cell line was plated at a density ranging from  $8 \times 10^4$  to  $10^5$  cells in 12 well plates (day 0), and incubated overnight. After 24-h (day 1), media was removed from non-control wells and 1 mL of fresh media with varying concentrations of IB-DNQ (0.1, 0.4, or 3.0  $\mu\text{M}$ ) was placed into respective wells and incubated for 1 h. Wells were then rinsed and replaced with 2 mL fresh media and incubated overnight. On days 2-5, serial repeats of day 1 procedures were performed until treatment wells had received a total of 5 treatments. After each sequential exposure to IB-DNQ, cell death was assessed by SRB daily for up to 5 days.

The SCCF3 cell line was plated at a density of  $8 \times 10^4$  cells in 12 well plates (day 0), and incubated overnight. After 24-h (day 1), media was removed from non-control wells and 1 mL of fresh media with varying concentrations of IB-DNQ (0.1, 0.4, or 3.0  $\mu\text{M}$ ) was placed into respective wells and incubated for 1 h. Wells were then rinsed and replaced with 2 mL fresh media and incubated overnight. On days 2-4, serial repeats of day 1 procedures were performed until treatment wells had received a total of 4 treatments. After each sequential exposure to IB-DNQ, cell death was assessed by SRB daily for up to 4 days.

The SCCF1 cell line was plated at a density of  $5 \times 10^4$  cells in 12 well plates (day 0), and incubated overnight. After 24-h (day 1), media was removed from non-control wells and 1 mL of fresh media with 3.0  $\mu\text{M}$  concentration of IB-DNQ was placed into respective wells and incubated for 15 min. Wells were then rinsed and replaced with 2 mL fresh media and incubated overnight. On days 2-4, serial repeats of day 1 procedures were performed until treatment wells had received a total of 4 treatments. After each sequential exposure to IB-DNQ, cell death was assessed by SRB daily for up to 4 days.

### **Animal dosing and sample collection**

Four, healthy, intact, female domestic shorthair cats weighing 4-5 kg were used for all pharmacokinetic and toxicologic studies. IB-DNQ was dissolved into HP $\beta$ CD and sterile water was administered intravenously (IV; 0.5 mg/kg, 1.0 mg/kg, or 2.0 mg/kg) and by oral gavage (PO; 1.0 mg/kg). Cats received a minimum of four doses of IB-DNQ (3 IV, 1 PO) with a minimum washout period of 2 weeks between dosing. Sample collection times for all methods of administration were 0, 10, 20, 30, 40, 60, 120, 240, 480 min and 24 h post administration. Cats were monitored peri- and post-IB-DNQ administration to document clinical symptoms. Upon completion of IB-DNQ administrations, the cats were monitored for an additional 9 months for assessment of delayed toxicity. All experiments with healthy research cats were approved by the University of Illinois Animal Care and Use Committee.

### **Plasma IB-DNQ quantification method**

Plasma samples were analyzed with the 5500 QTRAP LC/MS/MS system (Sciex, Framingham, MA) in Metabolomics Lab of Roy J. Carver Biotechnology Center, University of Illinois at Urbana-Champaign. Software Analyst 1.6.2 was used for data acquisition and analysis. The 1200 series HPLC system (Agilent Technologies, Santa Clara, CA) includes a degasser, an autosampler, and a binary pump. Multiple reaction monitoring (MRM) was used for quantification of IB-DNQ with DNQ as the internal standard. The detection limit of IB-DNQ was 1.0 ng/mL)

### **Pharmacokinetic profile of IB-DNQ**

Pharmacokinetic analyses were performed using a non-linear regression program (Winnonlin, version 5.1) (Pharsight Corporation, Cary, NC). The area under the curve (AUC), terminal half-life ( $t_{1/2}$   $\beta$ ), volume of distribution at steady state ( $V_{d_{ss}}$ ), total clearance (Cl), maximum drug concentration ( $C_{max}$ ) and time at which  $C_{max}$  was achieved ( $T_{max}$ ) were determined.

### **Hematologic and non-hematologic toxicity assessment**

Assessment of hematologic and non-hematologic tolerability in cats following IB-DNQ administration were performed on days 1, 3, 7 and 14 post IB-DNQ administration. Complete blood counts (CBC) and serum biochemical analysis were performed by the Veterinary Diagnostic Laboratory, University of Illinois at Urbana-Champaign.

### **Off-target oxidative injury assessment with 8-hydroxydeoxyguanosine ELISA**

Baseline (time 0) and 24-h post IB-DNQ serum samples were evaluated for changes in 8-hydroxydeoxyguanosine (8-OHdG) concentrations in all cats following the IV IB-DNQ administration at the lowest (0.5 mg/kg) and highest dosages (2.0 mg/kg). Concentrations of 8-OHdG were quantified with the commercially available ELISA kit (Abcam, Cambridge, MA, ab201734).

### **IR-induction of NQO1 expression.**

SCCF3 cells were seeded at 500,000 cells per well in 6 well plates in 2 mL of media and incubated overnight at 37°C, 5% CO<sub>2</sub>. Cells were irradiated at University of Illinois College of

Veterinary Medicine at doses of 2, 4, 6, or 8 Gy. Cell plates were incubated at 37°C, 5% CO<sub>2</sub> for varying amounts of time before harvesting at 1, 2, 4, 8, or 24 h post-radiation. Media was removed from wells and cells were washed once in 1 mL PBS, which was replaced by 0.5 mL trypsin. Cells were incubated for 2-3 min and then 1 mL RPMI 1640 media was added to quench trypsin. Cells were scrapped if not already detached and transferred to falconer tubes. Cells were centrifuged at 500 x g for 3 min. Media was aspirated off and pellet was resuspended in PBS before centrifuging at 500 x g for 3 min. This was repeated twice. Cells were kept at -80°C until Western Blot analysis or NQO1 activity assay.

### **Single agent IB-DNQ treatment in FOSCC patients**

Three patient cats with histologically-confirmed OSCC were recruited for a small pilot trial evaluating the tolerability and anticancer activities of IB-DNQ administered IV at a dosage of 1.0 mg/kg for 3-4 consecutive treatments over a 4-6 week period. Prior to IB-DNQ treatment, baseline complete blood counts and serum chemistry panels were performed, with diagnostic assessments repeated immediately prior to each successive IB-DNQ treatment. To quantify anticancer activities, computed tomography was performed in all cats prior to IB-DNQ treatment to objectively quantify treatment naïve tumor burden, and repeated computed tomography was performed 7-days following the last administered dosage of IB-DNQ. Immunohistochemical staining for NQO1 was performed on OSCC tissue samples collected from pet cats, and relative NQO1 staining intensity graded in comparison to A549. All experiments with pet cats diagnosed with OSCC were approved by the University of Illinois Animal Care and Use Committee.

## **Combination treatment IR and IB-DNQ in FOSCC patients**

Two patient cats with histologically-confirmed FOSCC were recruited for a small pilot trial evaluating tolerability and anticancer activity of IR irradiation at a dosage of 8 Gy followed by systemic administration of IB-DNQ IV at a dosage of 1 mg/kg 4 hours post-radiation for 4 consecutive treatments over a 4 week period. Prior to radiation, baseline complete blood counts and serum chemistry panels were performed, with diagnostic assessments repeated immediately prior to each successive treatment. To quantify anticancer activities, computed tomography was performed in all cats prior to treatment to objectively quantify treatment naïve tumor burden, and repeated computed tomography was performed 7-days following the last administered dosage of IB-DNQ. IHC staining for NQO1 was performed on OSCC tissue samples collected from pet cats, and relative NQO1 staining intensity graded in comparison to A549 cells. All experiments with pet cats diagnosed with OSCC were approved by the University of Illinois Animal Care and Use Committee.

## **Statistical analyses**

All in vitro experiments were repeated at least three times and results were expressed as mean  $\pm$  SD. Data was compared with lone-way ANOVA and differences of treatment groups relative to untreated controls were assessed with post-hoc Dunnet's test. A  $p$ -value  $<0.05$  was considered statistically significant;  $*p < 0.05$ ,  $**p < 0.01$ ,  $***p < 0.001$ .

## **2.7. References**

(1) Mak, I.W.; Evaniew, N.; Ghert, M. Lost in translation: animal models and clinical trials in cancer treatment. *Am. J. Transl. Res.* **2014**, *6*(2), 114-118.

- (2) Kamb, A. What's wrong with our cancer models? *Nat. Rev. Drug Discov.* **2005**, 4(2), 161-165.
- (3) Talmadge, J.E.; Singh, R.K.; Fidler, I.J.; Raz, A. Murine models to evaluate novel and conventional therapeutic strategies for cancer. *Am. J. Pathol.* **2007**, 170(3), 793-804.
- (4) Mestas, J.; Hughes, C.C. Of mice and not men: differences between mouse and human immunology. *J. Immunol.* **2004**, 172(5), 2731-2738.
- (5) Richmond A.; Su, Y. Mouse xenograft models vs GEM models for human cancer therapeutics. *Disease Models & Mechanisms* **2008**, 1(2-3), 78-82.
- (6) Khanna, C.; Linblad-Toh, K.; Vail, D.; London, C.; Bergman, P.; Barber, L.; Breen, M.; Kitchell, B.; McNeil, E.; Modiano, J.F.; Niemi, S.; Comstock, K.E.; Ostrander, E.; Westmoreland, S.; Withrow, S. The dog as a cancer model. *Nat. Biotechnol.* **2006**, 24(9), 1065-1066.
- (7) Paoloni, M.; Khanna, C. Translation of new cancer treatments from pet dogs to humans. *Nat. Rev. Cancer* **2008**, 8(2), 147-156.
- (8) LeBlanc, A.K.; Breen, M.; Choyke, P.; Dewhist, M.; Fan, T.M.; Gustafson, D.L.; Helman, L.J.; Kastan, M.B.; Knapp, D.W.; Levin, W.J.; London, C.; Mason, N.; Mazcko, C.; Olson, P.N.; Page, R.; Teicher, B.A.; Thamm, D.H.; Trent, J.M.; Vail, D.M.; Khanna, C. Perspectives from man's best friend: National Academy of Medicine's Workshop on Comparative Oncology. *Sci, Transl. Med.* **2016**, 8(324), 324ps5.
- (9) Paoloni, M.; Davis, S.; Lana, S.; Withrow, S.; Sangiorgi, L.; Picci, P.; Hewitt, S.; Triche, T.; Meltzer, P.; Khanna, C. Canine tumor cross-species genomics uncovers targets linked to osteosarcoma progression. *BMC Genomics* **2009**, 10, 625.



- (10) Angstadt, A.Y.; Motsinger-Reif, A.; Thomas, R.; Kisseberth, W.C.; Guillermo Couto, C.; Duval, D.L.; Nielsen, D.M.; Modiano, J.F.; Breen, M. Characterization of canine osteosarcoma by array comparative genomic hybridization and RT-qPCR: signatures of genomic imbalance in canine osteosarcoma parallel the human counterpart. *Genes Chromosom. Cancer* **2011**, *50*(11), 859-874.
- (11) Breen, M.; Modiano, J.F. Evolutionarily conserved cytogenetic changes in hematological malignancies of dogs and humans-man and his best friend share more than companionship. *Chromosome Res.* **2008**, *16*(1), 145-154.
- (12) Wypij, J.M.; A naturally occurring feline model of head and neck squamous cell carcinoma. *Pathol. Res. Int.* **2013**, *2013*, 502197.
- (13) Supsavhad, W.; Dirksen, W.P.; Martin, C.K.; Rosol, T.J. Animal models of head and neck squamous cell carcinoma. *Vet. J.* **2016**, *210*, 7-16.
- (14) Bilgic, O.; Duda, L.; Sanchez, M.D.; Lewis, J.R. Feline oral squamous cell carcinoma: clinical manifestations and literature review. *J. Vet. Dent.* **2015**, *32*(1), 30-40.
- (15) Stebbins, K.E.; Morse, C.C.; Goldschmidt, M.H. Feline oral neoplasia: a ten-year survey. *Vet. Pathol.* **1989**, *26*(2), 121-128.
- (16) Kundu, S.K.; Nestor, M. Targeted therapy in head and neck cancer. *Tumour. Biol.* **2012**, *33*(3), 707-721.
- (17) Parkinson, E.I.; Hergenrother, P.J. Deoxyxyboquinones as NQO1-activated cancer therapeutics. *Acc. Chem. Res.* **2015**, *48*(10), 2715-2723.
- (18) Parkinson, E.I.; Bair, J.S.; Cismesia, M.; Hergenrother, P.J. Efficient NQO1 substrates are potent and selective anticancer agents. *ACS. Chem. Biol.* **2013**, *8*, 2173-2183.

- (19) Parkinson, E.I.; Hergenrother, P.J. Runaway ROS as a selective anticancer strategy. *Chem. Med. Chem.* **2011**, *6*(11), 1957-1959.
- (20) Huang, X.; Dong, Y.; Bey, E.A.; Kilgore, J.A.; Bair, J.S.; Li, L.S.; Patel, M.; Parkinson, E.I.; Wang, Y.; Williams, N.S.; Gao, J.; Hergenrother, P.J.; Boothman, D.A. An NQO1 substrate with potent antitumor activity that selectively kills by PARP1-induced programmed necrosis. *Cancer Res.* **2012**, *72*(12), 3038-3047.
- (21) Yang, Y. Zhang, Y.; Wu, Q.; Cui, X.; Lin, Z.; Liu, S.; Chen, L. Clinical implications of high NQO1 expression in breast cancers. *J. Exp. Clin. Cancer Res.* **2014**, *33*, 14.
- (22) Lin, L.; Quin, Y.; Jin, T.; Liu, S.; Zhang, S.; Shen, X.; Lin, Z. Significance of NQO1 overexpression for prognostic evaluation of gastric adenocarcinoma. *Exp. Mol. Pathol.* **2014**, *96*(2), 200-205.
- (23) Cui, X.; Jin, T.; Wang, X.; Jin, G.; Li, Z.; Lin, L. NAD(P)H:quinone oxidoreductase-1 overexpression predicts poor prognosis in small cell lung cancer. *Oncol. Rep.* **2014**, *32*(6), 2589-2595.
- (24) Li, L.S.; Reddy, S.; Lin, Z.H.; Liu, S.; Park, H.; Chun, S.G.; Bornmann, W.G.; Thibodeaux, J.; Yan, J.; Chakrabarti, G.; Xie, X.J.; Sumer, B.D.; Boothman, D.A.; Yordy, J/S. NQO1-mediated tumor-selective lethality and radiosensitization for head and neck cancer. *Mol. Cancer. Ther.* **2016**, *15*(7), 1757-1767.
- (25) Ma, Y.; Kong, J.; Yan, G.; Ren, X.; Jin, D.; Jin, T.; Lin, L.; Lin, Z. NQO1 overexpression is associated with poor prognosis in small cell lung cancer. *BMC Cancer*, **2014**, *14*, 414.
- (26) Bey, E.A.; Bentle, M.S.; Reinicke, K.E.; Dong, Y.; Yang, C.R.; Girard, L.; Minna, J.D.; Bornmann, W.G.; Gao, J.; Boothman, D.A. An NQO1- and PARP-1-mediated cell death

pathway induced in non-small-cell lung cancer cells by beta-lapachone. *Proc. Natl. Acad. Sci. U.S.A.* **2007**, *104*(28), 11832-11837.

(27) Li, L.S.; Bey, E.A.; Dong, Y.; Meng, J.; Patra, B.; Yan, J.; Xie, X.J.; Brekken, R.A.; Barnett, C.C.; Bornmann, W.G.; Gao, J.; Boothman, D.A. Modulating endogenous NQO1 levels identifies key regulatory mechanisms of action of beta-lapachone for pancreatic cancer therapy. *Clin. Cancer Res.* **2011**, *17*(2), 275-285.

(28) Hill, A.S.; O'Neill, S.; Rogers, Q.R.; Christopher, M.M. Antioxidant prevention of Heinz body formation and oxidative injury in cats. *Am. J. Vet. Res.* **2001**, *62*(3), 370-374.

(29) Park, H.J.; Ahn, K.; Ahn, S.; Choi, E.; Lee, S. W.; Williams, D.; Kin, E.J.; Griffin, R.; Bey, E.A.; Bornmann, W.G.; Gao, J.; Park, H.J.; Boothman, D.A.; Song, C.S. Susceptibility of cancer cells to beta-lapachone is enhanced by ionizing radiation. *Int. J. Radiat. Oncol. Biol. Phys.* **2005**, *61*(1), 212-219.

(30) Suzuki, M.; Amano, M.; Choi, J.; Park, H.J.; Williams, B.W.; Ono, K.; Song, C.W. Synergistic effects of radiation and beta-lapachone in DU-145 human prostate cancer cells in vitro. *Radiat. Res.* **2006**, *165*(5), 525-531.

(31) Choi, E.K.; Terai, K.; Ji, I.M.; Kook, Y.H.; Park, K.H.; Oh, E.T.; Griffin, R.J.; Lim, B.U.; Kim, J.; Lee, D.S.; Boothman, D.A.; Loren, M.; Song, C.W.; Park, H.J. Upregulation of NAD(P)H:quinone oxidoreductase by radiation potentiates the effect of bioreductive beta-lapachone on cancer cells. *Neoplasia* **2007**, *9*, 643-642.

(32) Begleiter, A.; Leith, M.K.; Thliveris, J.A.; Digby, T. Dietary induction of NQO1 increases the antitumor activity of mitomycin C in human colon tumors in vivo. *Br. J. Cancer* **2004**, *91*, 1624-1631.

- (33) Park, H.J.; Choi, E.K.; Choi, J.; Ahn, K.J.; Kim, E.J.; Ji, I.M.; Kook, Y.H.; Ahn, S.D.; Williams, B.; Griffin, R.; Boothman, D.A.; Lee, C.K.; Song, C.W. Heat—induced up-regulation of NAD(P)H:quinone oxidoreductase potentiates anticancer effects of beta-lapachone. *Clin. Cancer Res.* **2005**, *11*(24), 8866-8871.
- (34) Song, C.W.; Chae, J.J.; Choi, E.K.; Hwang, T.S.; Kim, C.; Lim, B.U.; Park, H.J. Anti-cancer effect of bio-reductive drug beta-lapachon is enhanced by activating NQO1 with heat shock. *Int. J. Hyperthermia* **2008**, *24*, 161-169.
- (35) Terai, K.; Dong, G.; Oh, E.; Park, M.; Gu, Y.; Song, C.W.; Park, H.J. Cisplatin enhances the anticancer effect of beta-lapachone by upregulating NQO1. *Anti-Cancer Drugs* **2009**, *20*, 901-909.
- (36) Court, M.H. Feline drug metabolism and disposition: pharmacokinetic evidence for species differences and molecular mechanisms. *Vet. Clin. North Am. Small Anim. Pract.* **2013**, *43*(5), 1039-1054.
- (37) Booth, D.M. Drug therapy in cats: mechanisms and avoidance of adverse drug reactions. *J. Am. Vet. Med. Assoc.* **1990**, *196*(8), 1297-1305.
- (38) Vichai, V.; Kirtikara, K. Sulforhodamine B colorimetric assay for cytotoxicity screening. *Nat. Protoc.* **2006**, *1*, 1112-1116.

## Chapter 3. Enhancing the therapeutic window of IB-DNQ

### 3.1. The prodrug approach

Prodrugs are a common strategy in drug development as approximately 10% of all drug products are prodrugs.<sup>1</sup> As of 2009 15% of the top selling pharmaceutical products were prodrugs<sup>2</sup> further highlighting the usefulness and commercial appeal to these compounds. The concept of prodrugs is rather straight forward: First, a drug molecule is unable to access its target or exert its cytotoxic effect due to an obstacle present either inherently to the molecule itself or as a result of biology. These obstacles are anything that prevents or limits the usefulness of a drug molecule and often are classified into four broad categories:<sup>3-7</sup> (1) Pharmaceutical: insufficient chemical stability, poor aqueous solubility, offensive taste/odor, irritation or pain; (2) Pharmacokinetic: poor bioavailability, unfavorable distribution, short duration of action, or marked presystemic metabolism; (3) Pharmacodynamic: inadequate site specificity or toxicity; and (4) Economical: patent life expiration. In order to overcome or circumvent these obstacles, the drug is appended with certain functionalities, called the promoiety. The promoiety allows successful crossing of the obstacle and is then cleaved through either enzymatic and/or chemical biotransformations releasing the active drug molecule. The drug molecule now at its particular target and free of any inactivating modification can exert its cytotoxic action. This prodrug strategy is summarized in Fig 3.1.

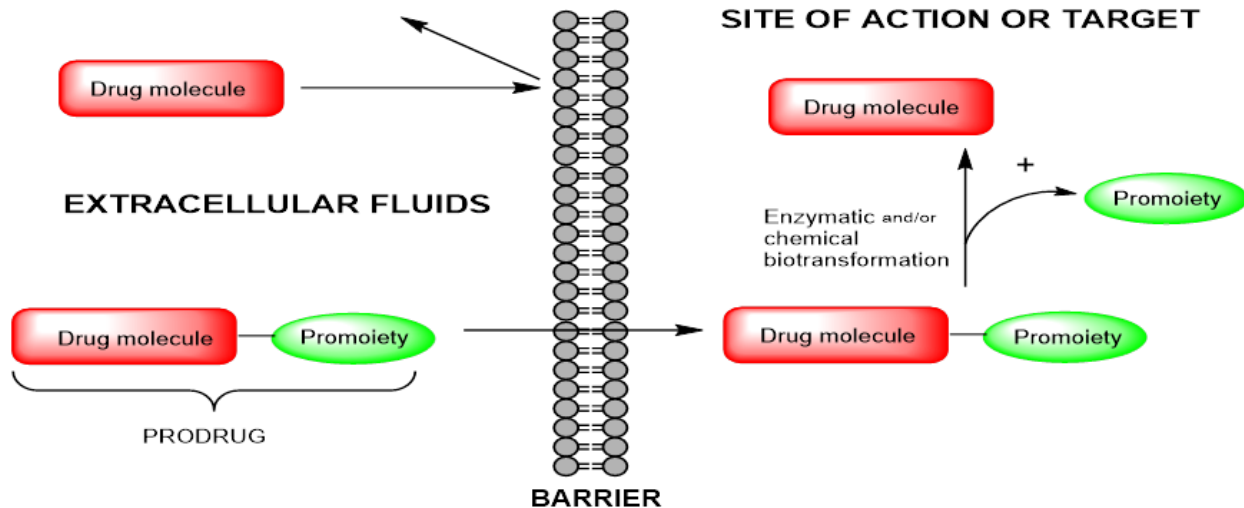


**Figure 3.1.** Schematic of the concept of prodrugs.

DNQ possesses the inherent pharmaceutical obstacle of poor aqueous solubility, something that was overcome, in part, with second generation derivatives including IB-DNQ. These derivatives possess additional steric bulk at the *N*-methyl position which likely disrupts intramolecular  $\pi$ - $\pi$  stacking interactions resulting in enhanced aqueous solubility.<sup>8-10</sup> While this improved solubility is satisfactory for in vitro cell and small animal in vivo experiments, in thinking about future translation into larger animals and perhaps humans, this solubility could become a significant obstacle. Also the pharmacodynamic obstacle of toxicity is a concern going further. In felines the dose administered is the same as the MTD making for a very narrow therapeutic window and a prodrug that masks the toxicity of the molecule could effectively open this window more widely.

Addressing the obstacle of aqueous solubility, the most common strategy is through the addition of a phosphate group to the drug molecule.<sup>11-15</sup> These prodrugs typically have good stability in the promoiety phosphate to the drug molecule, only undergoing bioconversion

through the action of alkaline phosphatases. This selective bioconversion allows for predictable behavior of the prodrug.<sup>14-17</sup> The appending of a phosphate group on the scaffold of IB-DNQ should be a good strategy for improving the aqueous solubility of the molecule to increase dose as well as help in formulation.

The pharmacokinetic obstacle of toxicity is more challenging as the mediators of the off target effects are still not clear. Due to the mechanism of action of DNQ and IB-DNQ and the low expression of NQO1 outside of the tumor, the prevailing hypothesis is that the adverse effects are mediated through the action of one-electron and other two-electron reductases.<sup>18</sup> Therefore a prodrug strategy in which the quinone portion of the molecule (the portion responsible for reduction and ROS generation) is masked by a promoiety should aid in reducing any non-NQO1-mediated ROS generation. Nearly half of all prodrugs make use of an ester promoiety<sup>6,17</sup> and this strategy has been used previously in conjunction with the NQO1 substrate  $\beta$ -lapachone.<sup>21-23</sup> In this case the active ortho-quinone when masked with an ester functionality, led to a 3.5-fold increase in MTD.<sup>21</sup> Given the similarities between the mechanism of  $\beta$ -lapachone and IB-DNQ, masking the para-quinone through similar functionality would be expected to provide similar results.

### **3.1.1. Phosphate prodrug**

Based on the structure and available functional groups of IB-DNQ, it was determined that there were three potential sites amenable to addition of a phosphate promoiety. First, a phosphate could theoretically be introduced on the secondary nitrogen of the  $\delta$ -lactam ring through a oxymethylene spacer (Fig 3.2). This strategy has been used elsewhere<sup>24-28</sup> and after cleavage of the phosphate through the action of alkaline phosphatases, formaldehyde would be

spontaneously released to provide the active drug molecule (Fig. 3.2). The second site is that of either amide carbonyl, which likely could be reduced and then conjugated with a phosphate moiety. The last site deemed amenable to addition of a phosphate functionality was that of the para-quinone. Reduction of the quinone to the hydroquinone and subsequent conjugation with phosphorylating agents, in theory would produce a prodrug that not only possessed greater aqueous solubility due to addition of a phosphate, but would also mask the active component of the molecule to prevent processing by off target enzymes. This potential dual benefit prioritized this site for phosphate prodrug synthesis.

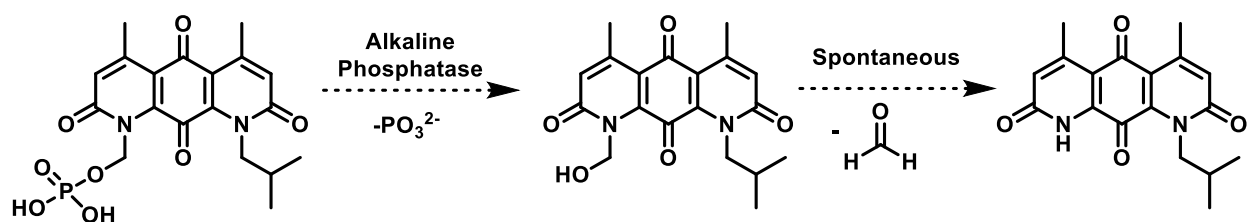
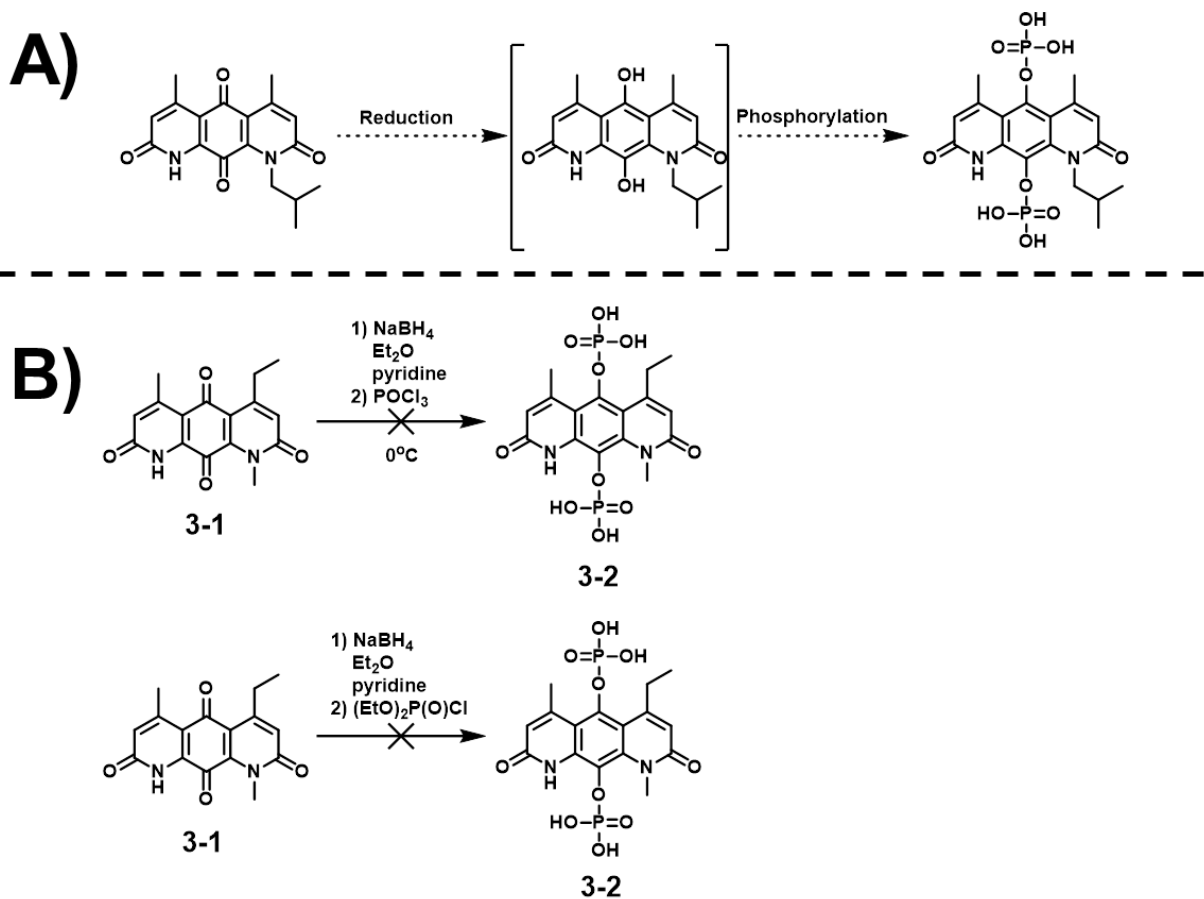


**Figure 3.2.** Rationale of N-oxymethylene phosphate prodrug of IB-DNQ.

In order to synthesize the phosphate masked quinone, it was thought that this could be accomplished via a reduction of the quinone to the hydroquinone and upon reduction the hydroquinone could be phosphorylated with a protected phosphate molecule and upon deprotection the desired prodrug would be obtained (Scheme 3.1). Due to the instability of the hydroquinone in the presence of oxygen, isolation of the hydroquinone did not seem trivial and necessitated that the reduction and phosphorylation be done in one pot. This strategy was applied to compound **3-1**, a DNQ derivative in which the  $\beta$ -methyl group of the tertiary  $\delta$ -lactam ring has been substituted for an ethyl group. Immediate addition of sodium borohydride to **3-1** resulted in the solvent changing from red to deep purple and within 15 min starting material had nearly been completely converted as judged from LCMS. Attempting to trap the hydroquinone with either  $\text{POCl}_3$  or diethyl chlorophosphate was unsuccessful and starting material was recovered. Even in



the presence of a large excess of phosphate (100 equivalents) no observable product was seen. It appears that the para-quinone of IB-DNQ can undergo reduction to the hydroquinone, but that introduction of the smallest amount of oxygen, possibly through co-addition with the phosphorylating agent, allows the re-oxidation to the quinones species and this reoxidation reaction is much more rapid than the phosphorylation reaction.



**Scheme 3.1.** Synthesis of masked quinone phosphate prodrugs. (a) Envisioned steps in synthesizing phosphate prodrug (b) failed attempts in attempting to produce the envisioned phosphate prodrug.

### 3.1.2. Developing a suitable model system

#### 3.1.2.1. Synthesis of quinolonedione model system

From the initial investigations on phosphate prodrugs it appeared that it would not be as straight forward to synthesize these compounds as previously anticipated therefore, a model system was desired to test initial reaction conditions to not waste the more valuable derivatives. The 5,8-quinolonedione scaffold presented itself as a useful surrogate for attempting to understand the chemistry of IB-DNQ as it possesses similar functionality in the para-quinone and adjacent lactam ring (Fig 3.3). In fact this system is as if **IB-DNQ** was separated into two halves, and provides a unique opportunity to understand the reactivity of the two halves of the molecule independently.

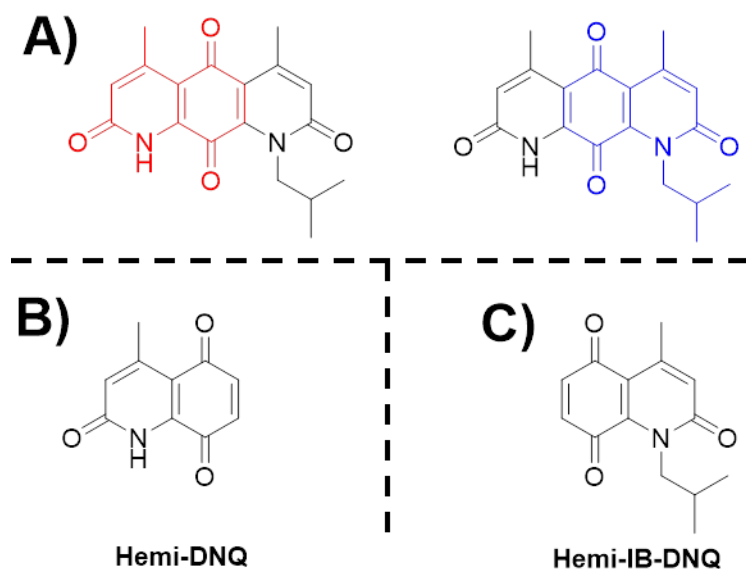
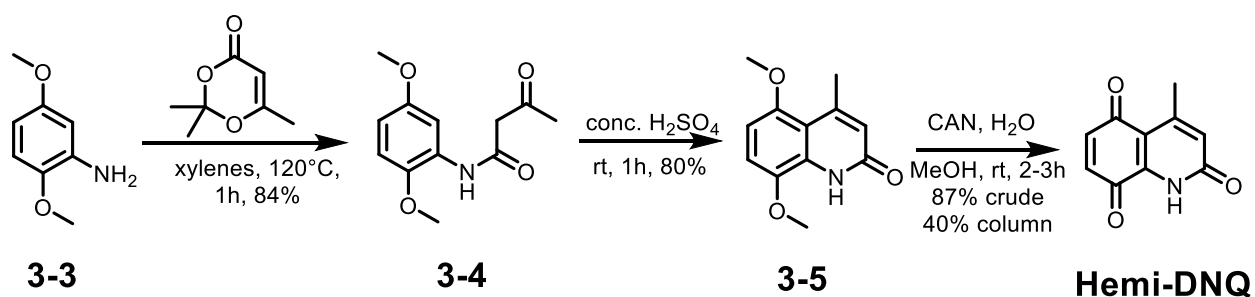


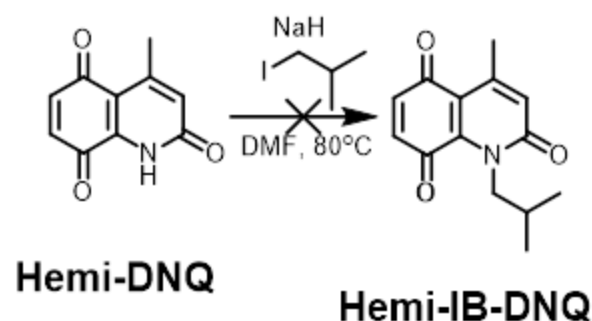
**Figure 3.3.** Model systems for IB-DNQ prodrugs. (a) highlighted in red and blue are the proposed breakdowns of the IB-DNQ scaffold that are of interest to study in this model system (b) the compound composed of the para-quinone and the unsubstituted N-methyl ring will be referred to as Hemi-DNQ while (c) Hemi-IB-DNQ refers to the compound comprised of the para-quinone and the N-isobutyl ring.

A previously reported synthesis of derivatives of this system provided a useful guideline for synthesizing these compounds<sup>29,30</sup> (Scheme 3.2). 2,5-dimethoxyaniline (compound **3-3**) was dissolved in xylenes and treated with 2,2,6-trimethyl-4*H*-1,3-dioxin-4-one with heat to yield 2,5-dimethoxyacetoacetanilide (compound **3-4**) in 84% yield. Knorr cyclization of compound **3-4** provided the quinolone compound **3-5** in 80% yield. Finally oxidation of **3-5** with ceric ammonium nitrate (CAN) produced the desired quinolonedione, **Hemi-DNQ**, in 87% crude yield.



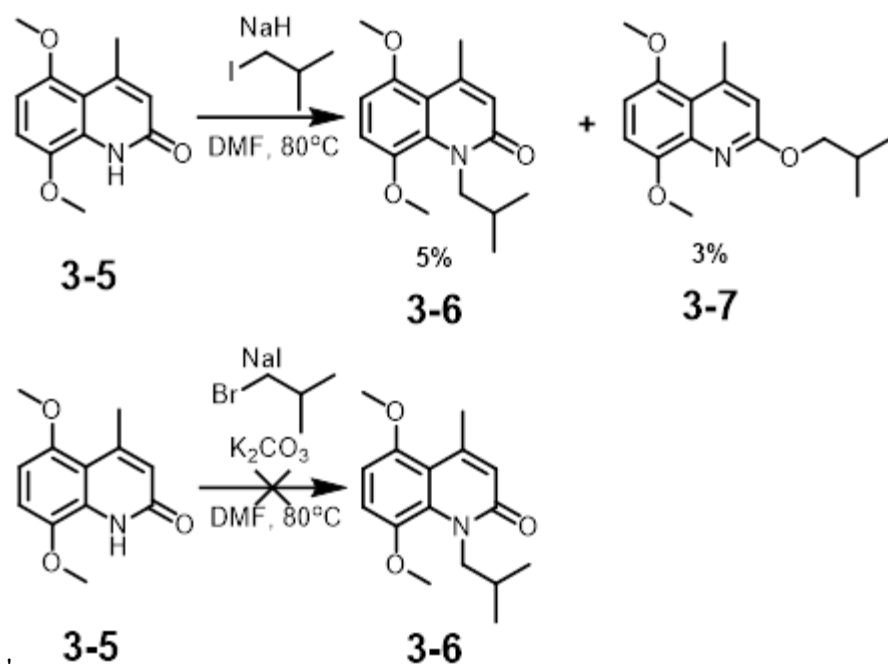
**Scheme 3.2.** Synthetic route to Hemi-DNQ.

From **Hemi-DNQ**, it was envisioned that a late stage alkylation of the  $\delta$ -lactam nitrogen would be able to yield **Hemi-IB-DNQ**, the complementary half of the IB-DNQ molecule (Scheme 3.3). **Hemi-DNQ** was treated with sodium hydride under inert atmosphere for 15 min before the addition of 1-iodo-2-methylpropane. Upon workup; no desired product could be isolated, only starting material was isolatable.



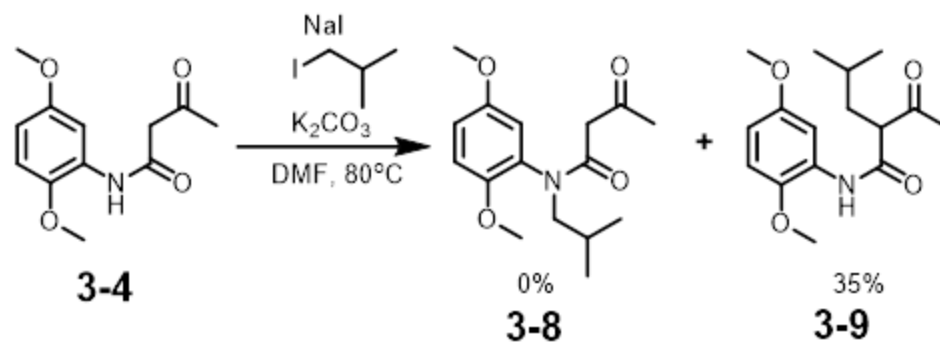
**Scheme 3.3.** Late stage functionalization for synthesis of Hemi-IB-DNQ.

The late stage functionalization on **Hemi-DNQ** seemed problematic as potential contamination could be preventing the reaction. Attempts to purify Hemi-DNQ through column chromatography led to the discovery that the molecule was unstable to silica and decomposition was observed. Rather than using the crude reaction mixture, it was thought that alkylation on the Knorr cyclized product, **3-5** might be more fruitful. The reaction conditions used in the attempted conversion of Hemi-DNQ to Hemi-IB-DNQ were then applied to **3-5**. The reaction was extended overnight and heated at 80°C and the desired product **3-6** was produced in 5% yield along with the 3% of side product **3-7**. The Knorr cyclization product was also subjected to sodium iodide, potassium carbonate and 1-Bromo-2-methylpropane overnight at elevated temperatures; however only starting material was recovered.



**Scheme 3.4.** Synthesis of Hemi-IB-DNQ through late stage alkylation of compound **3-5**.

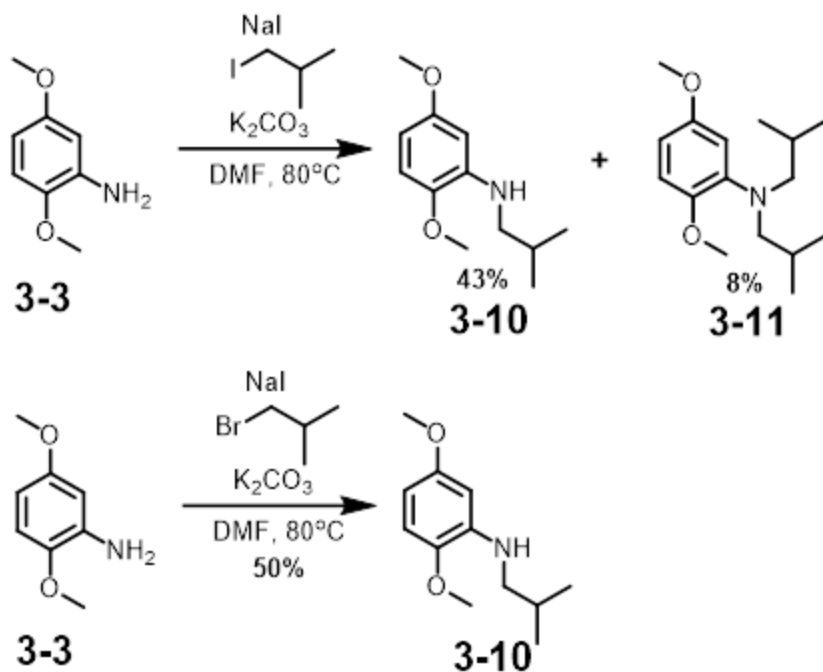
Due to the low yields and formation of side product in approximately equal yields in the alkylation of compound **3-5**, alkylation of compound **3-4** was pursued. The desired alkylation product **3-8** was not produced when **3-4** was stirred in the presence of sodium iodide, potassium carbonate and 1-iodo-2-methylpropane for 48h. Instead alkylation at the  $\alpha$ -carbon was observed. The increased acidity of this  $\alpha$ -proton makes it optimal for deprotonation by potassium carbonate which can then undergo substitution reaction with the alkyl halide biasing the reaction for **3-9** not **3-8**.



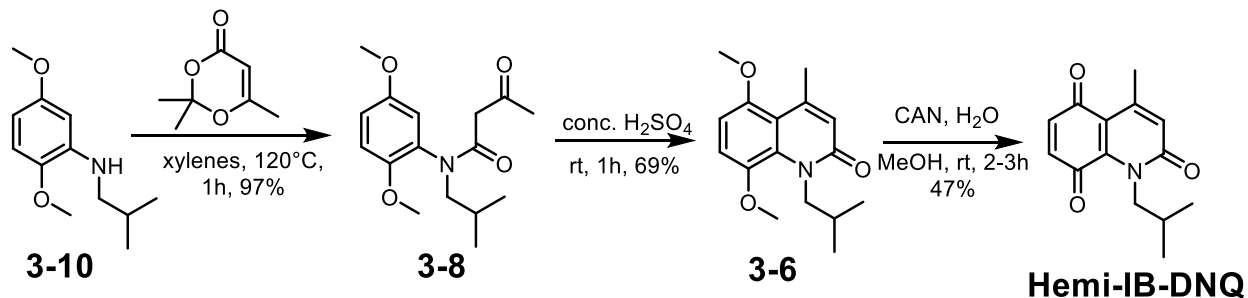
**Scheme 3.5.** Synthesis of tertiary amide **3-8**.

Late stage alkylation of the quinolonedione scaffold route proved uncooperative; therefore a strategy incorporating the alkylation from the onset was implemented (Scheme 3.6). The alkylating conditions of sodium iodide, potassium carbonate and 1-iodo-2-methylpropane used in previous attempts of late stage functionalization of the  $\delta$ -lactam nitrogen were applied to 2,5-dimethoxyaniline (**3-3**). The reaction yielded the desired compound **3-10** in 43% yield along with small amounts of the di-alkylated compound **3-11** (8%) and starting material. Substitution of 1-iodo-2-methylpropane for 1-bromo-2-methylpropane yielded compound **3-10** in 50% yield without observable quantities of the di-alkylation product **3-11**.

The synthetic scheme then proceeded as detailed for **Hemi-DNQ** (Scheme 3.7). Treatment of **3-10** with 2,2,6-trimethyl-4*H*-1,3-dioxin-4-one provided compound **3-8** in 97% yield. Knorr cyclization proceeded in 69% yield to yield compound **3-6** and CAN-mediated oxidation to **Hemi-IB-DNQ** proceeded in 47% yield and interestingly this compound was stable to column conditions.



**Scheme 3.6.** Synthetic route to alkyl substitution on aniline.



**Scheme 3.7.** Synthetic route to **Hemi-IB-DNQ**.

### 3.1.2.2. In vitro cytotoxicity of model compounds

With both model compounds in hand, it was of interest to see how well these compounds mimicked the potency of the parent compound. **Hemi-DNQ** and **Hemi-IB-DNQ** were evaluated head to head against IB-DNQ for cytotoxicity in A549 cells (Fig 3.4). The cytotoxicity of IB-DNQ ( $0.17 \pm 0.05 \mu\text{M}$ ) was significantly greater than either of the two model compounds ( $14.6 \pm$

5.0  $\mu\text{M}$  and  $7.5 \pm 1.0 \mu\text{M}$  for **Hemi-DNQ** and **Hemi-IB-DNQ**, respectively). Interestingly when coincubated with the NQO1 inhibitor dicoumarol, whereas dicoumarol provided protection from IB-DNQ-mediated cytotoxicity ( $2.9 \pm 0.5 \mu\text{M}$ ; 17-fold change), both compounds were equally cytotoxic in the presence of dicoumarol ( $9.6 \pm 0.7 \mu\text{M}$  and  $6.9 \pm 1.7 \mu\text{M}$  for **Hemi-DNQ** and **Hemi-IB-DNQ**). This suggest that these compounds are not substrates by NQO1 and likely exert their cytotoxicity through another mechanism.

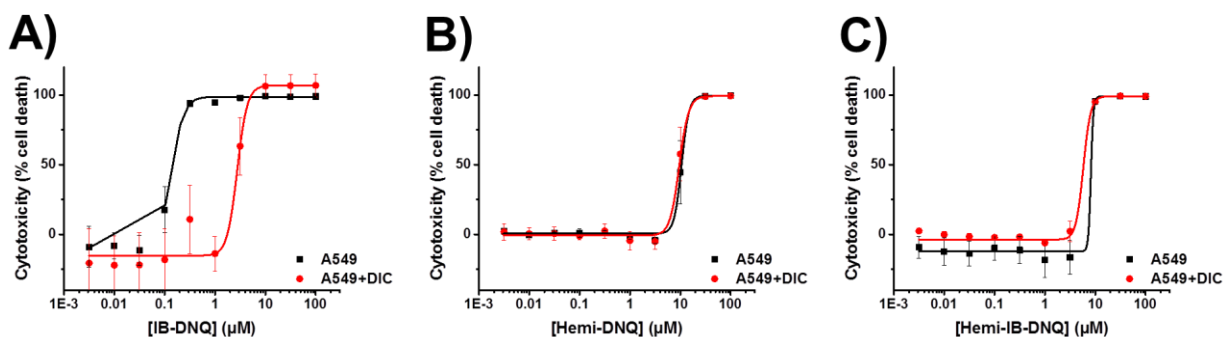
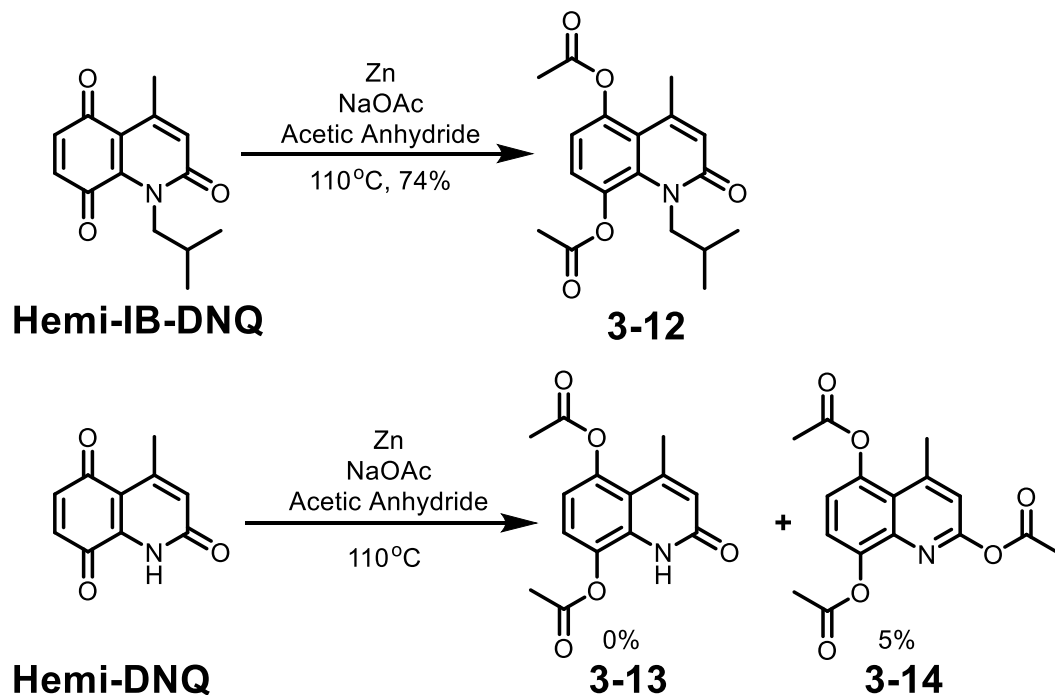


**Figure 3.4.** Dose-dependent cytotoxic effects of (a) **IB-DNQ** and model compounds (b) **Hemi-DNQ** and (c) **Hemi-IB-DNQ** in A549 cell lines, in the presence or absence of dicoumarol (25  $\mu\text{M}$ ). Increased susceptibility of A549 cell lines to **Hemi-DNQ** and **Hemi-IB-DNQ** in the presence of dicoumarol suggests these compounds are detoxified through the action of NQO1.

### 3.1.2.3. Esterification of model compound quinone

Next, the model quinolonedione compounds were subjected to reductive esterification reactions (Scheme 3.8), utilized in the synthesis of ester prodrug forms of  $\beta$ -lapachone.<sup>22</sup> The reaction with **Hemi-IB-DNQ** provided compound **3-12** in 74% yield. The reaction with **Hemi-DNQ**, however, did not provide the expected di-esterified product **3-13**, but instead a tri-esterified product, **3-14** in low yield  $\sim 5\%$ . The possibilities for the third ester site were either the oxygen of the amide carbonyl or the nitrogen of the carbonyl, but with a carbon chemical shift of 156.52 ppm, this is consistent with the esterification to the oxygen atom of the carbonyl not the nitrogen atom in the amide.





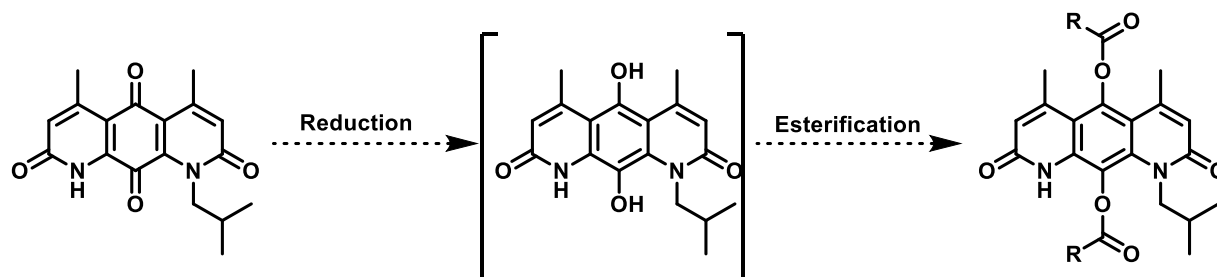
**Scheme 3.8.** Synthesis of esterified model compounds.

### 3.1.3. Ester prodrug

It is hypothesized that if the quinone in IB-DNQ could be masked through a promoiety, that the tolerability of IB-DNQ could be enhanced. In a compound with a similar mechanism of action, 2-electron reduction by NQO1 to induce redox cycling, an ester masking of the ortho-quinone of  $\beta$ -lapachone was able to increase the MTD by 3.5-fold.<sup>21</sup> Since the esters mask the portion of the molecule responsible for cytotoxic action, it is presumed that this prodrug form of  $\beta$ -lapachone would be processed less by more promiscuous reductases and is the reason for the improved MTD. This would suggest that if applied to IB-DNQ, similar improvements in MTD should be observed.

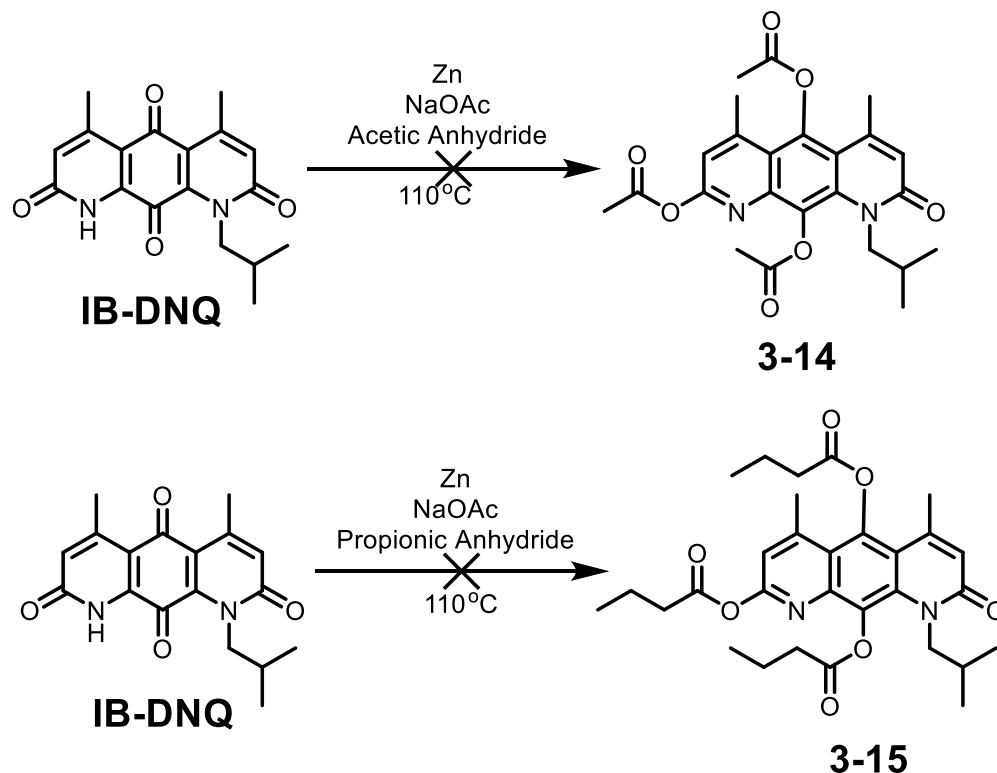
Previously phosphorylation of the quinone to create a masked quinone prodrug form of IB-DNQ was attempted and proved unsuccessful, likely because the phosphorylation reaction

was slower than reoxidation to the quinone. Given its success with  $\beta$ -lapachone, however, we were optimistic that the esterification reaction may occur more quickly and could be used to mask the quinone (Scheme 3.9).



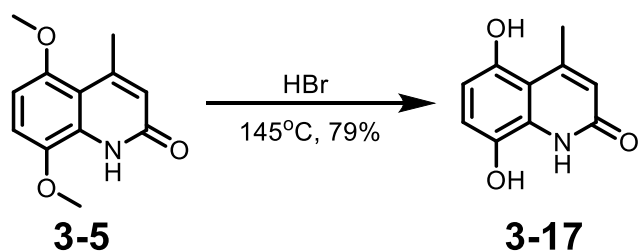
**Scheme 3.9.** Envisioned route to quinone-masked ester prodrug of IB-DNQ.

The esterification conditions used in the model compounds series were then applied to IB-DNQ. The reduction of the quinone was mediated by zinc dust and the acetic anhydride was provided in large excess in order to attempt to trap the hydroquinone as a di-ester. After 2 h the reaction had appeared complete, however upon workup and column chromatography the tri-esterified product **3-15** (predicted from studies of the model system esterification reactions) was not isolated. Likely the ester trapping of the hydroquinone was labile enough that the product was not observed. Trapping with propionic anhydride, was attempted under the assumption that the longer chain of the ester would render it more stable, but these conditions also did not provide the desired trimester prodrug **3-16**.



**Scheme 3.10.** Attempted synthesis of quinone-masked ester prodrug of IB-DNQ.

Compound **3-17** was able to be isolated as the hydroquinone following deprotection of **3-5** with concentrated HBr, and likely the success of esterification of the quinone in these model compounds is due to the enhanced stability of their hydroquinones whereas the intact IB-DNQ scaffold does not allow for sufficient time as the hydroquinone to undergo efficient esterification of the quinone. Cell culture experiments between IB-DNQ and model compounds seem to support this less stable hydroquinone hypothesis, as NQO1 could detoxify **Hemi-DNQ** and **Hemi-IB-DNQ** and not IB-DNQ, which would only result if the hydroquinone form of the model compounds were stable enough to undergo conjugation.



**Scheme 3.11.** Isolation of hydroquinone form of Hemi-DNQ.

## 3.2. DNQ derivatives

### 3.2.1. Novel DNQ derivatives

#### 3.2.1.1. SAR of DNQ

Previously work had been done to establish a correlation between NQO1 processing and cell culture toxicity using a panel of 25 DNQ derivatives and constitutes the entire known structure activity relationship of DNQ.<sup>8</sup> Primarily consisting of alkyl substitutions, modifications were made solely to the methyl position on the secondary  $\delta$ -lactam ring (blue circle), the methyl position on the tertiary  $\delta$ -lactam ring (green circle), the N-methyl position (red circle) or the unsubstituted nitrogen (yellow circle) or to a combination of 2, 3 or all of these sites (Fig, 3.5). Multiple substitutions at these four sites resulted in less efficient processing of the derivatives as compared to DNQ (up to 30-fold). Small substitutions at either  $\delta$ -lactam ring, such as a methyl to ethyl substitution, were tolerated, however the potency of these compounds were 10-fold lower. Longer chain, more sterically encumbering substitutions at these positions reduced the processing efficiency as well as potency of the derivatives. Substitution at the N-methyl position (red circle Fig 3.5) with longer and more bulky alkyl chains was largely tolerated without

significant reduction in either NQO1 processing or cellular potency.<sup>8</sup> These derivatives also tended to have improved MTDs in mice compared to DNQ.<sup>10</sup> However, as it stands currently, the SAR of DNQ has been limited to these few specific site manipulations that have been entirely composed of alkyl substitutions. Investigation into the SAR of other positions around the DNQ scaffold, as well as studying of the electronic effects of substituents on the processing and cytotoxicity of DNQ could provide new, interesting derivatives that may possess more favorable in vivo pharmacokinetics and tolerability.

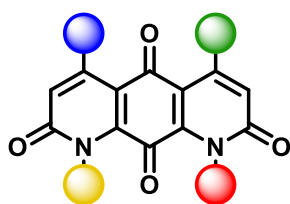


**Figure 3.5.** Structure activity relationship of DNQ scaffold.

### 3.2.1.2. Modeling evidence

The most obvious site for further investigation into the SAR of DNQ is that of the  $\alpha$ -carbon of the  $\delta$ -lactam ring. Computational modeling of molecules generated in silico with alkyl substitutions at this position suggested that modification at this position should minimally perturb NQO1 processing while perturbing to a greater extent processing by NADPH cytochrome P450 reductase (P450R), a one-electron reductase thought to be responsible for possible off target effects of DNQ (Fig. 3.6).<sup>18</sup> From the modeling data  $\alpha$ -carbon substitutions should lead to steric clashing of the derivative with the active site cofactors, which, upon resolving and adopting a minimal energy conformation, would place the quinone portion outside of the active site and lead to less efficient electron transfer (compounds **3-18**, **3-19**). Therefore it was hypothesized that these derivatives would have more selectivity for 2-electron reduction by

NQO1 over one-electron reduction by other reductases and that this selectivity would translate into more tolerability in vivo.

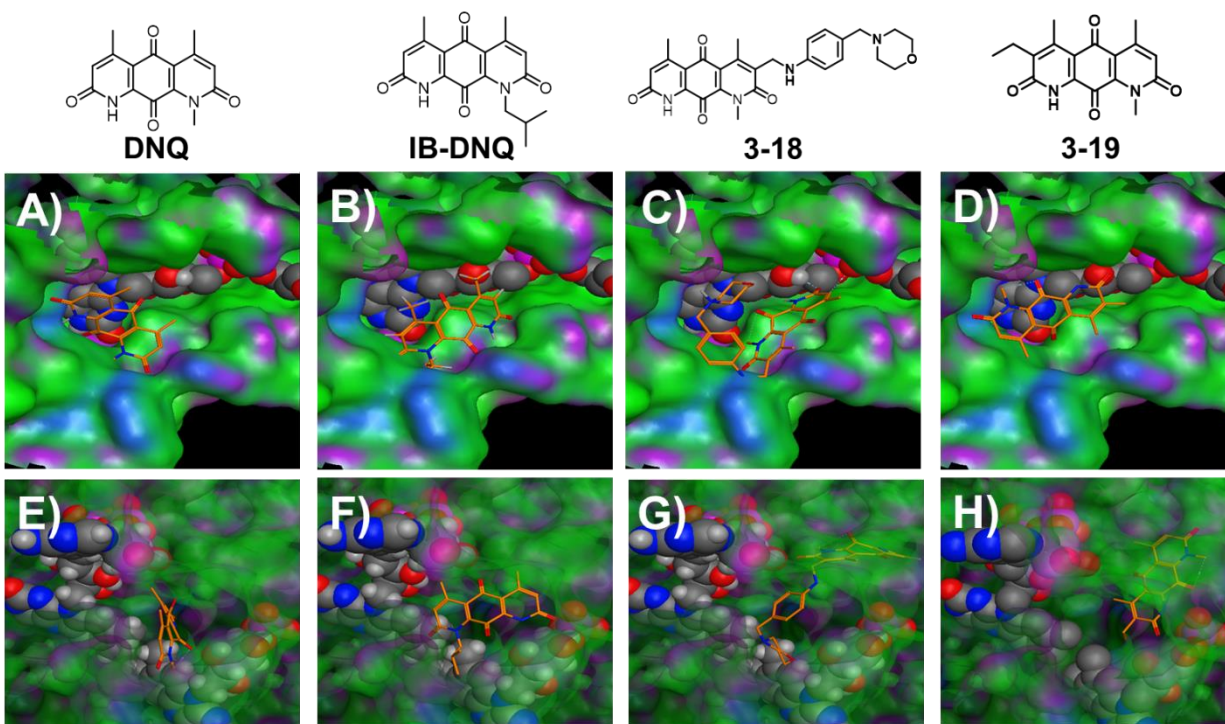
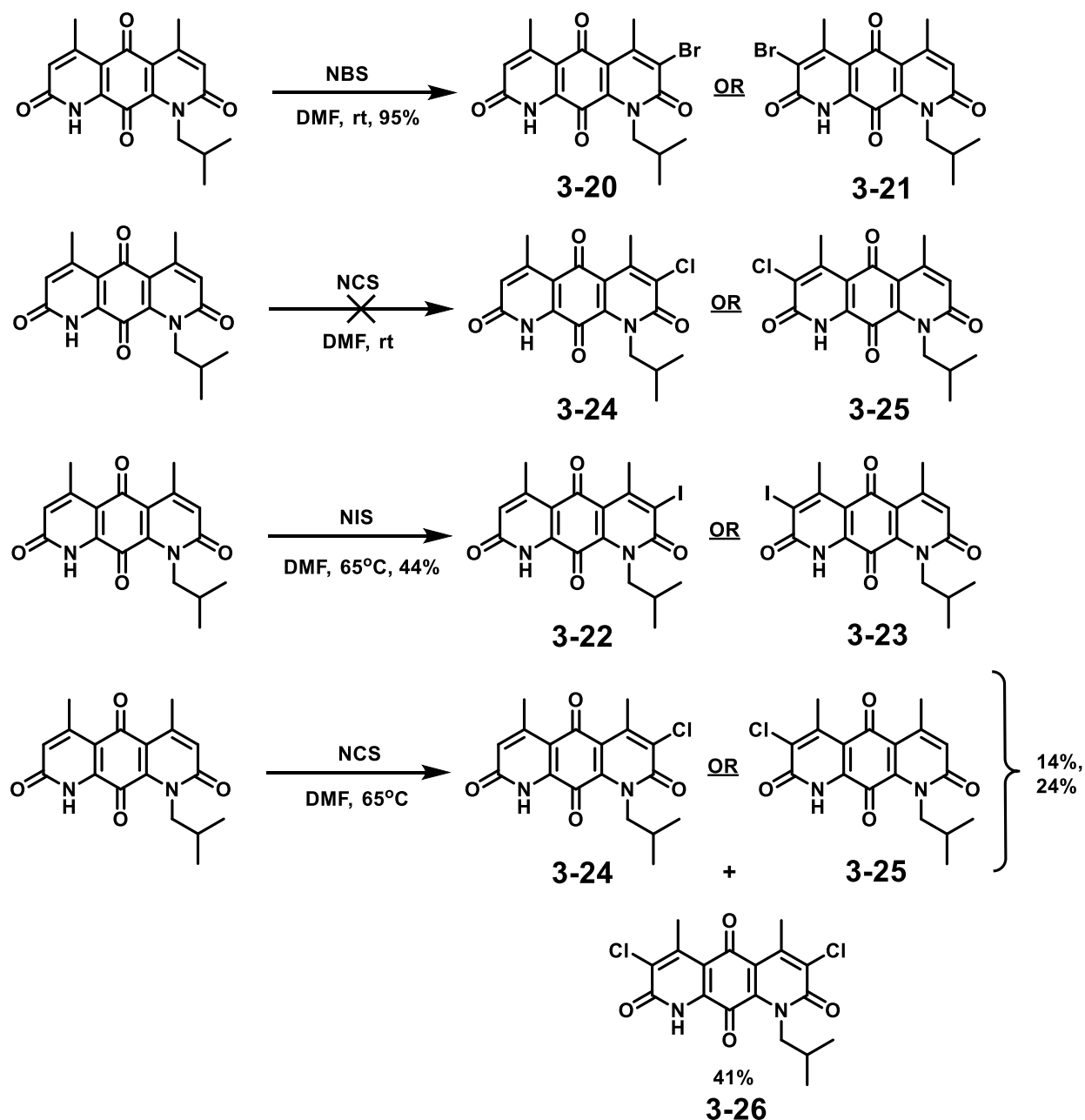


**Figure 3.6.** Computational modeling of DNQ, IB-DNQ and two novel molecules suggests that modification of the  $\alpha$ -carbon should not perturb NQO1 processing (**a-d**) while influencing to a greater extent one electron processing as modeled by P450R (**e-h**).

### 3.2.1.3. Synthesis

From the current synthesis of IB-DNQ it appeared challenging to synthesize an iodoamide cross coupling partner with substitution at the desired position, so a late stage functionalization strategy was adopted instead. It was hypothesized that if IB-DNQ could be halogenated at the position then this could facilitate a Suzuki-cross coupling reaction that would be able to be adaptable to a diverse set of cross coupling partners to create a vast set of derivatives. Addition of NBS to IB-DNQ overnight was able to produce a single brominated product **3-20** OR **3-21** in 95% yield. Since the location of the bromine and identity of which compound the product is has not been determined this compound will be referred to as **Br-IB-**

**DNQ**. Similarly the reaction with NIS afforded a single product **I-IB-DNQ** (either **3-22** or **3-23**), although mild heating was necessary, in 44% yield. The reaction with NCS yielded three products, two singly chlorinated (**3-24** and **3-25**) in 14% (**Cl<sub>a</sub>-IB-DNQ**) and 24% (**Cl<sub>b</sub>-IB-DNQ**) yield and one doubly chlorinated compound, **3-26** or **Cl<sub>2</sub>-IB-DNQ** (41%), that were separable by column chromatography. The iodinated and brominated IB-DNQ derivatives could serve as potential platforms for subsequent Suzuki coupling reactions.



**Scheme 3.12.** Synthesis of halogenated IB-DNQ derivatives.

#### 3.2.1.4. Cytotoxicity of Halo-IB-DNQ derivatives

The five halogenated IB-DNQ derivatives (**I-IB-DNQ**, **Br-IB-DNQ**, **Cl<sub>a</sub>-IBDNQ**, **Cl<sub>b</sub>-IBDNQ**, **Cl<sub>2</sub>-IBDNQ**) were selected to evaluate their abilities to induce cancer cell death in an



NQO1 expressing non-small cell lung carcinoma cell line (A549). Cells were exposed to a range of concentrations in both the presence and absence of NQO1 inhibitor ES936. Compared to the cytotoxicity of IB-DNQ ( $0.17 \pm 0.05 \mu\text{M}$ ) all five derivatives saw at least 40-fold decrease in potency (Table 3.1). Among the chlorinated derivative series there was an observable difference between the two mono-chlorinated compounds ( $7.9 \pm 1.4 \mu\text{M Cl}_b\text{-IB-DNQ}$  vs.  $13 \pm 1 \mu\text{M Cl}_a\text{-IB-DNQ}$ ) and an additional chlorine atom resulted in a drastic decrease in potency over both of the mono-chlorinated compounds. ES936 provided protection from cytotoxicity in all cases, indicating that these are still substrates for NQO1, able to be processed and undergo redox cycling. It may be that the electron-withdrawing nature of the halogen substituents is able to inductively pull electron density from the quinone core and as a result make it more difficult for NQO1 to mediate the two electron reduction to the hydroquinone. Alternatively the electron withdrawing nature may help to stabilize the molecule as the hydroquinone and the prolonged existence of the hydroquinone form would enable more conjugation and excretion from the cell leading to less efficient cytotoxic redox cycling. However, in this second case it might be expected that in the presence of NQO1 inhibitor these compounds would become more cytotoxic, which is in opposition to what is seen in cell culture. Therefore it is more likely that these compounds are less potent due to the more difficult reduction of the quinone and derivatives possessing either an alkyl or electron donating substituent in this position would be interesting candidate compounds to test this hypothesis.

An alternative explanation for the decrease in potency in the Halo-IB-DNQ derivatives could be that the molecule does not sterically tolerate any derivatization at this position. A decrease in potency does correlate with the atomic radius of the halogen, with the chlorinated derivative being most potent and having smallest atomic radius and the iodinated derivative

being least potent and having the largest atomic radius, with the brominated derivative somewhere in between. However, from the computational modeling experiment performed in Section 3.2.1.2 derivatization at this position should be tolerated and it is more likely that this decrease in potency relates to the electronic effects rather than any steric effects.

**Table 3.1.** Potency of Halo-IB-DNQ derivatives in A549 cells

Compound	IC <sub>50</sub> (μM)	IC <sub>50</sub> +ES936/DIC (μM)	Fold protection
IB-DNQ	0.17 ± 0.05	2.9 ± 0.5	17
Cl <sub>a</sub> -IB-DNQ	13 ± 1	48 ± 8	4
Cl <sub>b</sub> -IB-DNQ	7.9 ± 1.4	59 ± 15	7
Cl <sub>2</sub> -IB-DNQ	59 ± 9	> 100	> 1.7
Br-IB-DNQ	9.3 ± 0.3	48 ± 5	5
I-IBDNQ0	21 ± 4	65 ± 13	3

### 3.2.2. Revisiting previously synthesized derivatives

In previous work,<sup>8</sup> derivatives of DNQ had been synthesized according to a modular route to establish a correlation between NQO1 processing activity and in vitro cytotoxicity. A diverse set of 25 DNQ derivatives was created which led to the discovery of IB-DNQ. Due to the increased solubility over DNQ and better in vivo tolerability in mouse models (14 mg/kg vs 9 mg/kg), IB-DNQ proceeded as the molecule of choice. The progression into animal models larger than mice necessitated large amounts of compound and the relatively cheap price of isobutylamine made it more attractive than other derivatives. After observing the effectiveness in of IB-DNQ in feline OSCC patients, we wanted to take a step back and evaluate if IB-DNQ would in fact be the best compound to proceed forward with or if maybe there was a previously synthesized derivative that would have greater therapeutic potential.

In revisiting this set of 25 derivatives,<sup>10</sup> four derivatives were identified with improved MTD over IB-DNQ in mouse models: propyl-DNQ or **P-DNQ** (17 mg/kg), Isopentyl-DNQ or

**IP-DNQ** (15 mg/kg), neopentyl-DNQ (21 mg/kg) or **NP-DNQ** and 3,3-dimethylbutyl-DNQ (22 mg/kg) or **3,3-DMB-DNQ**. Furthermore, these derivatives possessed similar catalytic efficiencies and maintained similar potencies in breast cancer and lung cancer cell lines to IB-DNQ. (Fig. 3.7) Therefore these compounds were selected for synthesis and evaluation for potential improvements in pharmacokinetics and MTD over IB-DNQ, to help inform decision of which derivative to move forward with into the clinic.

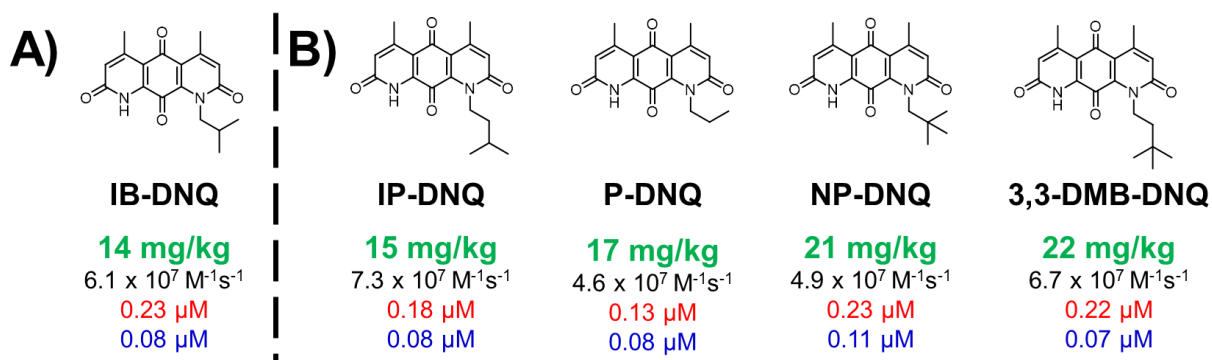


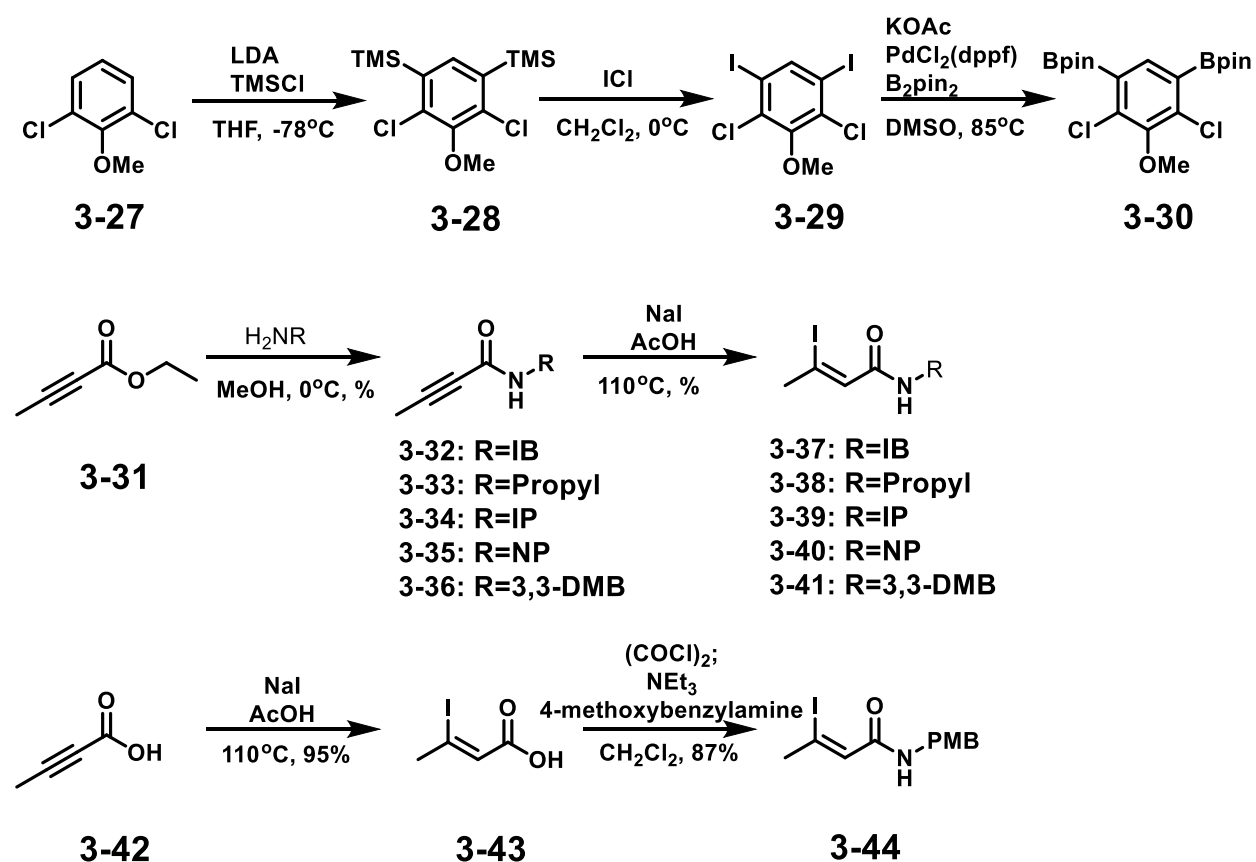
**Figure 3.7.** Properties of previously synthesized DNQ derivatives. (a) IB-DNQ (b) derivatives to be evaluated and compared to IB-DNQ. MTD (green), catalytic efficiency (black),  $\text{IC}_{50}$  against MCF-7 breast cancer cell line (red),  $\text{IC}_{50}$  against A549 cell line (blue) demonstrate the similarities and differences between IB-DNQ and potential derivatives.

### 3.2.2.1. Synthetic scheme

The synthesis of previous derivatives could be achieved by the previous synthetic route<sup>8,31</sup> (Schemes 3.13 and 3.14). From 2,6-dichloroanisole (**3-27**), deprotonation with lithium disopropylamide (LDA) and quenching with trimethylsilyl chloride provided selective silylation at the 3- and 5-positions of the anisole (**3-28**). Iododesilylation was then carried out on **3-28** through the action of iodine monochloride at 0°C to produce **3-29**. Subjection of **3-29** to Miyaura borylation conditions provided the cross-coupling partner **3-30** in yields in line with previous reports.<sup>31</sup>

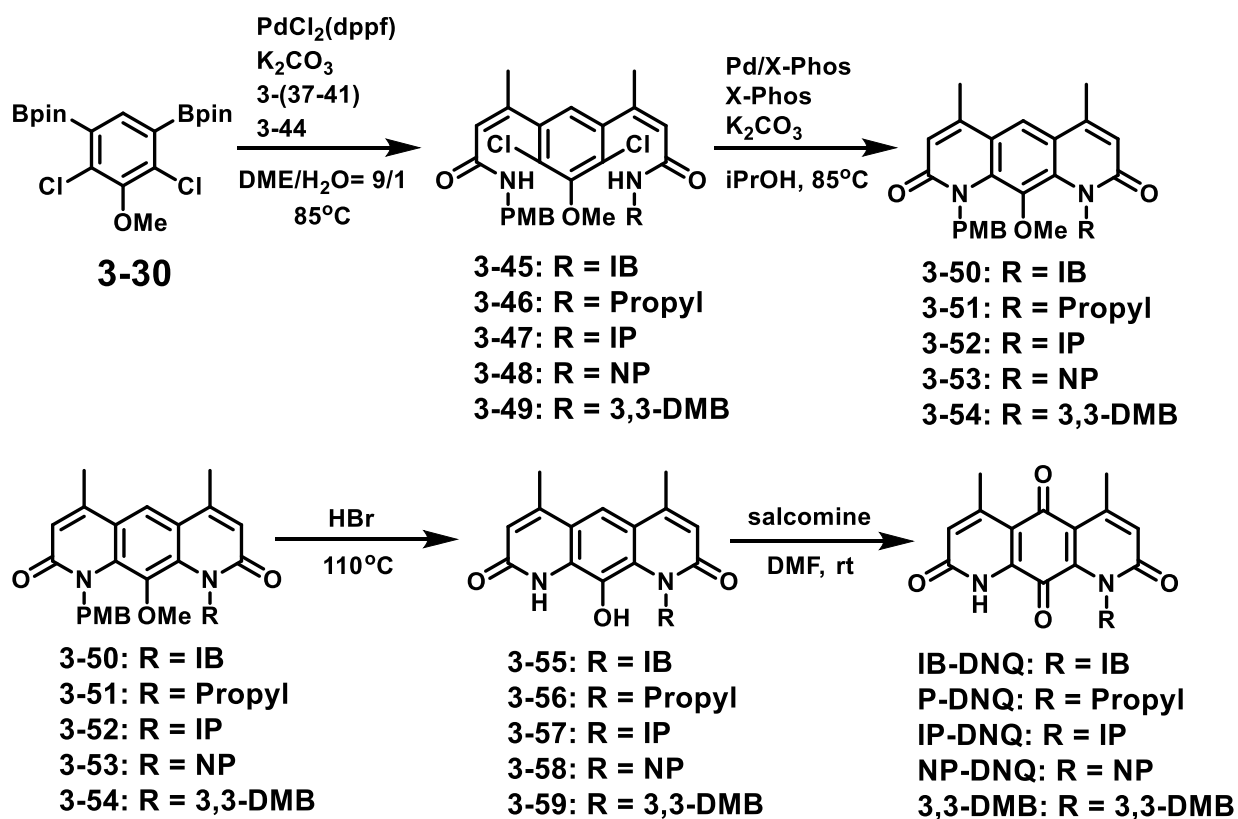
The alkyl-iodoamide coupling partner was synthesized via an amide coupling of ethyl 2-butynoate (**3-31**) and the desired alkyl amine and through the action of sodium iodide in acetic acid was converted to the (*Z*)-iodoolefin.

Due to the lability of the para-methoxybenzyl (PMB) group under acidic conditions, the PMB-iodoamide coupling partner was synthesized from 2-butynoic acid (**3-42**) first through the action of sodium iodide and acetic acid to produce the (*Z*)-iodoolefin carboxylic acid, **3-43**, and then through the conversion of the carboxylic acid to the PMB-amide, **3-44**, in two steps via an acyl chloride intermediate.



**Scheme 3.13.** Synthesis of cross coupling partners. (top) center piece, (middle) alkyl iodoamides, and (bottom) PMB-amide.

Both the alkyl-iodoamide (**3-37-41**) and PMB-iodoamide, **3-44**, were utilized in a mixed Suzuki cross coupling reaction with coupling partner **3-30**. After purification via flash chromatography to isolate the desired product, a Buchwald-Hartwig amidation was performed to form the tricyclic ring system. Reflux in concentrated HBr yielded the deprotected monophenol. The monophenol was subjected to salcomine-catalyzed oxidation in the presence of oxygen atmosphere to produce desired DNQ derivatives (Scheme 3.14).



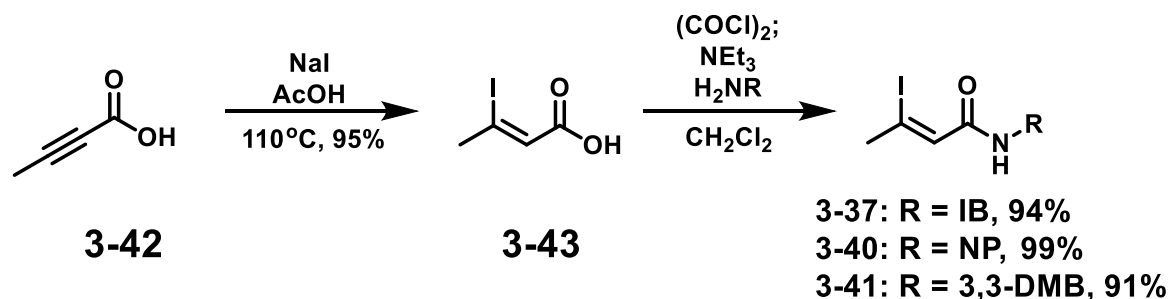
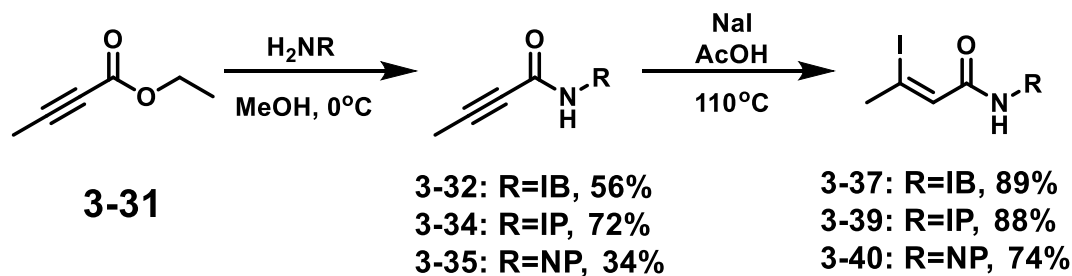
**Scheme 3.14.** General synthesis of DNQ derivatives from cross coupling partners.

Application of this scheme was able to produce IB-DNQ, IP-DNQ and P-DNQ in useful amounts for clinical experiments; however NP-DNQ was much more difficult. It became apparent that there were two steps in the reaction scheme that could be altered to increase

productivity, the first being the amine coupling reaction with ethyl 2-butynoate and the second being the final salcomine-mediated oxidation reaction.

While the amine coupling produces isopentylamine and isobutylamine derived products in 72% and 56% yield, the coupling with neopentylamine is less efficient (34% yield). Due to the cost associated with these more sterically encumbered amines and also the lower quantity available to utilize in the synthetic scheme, a more efficient way of synthesizing these iodoamides was necessary. The steric bulk of the amine likely causes a sluggish reaction, therefore it was thought that conversion of the ester to a more reactive carbonyl may facilitate the speed of the reaction and lead to improved yields. Such a route is implemented in the synthesis of PMB-iodoamide, necessary due to the sensitivity of the PMB group to acidic conditions, in which the carboxylic acid is converted to an acyl chloride before undergoing reaction with amine. Since this route is used due to the PMB group's sensitivity to the conditions of the iodination reaction, we saw no reason why this could not be applied to synthesis of the alkyl iodoamides as well.

Conversion of **3-42** to the **3-43** through sodium iodide and acetic acid produced the **3-43** in 95% yield. This compound was then converted to the corresponding acyl chloride through the action of oxalyl chloride and then in the same pot, in the presence of triethylamine, the desired alkyl amine was added. The yield for the sterically encumbered neopentylamine was nearly quantitative (99% yield) and high yields were also obtained for the other alkyl amines: 3,3-dimethylbutylamine 91%, isobutylamine 94%. Comparison of the two steps yields of the old route and this modified route increased 50% to 89% for **3-37** and 27% to 94% for **3-40**.



**Scheme 3.15.** Comparison of old and modified routes for synthesizing alkyl-iodo-amides for cross coupling reactions.

With no longer limiting amounts of iodoamides, attention was turned to the oxidation step of the reaction scheme. Yields for these derivatives ranged anywhere from 15 to 30% and these low yields were limiting the production of the larger quantities of alternative DNQ derivatives necessary for clinical experiments. Four hypotheses were developed in an attempt to explain the low yield in this reaction. The first was that excess salt in the phenol starting material may be inflating starting material mass leading to artificially low yields. Therefore the product was suspended in DI water, sonicated to remove salts, centrifuged and filtered to yield “purified” starting material. However this did not appear to be a significant contributor as the yield of **IB-DNQ** only increased from 15% to 23% when using “purified” compound.

Since the phenol compound is extremely insoluble, the second hypothesis was that not all of the starting material is going into solution to allow for the transformation. Testing this

hypothesis, the phenol was heated until the solution was clear to create a supersaturated solution before being subjected to the normal reaction conditions. Unfortunately no change in the yield of the reaction was observed with this modification, eliminating it as a potential contributor to the low reaction yields.

A third hypothesis was that the oxygen was not sufficiently available to induce oxidation of the compound. As the reaction typically is set up so that the flask is kept under an oxygen atmosphere by placing a balloon full of O<sub>2</sub> over the opening of the flask, the oxygen may only be present at the solution-atmosphere interface. To enhance contact with oxygen, O<sub>2</sub> was bubbled into the solution instead of just presenting an oxygen atmosphere. Implementing this change into the reaction protocol increased the yield of the oxidation reaction of **IB-DNQ** from 15% to 30%.

The last hypothesis was that over the time frame of the reaction, the salcomine catalyst was undergoing deactivation and that this deactivation was no longer allowing for conversion of starting material to product. Deactivation of salcomine had previously been reported in a study looking at the oxidation of monophenols to quinones.<sup>32</sup> To compensate for any deactivation, additions of 6 mol% catalyst were added to the solution every three hours for up to three additions. The resulting yield of the reaction increased from 15% to 40%. A further bump in yield (40 to 49%) was observed when combining the O<sub>2</sub> and catalyst modifications.

#### **3.2.2.2. Pharmacokinetics of derivatives**

Pharmacokinetics were derived from 4 healthy research cats, following single-dose, IV administration at 2.0 mg/kg of **P-DNQ**, **IP-DNQ** and **NP-DNQ**; average peak plasma concentration levels were 6270.5 ± 685.2 ng/mL (20.1 ± 2.2 μM), 2535.1 ± 614.8 ng/mL (7.4 ± 1.8 μM), and 3992.5 ng/mL ± 1873.9 (11.7 ± 5.5 μM), respectively (Fig 3.8). Terminal



elimination half-life at 2.0 mg/kg IV was  $606 \pm 90$  min,  $496.2 \pm 141.0$  min, and  $294 \pm 72$  min for P-DNQ, NP-DNQ and IP-DNQ, respectively. Full pharmacokinetic parameters for DNQ derivatives administered IV are detailed in Table 3.2.

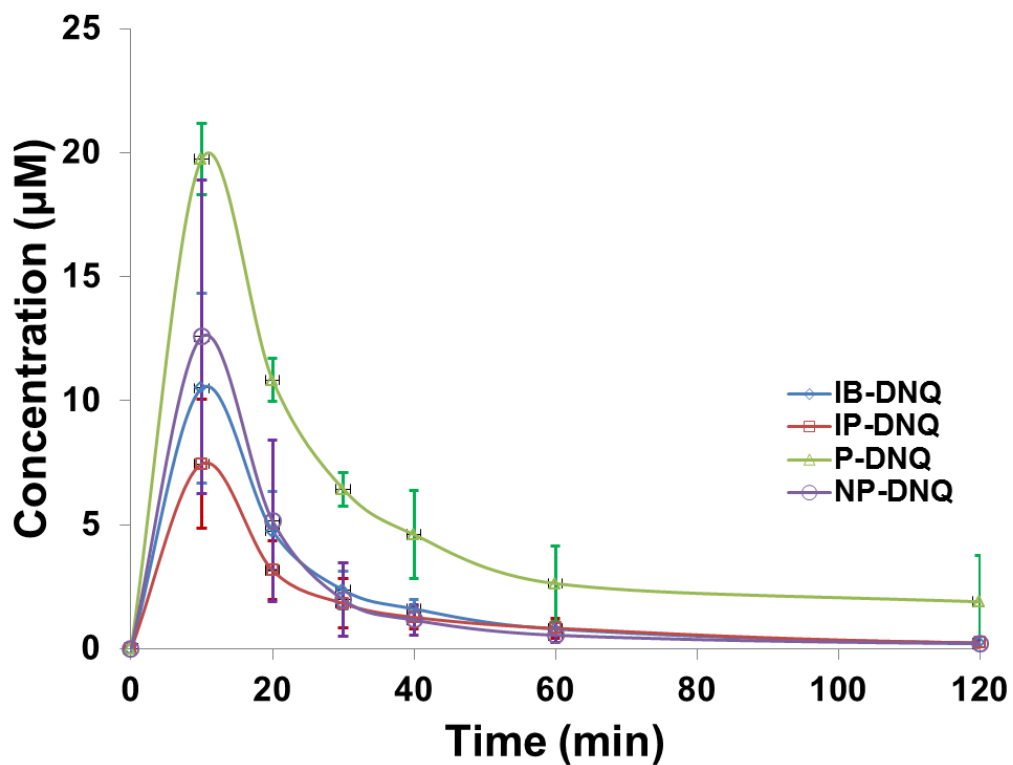


**Figure 3.8.** Pharmacokinetic profile of intravenous DNQ derivatives dosed at 2.0 mg/kg as an aqueous solution in HP $\beta$ CD. Data represented as average  $\pm$  SD.

**Table 3.2.** Pharmacokinetic parameters of IB-DNQ following 2.0 mg/kg IV administration

	IP-DNQ	NP-DNQ	P-DNQ	IB-DNQ
AUC <sub>0-inf</sub> (ng x hr/mL)	1539.8 ± 560.4	1871.5 ± 736.3	10025.4 ± 7743.9	1884.4 ± 780.7
K10-HL (min)	24.6 ± 3.0	21.0 ± 3.6	66 ± 54	13.7 ± 1.5
α (1/min)	0.0 ± 0.0	0.0 ± 0.0	0.0 ± 0.0	0.1 ± 0.0
β (1/min)	0.0 ± 0.0	0.0 ± 0.0	0.0 ± 0.0	0.0 ± 0.0
t <sub>1/2</sub> α (min)	23.4 ± 2.4	17.4 ± 1.8	22.2 ± 5.4	10.9 ± 1.5
t <sub>1/2</sub> β (min)	294 ± 72	496.2 ± 141.0	606.0 ± 234.0	115.8 ± 90.7
A (ng/mL)	2481.3 ± 597.9	3969.3 ± 1867.3	5898.6 ± 807.3	5582.9 ± 2395.2
B (ng/mL)	53.8 ± 21.4	23.2 ± 7.3	371.9 ± 289.8	198.5 ± 162.5
C <sub>max</sub> (ng/mL)	2535.1 ± 614.8	3992.5 ± 1873.9	6270.5 ± 685.2	3426.3 ± 1249.7
Cl (mL/min)	92.5 ± 39.8	79.3 ± 36.9	20.3 ± 10.6	73.9 ± 39.8
AUMC <sub>0-inf</sub> (ng x hr x hr/mL)	3423.3 ± 2122.6	3609.9 ± 367.1	143,614.8 ± 173,487.9	2138.3 ± 2455.4
MRT (min)	120.0 ± 34.2	156.0 ± 96.0	552.0 ± 402.0	57.7 ± 51.0
V <sub>ss</sub> (mL)	9902.9 ± 1716.6	15,715.5 ± 15,834.4	7030.2 ± 2001.2	3409.0 ± 1857.8
V <sub>2</sub> (mL)	6817.8 ± 813.4	13,133.2 ± 14,203.5	5865.1 ± 2048.3	1956.2 ± 2043.2
Cl <sub>d2</sub> (mL/min)	1395.0 ± 582.2	1139.8 ± 1100.5	10006.5 ± 257.4	13.5 ± 5.0

Parameters derived from 4 research cats and expressed as average ± SD

### 3.2.2.3. Tolerability of derivatives

To assess the tolerability of **P-DNQ**, **IP-DNQ** and **NP-DNQ**, we evaluated hematologic, non-hematologic, and clinical observational toxicities associated with each administration. Each feline subject was monitored for the development of acute clinical side effects peri-infusion and post-infusion (30 min). Side effects are comparable to **IB-DNQ** with the most notable clinical symptoms being hyper-salivation, mucous-y defecation, urination and tachypnea. **P-DNQ** the effects are significantly more severe than **IB-DNQ** with cats becoming very reactive during the infusion (increased vocalization and jumping). Hyper-salivation and tachypnea were both more severe and persisted longer. Cats seemed lethargic for multiple hours post infusion, whereas with **IB-DNQ** these effects lasted an hour at the longest. **IP-DNQ** shows similar severity to effects seen with **IB-DNQ**. **NP-DNQ** had no observable signs of hyper-salivation or tachypnea but more labored breathing during and immediately post-administration may indicate some degree of a respiratory side effect.

#### 3.2.2.4. NQO1-independent ROS generation

The ideal compound would produce maximal levels of ROS and cell death in cancers expressing NQO1 while producing minimal levels of ROS and cell death in normal tissues that do not express NQO1 to any appreciable amount. A compound that was able to do this would theoretically have the largest therapeutic window and should be prioritized going forward. The four derivatives (**IB-DNQ**, **P-DNQ**, **IP-DNQ**, and **NP-DNQ**) along with **DNQ** were evaluated for their ability to induce superoxide (ROS) and cell death at various concentrations in the NQO1-deficient head and neck cancer cell line, JHU029 (Fig 3.9., Table 3.3, Fig. 3.10, Table 3.4). At relevant biological concentrations (5-10  $\mu\text{M}$ ), **NP-DNQ** was able to exert the greatest cytotoxicity in these NQO1-deficient cells (Fig. 3.9, Table 3.3), in contrast to what was expected based on the previous tolerability studies. Across these same concentrations **IP-DNQ** showed the lowest levels of cytotoxicity while **DNQ**, **IB-DNQ** and **P-DNQ** all showed intermediate levels that did not really differentiate from each other. **NP-DNQ** showed the highest levels of ROS (assessed as MitoSox Red staining of mitochondrial superoxide) with **IB-DNQ** also demonstrating high levels of ROS (Figure 3.10, Table 3.4). This seems to suggest that **NP-DNQ** and **IB-DNQ** may be more susceptible to NQO1-independent redox cycling than **IP-DNQ** or **P-DNQ**

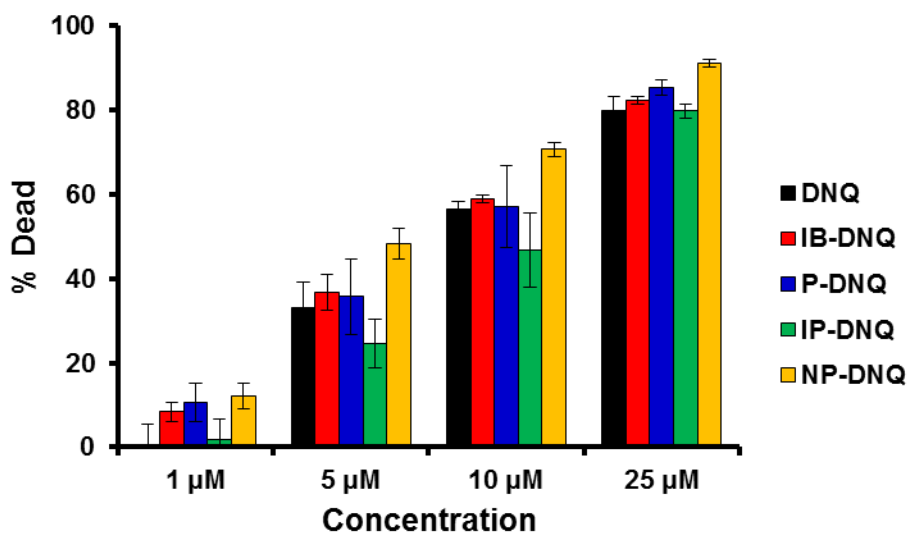


**Figure 3.9.** Cytotoxicity responses of DNQ derivatives in JHU029 cells. Experiment was conducted by Dr. Hyang Yeon.

**Table 3.3.** Cytotoxicity of DNQ derivatives in JHU029 cells

Concentration	DNQ	IB-DNQ	P-DNQ	IP-DNQ	NP-DNQ
1 μM	0.49 ± 4.85	8.36 ± 2.27	10.63 ± 4.67	1.92 ± 4.62	11.97 ± 3.03
5 μM	33.05 ± 6.02	36.60 ± 4.26	35.65 ± 8.88	24.57 ± 5.73	48.34 ± 3.62
10 μM	56.38 ± 1.87	58.83 ± 0.99	57.12 ± 9.67	46.71 ± 8.75	70.61 ± 1.72
25 μM	79.87 ± 3.27	82.13 ± 0.93	85.20 ± 1.81	79.75 ± 1.71	91.04 ± 0.95

\*Data expressed as Mean ± SD.

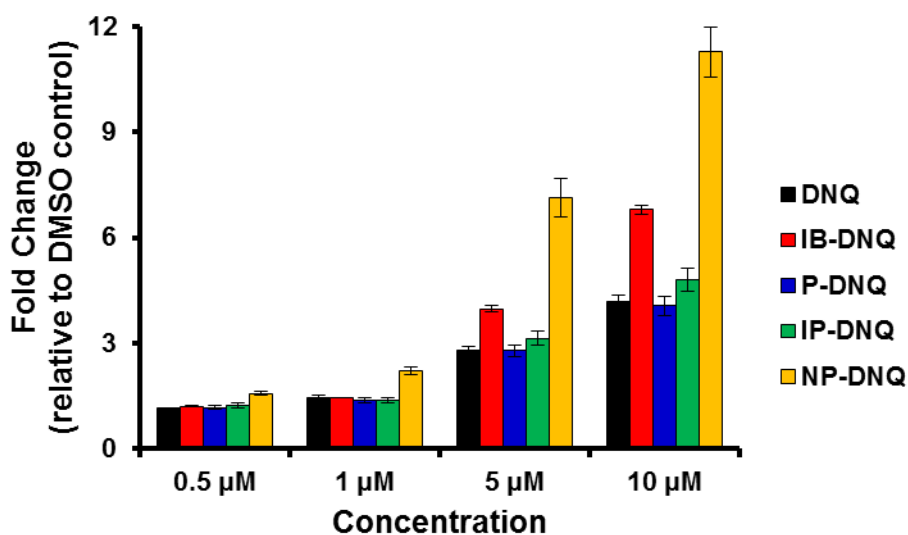


**Figure 3.10.** Mitochondrial superoxide generation of DNQ derivatives in JHU029 cells. Experiment was conducted by Dr. Hyang Yeon.

**Table 3.4.** Fold change in mitochondrial superoxide generation in JHU029 cells

<b>Concentration</b>	<b>DNQ</b>	<b>IB-DNQ</b>	<b>P-DNQ</b>	<b>IP-DNQ</b>	<b>NP-DNQ</b>
<b>0.5 <math>\mu</math>M</b>	1.15	1.21	1.18	1.23	1.58
<b>1 <math>\mu</math>M</b>	1.44	1.46	1.38	1.39	2.21
<b>5 <math>\mu</math>M</b>	2.81	3.98	2.79	3.14	7.14
<b>10 <math>\mu</math>M</b>	4.20	6.79	4.07	4.81	11.27

\*Data expressed as Mean

These derivatives were then evaluated in an isogenic cell line pair for their ability to cause cell death and generate superoxide. MDA-MB-231 breast cancer cells transfected with NQO1 showed extreme sensitivity to all derivatives even at the lowest concentration tested (1  $\mu$ M) and no significant differences were observed in cell death between the derivatives (Fig 3.11, Table 3.5). All derivatives produced high levels of ROS (at least a 7.5-fold increase in ROS levels compared to DMSO treated controls) (Fig. 3.12, Table 3.6), with **NP-DNQ** demonstrating the most robust superoxide formation. In the isogenic NQO1-deficient MDA-MB-231 cells, the cytotoxicity was significantly diminished; however, **NP-DNQ** was able to exert a much greater amount of cell death than any of the other derivatives (Fig 3.11, Table 3.5). Superoxide formation was also much higher in cells treated with **NP-DNQ**, (Fig. 3.12, Table 3.6) and mirrored that seen with the JHU029 cell line (Fig. 3.10, Table 3.4). Comparisons in superoxide formation between isogenic cell line pair for each derivative can be found in Table 3.7.

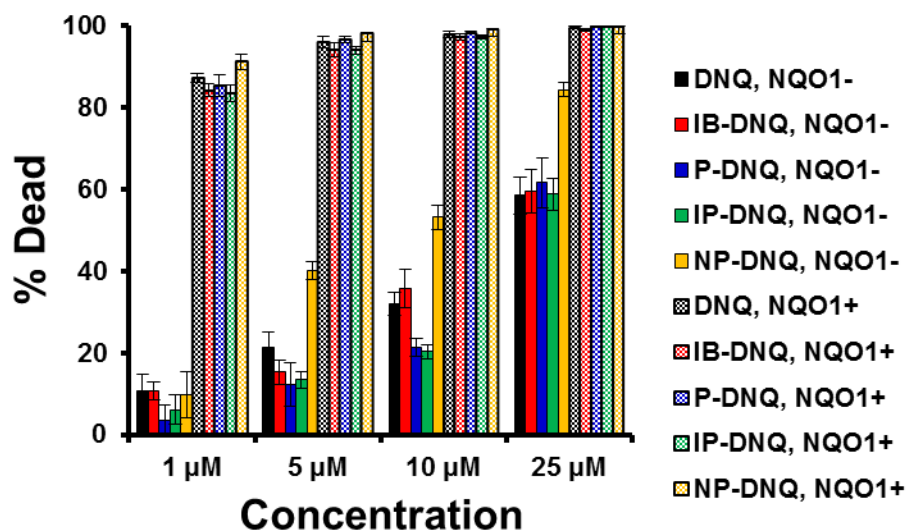


**Figure 3.11.** Cytotoxicity responses of DNQ derivatives in MDA-MB-231 cells transfected with NQO1 (NQO1+) or empty vector (NQO1-). Experiment was conducted by Dr. Hyang Yeon.

**Table 3.5.** Cell death of DNQ derivatives in isogenic MDA-MB-231 cell lines

		Concentration	DNQ	IB-DNQ	P-DNQ	IP-DNQ	NP-DNQ
NQO1 <sup>-</sup>	1 μM		10.84 ± 3.86	10.85 ± 2.22	3.70 ± 3.70	6.17 ± 3.66	9.74 ± 5.56
	5 μM		21.44 ± 3.56	15.34 ± 2.95	12.38 ± 5.29	13.41 ± 1.93	40.24 ± 2.16
	10 μM		32.00 ± 2.85	35.82 ± 4.66	21.25 ± 2.21	20.30 ± 1.68	53.15 ± 2.97
	25 μM		58.45 ± 4.52	59.47 ± 5.36	61.53 ± 5.97	58.76 ± 4.01	84.34 ± 1.73
NQO1 <sup>+</sup>	1 μM		87.18 ± 1.18	84.20 ± 1.68	85.36 ± 2.58	83.54 ± 2.03	91.11 ± 1.83
	5 μM		95.84 ± 1.46	93.94 ± 1.66	96.49 ± 0.69	93.96 ± 1.00	97.97 ± 0.25
	10 μM		97.78 ± 0.72	97.19 ± 0.85	98.22 ± 0.21	97.10 ± 0.41	99.01 ± 0.08
	25 μM		99.40 ± 0.28	99.01 ± 0.33	99.59 ± 0.17	99.54 ± 0.10	99.72 ± 0.05

\*Data expressed as Mean ± SD.

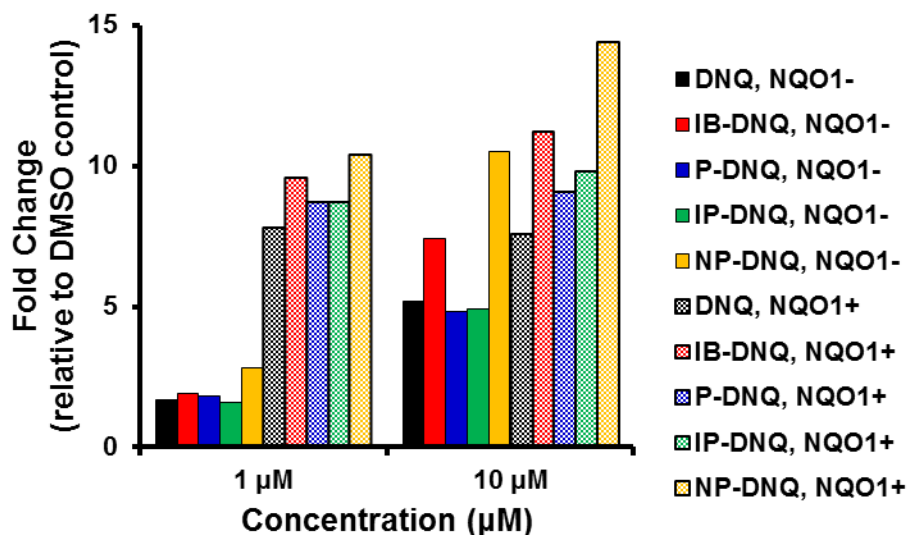


**Figure 3.12.** Mitochondrial superoxide generation elicited by DNQ derivatives in MDA-MB-231 isogenic cell line pairs transfected with NQO1 (NQO1+) or empty vector (NQO1-). Experiment was conducted by Dr. Hyang Yeon.

**Table 3.6.** Fold change in mitochondrial superoxide generation of DNQ derivatives in isogenic MDA-MB-231 cell line pairs

Concentration	MDA-MB-231 (NQO1 <sup>+</sup> )		MDA-MB-231 (NQO1 <sup>-</sup> )	
	1 μM	10 μM	1 μM	10 μM
DNQ	7.8	7.6	1.7	5.2
IB-DNQ	9.6	11.2	1.9	7.4
P-DNQ	8.7	9.1	1.8	4.8
IP-DNQ	8.7	9.8	1.6	4.9
NP-DNQ	10.4	14.4	2.8	10.5

**Table 3.7.** Comparison between mitochondrial superoxide generation in isogenic MDA-MB-231 cell line pairs for DNQ derivatives

Compound	NQO1 <sup>+</sup> ROS: NQO1 <sup>-</sup> ROS
DNQ	4.6
IB-DNQ	5.1
P-DNQ	4.8
IP-DNQ	5.4
NP-DNQ	3.7

### 3.3. Summary

Recent clinical evaluations of IB-DNQ in felines have provided optimism for the future of NQO1-targeted therapies not only in companion animal disease but for the translation into humans as well. However, as it currently stands the effective dose of IB-DNQ in felines is the same as its maximum tolerated dose which offers a very narrow therapeutic window. Therefore developing strategies for widening the therapeutic window of IB-DNQ is essential for its future development and we cannot simply hope that humans will respond as favorably to dosing at the MTD as our feline counterparts seem to tolerate.

Often this window can be extended through creating a prodrug form of the drug molecule to mitigate off-target toxicity. While conceptually this appears to be a useful strategy for IB-DNQ, through masking of the active para-quinone moiety with promoiety functional groups, it is not straightforward. The ability of para-quinone of IB-DNQ to undergo reduction to a hydroquinone and quickly reoxidize back to the parent quinone is a property of the molecule which makes it the most efficient NQO1 redox substrate known to date. Unfortunately this same property appears to make it challenging to mask the quinone in a prodrug, as the reoxidation appears to occur much faster than any conjugation reaction. While this strategy was able to be implemented with fellow NQO1 substrate  $\beta$ -lapachone,  $\beta$ -lapachone also is not processed as efficiently by NQO1 as IB-DNQ which may be a result of slower reoxidation kinetics which facilitate esterification of the quinone. While a strategy to prodrug IB-DNQ still may remain possible, it would appear challenging to accomplish.

Alternative derivatives of IB-DNQ may be the key to extending the therapeutic window. The SAR of IB-DNQ at the  $\alpha$ -carbons of the  $\delta$ -lactam rings remain largely unexplored. While introduction of a halogen at this position seems to abolish potency, the effects of substitution at

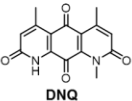
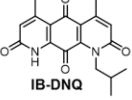
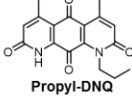
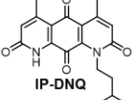
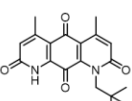
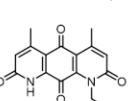


this position are incomplete. Bromination and iodination at this position prime the compound for quick diversification through cross coupling reactions in order to further interrogate the structure activity relationship of the molecule, which will hopefully yield exciting compounds in the future. Parallel to this quest for new derivatives is the re-evaluation of older derivatives. Through improvements in the synthetic yields of alkyl iodoamides and salcomine-mediated oxidation, derivatives with more sterically encumbering, expensive amines can now be evaluated to a greater extent in animal models, which may lead to the discovery of a better derivative to move forward with in the clinic. We can already see differences between the pharmacokinetics and tolerability of some of these derivatives; however, at this point no compound has significantly better properties than IB-DNQ (Fig. 3.13).

It appears that IB-DNQ should proceed as the derivative of choice in felids with OSCC, as preliminary findings show it is effective and toxicity has not yet been an issue even though dosing is conducted at the MTD. Potentially IP-DNQ might be considered for further use. While side effects are similar to that of IB-DNQ in appearance, duration and severity, IP-DNQ possesses a slightly longer half-life than that of IB-DNQ. Despite having a lower  $C_{\max}$  than IB-DNQ, this prolonged half-life may allow effective concentrations of IP-DNQ to persist in vivo for a longer duration than IB-DNQ while also avoiding any potential off-target effects that could result from a high  $C_{\max}$ . Also the greater ratio of  $\text{NQO1}^{\cdot-}:\text{NQO1}^-$  ROS experienced by IP-DNQ in isogenic cell lines suggests that the therapeutic window of IP-DNQ could be larger than that of IB-DNQ.

At this point in the development of deoxynyboquinones as anticancer agents for HNSCC, either IB-DNQ or IP-DNQ should be considered moving forward. To this point neither derivative possesses properties that would be considered superior to the other; however, IP-DNQ

does appear to have some improved properties and perhaps these could eventually differentiate themselves in other species, similar to what is seen in mice. In felines the MTD window of these derivatives may be compressed due to the sensitivity of felids to oxidative damage, and in a species, like canines, that are less sensitive to oxidative stress perhaps one of these derivatives would begin to show superiority. Other assays such as methemoglobin formation assays and tumor penetrance assays could be used to aid in this decision of which derivative to move forward with.

Name/Structure	MTD (mice) <i>Tox (cat)</i>	NQO1 catalytic efficiency	IC <sub>50</sub> A549	IC <sub>50</sub> MCF-7	C <sub>max</sub> (cat)	t <sub>1/2</sub> (cat)	NQO1*:NQO1- ROS
 DNQ	<b>5 mg/kg</b>	6.2 x 10 <sup>7</sup> M <sup>-1</sup> s <sup>-1</sup>	0.06 μM	0.13 μM			4.6
 IB-DNQ	<b>14 mg/kg</b>	6.1 x 10 <sup>7</sup> M <sup>-1</sup> s <sup>-1</sup>	0.08 μM	0.23 μM	10.5 μM	116 min	5.1
 Propyl-DNQ	<b>17 mg/kg</b> <i>more severe than IB-DNQ*</i>	4.6 x 10 <sup>7</sup> M <sup>-1</sup> s <sup>-1</sup>	0.11 μM	0.23 μM	20.1 μM	606 min	4.8
 IP-DNQ	<b>15 mg/kg</b> <i>same as IB-DNQ*</i>	7.3 x 10 <sup>7</sup> M <sup>-1</sup> s <sup>-1</sup>	0.08 μM	0.18 μM	7.4 μM	294 min	5.4
 NP-DNQ	<b>21 mg/kg</b> <i>less severe than IB-DNQ*</i>	4.9 x 10 <sup>7</sup> M <sup>-1</sup> s <sup>-1</sup>	0.08 μM	0.23 μM	11.7 μM	496 min	3.7
 3,3-DMB-DNQ	<b>22 mg/kg</b>	6.7 x 10 <sup>7</sup> M <sup>-1</sup> s <sup>-1</sup>	0.07 μM	0.22 μM			

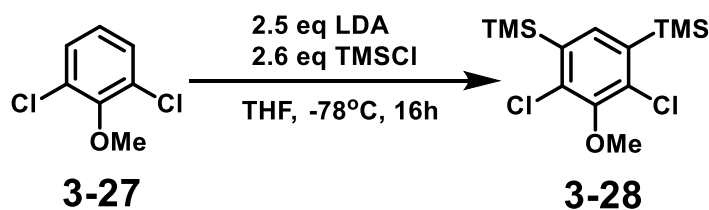
**Figure 3.13.** Head to head comparison chart of DNQ derivatives and performance in assays done to date. \*observable adverse effects with IB-DNQ persisted for 1h and included: ptyalism, tachypnea, urination, emesis, and lethargy.

### 3.4. Materials and methods

General chemical reagents were purchased from Sigma Aldrich. Pd/X-Phos catalyst and X-Phos ligand were purchased as a 1:1 admixture from Strem Chemicals, Inc. (Newburyport,

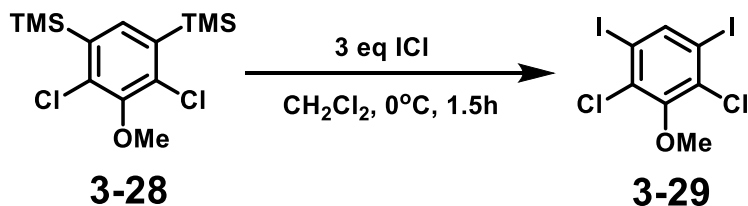
MA). Lithium diisopropylamide was purchased as a 2.0 M solution in THF from Acros Organics (Morris Plains, NJ). Ethyl 2-butynoate, 1,2-dimethoxyethane and iodine monochloride were purchased from GFS Chemicals (Powell, OH). 2-butynoic acid and neopentylamine were purchased from Oakwood Chemical (Estill, SC). PdCl<sub>2</sub>(dppf) catalyst and bis-pinacolboronate were purchased from CombiPhos Catalysts (Princeton, NJ). 2,6-dichloroanisole was purchased from TCI America (Portland, OR). 4-methoxybenzylamine and oxalyl chloride were purchased from Alfa Aesar (Heysham, Lancashire, United Kingdom). All reagents were used without further purification unless otherwise noted. Solvents were dried by passage through columns packed with activated alumina (THF, CH<sub>2</sub>Cl<sub>2</sub>, DMSO).

<sup>1</sup>H-NMR and <sup>13</sup>C-NMR were recorded on Varian Unity spectrometers at 400/500 MHz and 125 MHz, respectively. Spectra generated from a solution of CDCl<sub>3</sub> were referenced to residual chloroform (<sup>1</sup>H: δ 7.26 ppm; <sup>13</sup>C: δ 77.16 ppm). Spectra generated from a solution of CD<sub>3</sub>OD were referenced to residual methanol (<sup>1</sup>H: δ 3.31 ppm).

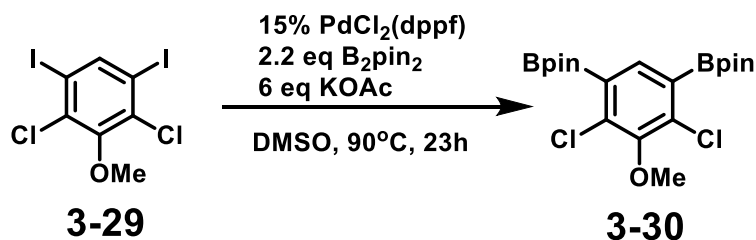


To an oven-dried flask and stir bar under nitrogen was added 2,6-dichloroanisole (**3-27**, 10.8 mL, 78.8 mmol) and dry THF (80 mL). The flask was chilled in a dry ice/isopropanol bath and lithium diisopropylamine (100 mL, 2.0M solution) was added dropwise via syringe. The reaction was stirred for 4h and kept at temperature -78°C. TMSCl (26 mL, 204.9 mmol) was added and mixture was stirred overnight warming to room temperature. A white precipitate had formed and reaction was quenched with distilled water (60 mL), which also dissolved the precipitate. Mixture was diluted with 1M HCl and separated after addition of ether. Aqueous

fraction was extracted once more with ether and then the combined organic fractions were washed with brine, dried over  $\text{MgSO}_4$  and evaporated to a pale yellow oil that solidified under vacuum over the course of the following week. Reaction yielded **3-28** (22.23 g, 69.1 mmol) in 88% yield that was used in further reactions without additional purification. Spectra of **3-28** was consistent with that previously report.<sup>31</sup>

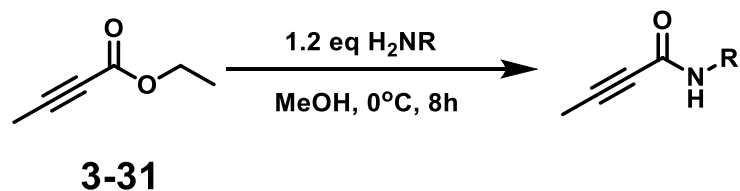


Iodine monochloride (33.88 g, 209 mmol) was weighed into a round-bottom flask with stir bar and dissolved in  $\text{CH}_2\text{Cl}_2$ . The flask was chilled in an ice-water bath and flask was adapted with addition funnel. **3-28** (22.23g, 69.1 mmol) was dissolved in minimal  $\text{CH}_2\text{Cl}_2$  (10 mL) and added to addition funnel. Stopcock was opened to add **3-28** to flask in a dropwise manner over the span of 1h, keeping solution temperature below  $20^\circ\text{C}$ . After addition used additional  $\text{CH}_2\text{Cl}_2$  to wash addition funnel and let stir for 0.5h. Added distilled water to flask and transferred to an Erlenmeyer with aid of  $\text{CH}_2\text{Cl}_2$ . Added sodium sulfite until color dissipated and separated. Extracted aqueous fraction with  $\text{CH}_2\text{Cl}_2$  three times and washed combined organic fraction with brine before drying over  $\text{MgSO}_4$ . Filtered and rotovapped to yield a hairy white-brown solid, **3-29** (27.75 g, 64.73 mmol, 94% yield). Spectra of **3-29** was consistent with that previously report.<sup>31</sup>



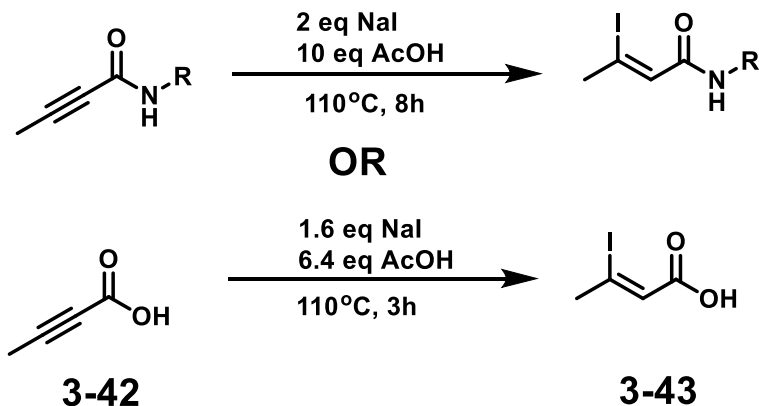
To a hot oven-dried flask with stir bar was added KOAc (35.98 g, 366.6 mmol) and vacuum was applied to dry the salt until flask was cool. To this flask was added **3-29** (26.19 g, 61.1 mmol), PdCl<sub>2</sub>(dppf) (7.48 g, 9.16 mmol, 15 mol%), and B<sub>2</sub>pin<sub>2</sub> (34.15 g, 134.5 mmol). Flask was evacuated and backfilled with nitrogen three times. Dry DMSO was added via syringe and mixture was placed in an oil bath at 90°C. Mixture was allowed to stir for 23h and then after cooling was poured into a separatory funnel with additional DMSO. Mixture was extracted with hexanes and combined hexane fractions were washed with water until the organic layer was clear. Organic fraction was then dried over MgSO<sub>4</sub> and evaporated to an off-white solid. The reaction yielded **3-30** (18.31 g, 31.0 mmol) in 70% yield that was used in subsequent Suzuki cross couplings without further purification. Spectra of **3-30** was consistent with that previously report.<sup>31</sup>

**General protocol for Amidation of ester:**



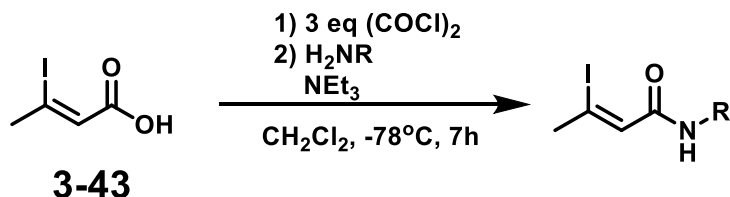
To a solution of chilled ethyl 2-butynoate, **3-31**, (1 equiv.) in methanol in an ice-water bath, alkyl amine (1.2 equiv.) was added. The reaction was stirred at 0°C overnight. Solvent was evaporated from the flask and residue was purified by silica gel chromatography (9:1 hexanes:ethyl acetate to 1:1 hexanes:ethyl acetate) to yield the desired alkynyl amide as a mixture of rotamers. Spectra of **3-32**, **3-33**, **3-34**, **3-35**, and **3-36** were consistent with that previously report.<sup>REF</sup>

**General protocol for hydroiodination of alkynes:**



Alkynyl amide (1 equiv), sodium iodide (2 equiv.) and acetic acid (10 equiv.) were combined and heated to 110°C for 8h. In the case of the alkynyl acid, 2-butynoic acid, **3-42**, (1 equiv.), sodium iodide (1.6 equiv.) and acetic acid (6.4 equiv.) were combined and heated to 110°C for 3h. After cooling to room temperature, the deep red reaction mixture was diluted with water (1-2 mL/mmol alkyne) and CH<sub>2</sub>Cl<sub>2</sub>. The mixture was treated with sodium sulfite until colorless and then carefully neutralized with a saturated aqueous solution of sodium bicarbonate. Organic fraction was separated and aqueous fraction was extracted twice with CH<sub>2</sub>Cl<sub>2</sub>. The combined organic fractions were washed with brine, dried over MgSO<sub>4</sub> and evaporated to yield the desired iodoamide. Spectra of **3-37**, **3-38**, **3-39**, **3-40**, **3-41** and **3-43** were consistent with that previously report.<sup>8,31</sup>

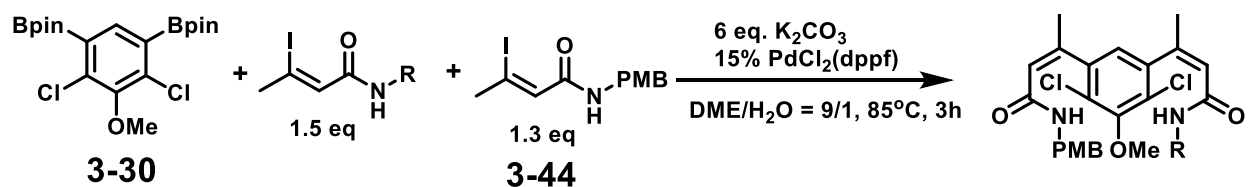
#### General protocol for amidation of acid chloride



To an oven-dried Schlenk flask with a stirbar was added the iodoacid, **3-43**, after which the flask was evacuated and backfilled with nitrogen. Dry CH<sub>2</sub>Cl<sub>2</sub> (0.4 M **3-43**) was added and the

solution was chilled on an ice-water bath. Oxalyl chloride (3 equiv.) was added via syringe and cold bath was removed following addition. After 5h at room temperature the volatile components were evaporated and dry  $\text{CH}_2\text{Cl}_2$  (0.5 M) was added to the residual yellow oil. Flask was chilled in a dry ice/isopropanol bath. 4-methoxybenzylamine or alkyl amines (1.1 equiv.) were added dropwise by syringe followed by dropwise addition of  $\text{NEt}_3$  (1 equiv.) The mixture was allowed to stir overnight, warming to RT. 1 M HCl (1.5 mL per mmol) was added and the solution was separated with help of  $\text{CH}_2\text{Cl}_2$ . The aqueous fraction was extracted three times with  $\text{CH}_2\text{Cl}_2$  and then dried over  $\text{MgSO}_4$  and evaporated. Spectra of **3-37**, **3-38**, **3-39**, **3-40**, **3-41** and **3-44** were consistent with that previously report.<sup>8,31</sup>

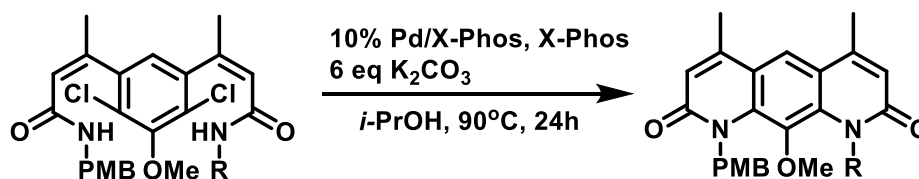
#### General protocol for Suzuki cross-coupling



To a flask with a stir bar was added **3-30** (1 equiv.),  $\text{PdCl}_2(\text{dppf})$ ,  $\text{K}_2\text{CO}_3$  (6 equiv.), **3-44** (1.3 equiv.) and alkyl iodoamide (1.5 equiv.). Flask was evacuated and backfilled with nitrogen three times. (Water 1 mL per mmol of **3-30**) and 1,2-dimethoxyethane (9 mL per mmol of **3-30**) were added via syringe after degassing the solvents by bubbling with nitrogen for 45 min. The flask was placed into an oil bath at  $85^\circ\text{C}$  for 3h. Once cool the mixture was poured into a separatory funnel, diluted with water and rinsed with EtOAc. The mixture was extracted with EtOAc three times and the combined organic extracts were dried over  $\text{MgSO}_4$  and evaporated to a deep red oil. The crude product was dissolved in  $\text{CH}_2\text{Cl}_2$  and separated by silica gel chromatography (1:1

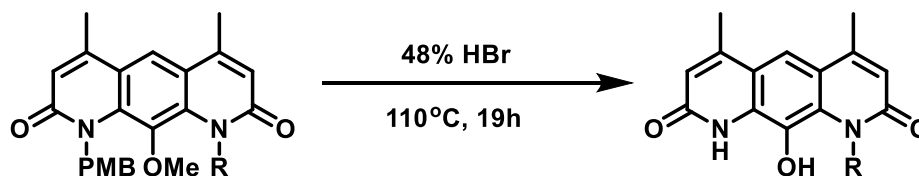
CH<sub>2</sub>Cl<sub>2</sub>:ethyl acetate). The cross coupled product could be found at rf ~0.4 depending on derivative and was rotovapped to a brown foam.

### General protocol for Buchwald-Hartwig amidation



In a flask containing the cross-coupled product (1 equiv.), K<sub>2</sub>CO<sub>3</sub> (6 equiv.) and Pd/X-Phos, X-Phos (1:1 admixture, 10 mol%) were added. The flask was evacuated and backfilled with nitrogen three times. *i*-PrOH ( mL per mmol cross-coupled product) was added via syringe after degassing of the solvent by bubbling with nitrogen for 45 min. The mixture was heated to 85°C with stirring for 24h. Insoluble materials were removed by filtration through Celite and rinsed with CH<sub>2</sub>Cl<sub>2</sub>. The filtrate was evaporated to a brown oil that was purified by silica gel chromatography (1:1 CH<sub>2</sub>Cl<sub>2</sub>:ethyl acetate, rf ~0.5).

### General protocol for HBr deprotection

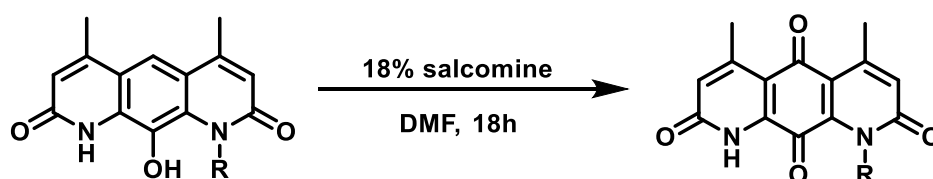


The ring-closed diazanthracene product was dissolved in 48% HBr and heated to 110°C. After 19 hours the reaction was removed from heat and allowed to cool to room temperature. The flask was cooled on an ice bath and rendered basic through addition of 10 M NaOH. Residual insoluble material was removed by filtration through hardened filter paper. The filtrate was



rendered acidic with 1 M HCl to form a colloidal precipitate. Mixture was filtered through hardened filter paper and dried under vacuum to yield the desired product.

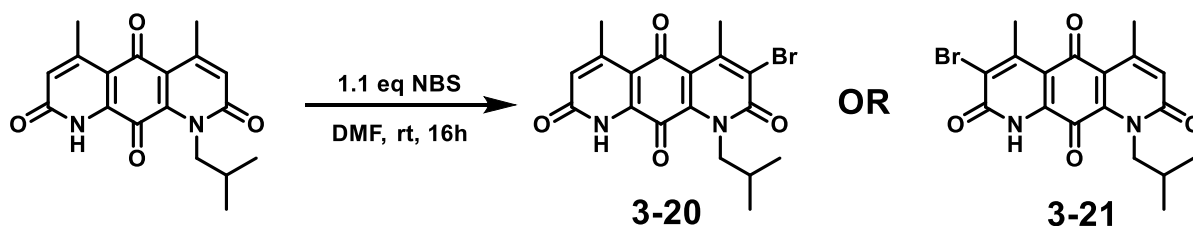
### General protocol for salcomine oxidation



Salcomine (6 mol%) was added to a flask containing the deprotected monophenol starting material (1 equiv.) and DMF (1 mL per 12 g monophenol). Flask was capped with septum and a syringe needle was placed into the solution. The needle was attached to a short piece of tubing and connected to a terminal 90 degree gas inlet adapter to which a balloon containing O<sub>2</sub> was fitted. An outlet needle was allowed to puncture the septum for 1-2 min to purge atmosphere and was continued stirring for 3h. At three hours another portion of salcomine (6 mol%) was added to the flask. A third addition of salcomine (6 mol%) was added three hours later and reaction was left to run for 12h. Balloon was removed and DMF was blown off to produce dark red-brown residue. Residue was dissolved in CH<sub>2</sub>Cl<sub>2</sub>, filtered and rotovapped to dark red oil. Oil was dissolved in CH<sub>2</sub>Cl<sub>2</sub> and loaded onto a chromatography column consisting of a layer of basic alumina under a layer of silica gel. The column was run with increasing amounts of methanol (2-5%) in CH<sub>2</sub>Cl<sub>2</sub> until the red product band entered the alumina layer which retained the product and allowed coeluting impurities to be removed. The product was released upon the addition of 1% HOAc to the mobile phases. Fractions that were visibly red in color were evaporated and further purified through silica gel chromatography (5% MeOH in CH<sub>2</sub>Cl<sub>2</sub>) to yield the desired

DNQ derivative as a reddish solid. Spectra of **IB-DNQ**, **P-DNQ**, **IP-DNQ**, **NP-DNQ** and **3,3-DMB-DNQ** were consistent with that previously report.<sup>8</sup>

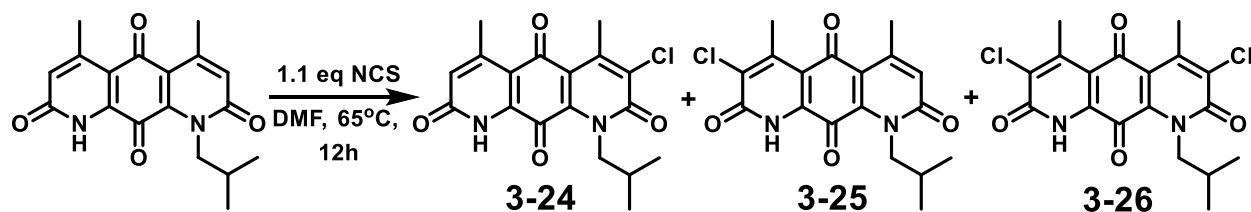
### Halogenation reactions



*N*-bromosuccinimide (9.8 mg, 0.06 mmol.) was added to a solution of **IB-DNQ** (16.3 mg, 0.05 mmol) in DMF (1 mL, 0.05 M). Within 15 minutes the reaction mixture had turned dark red. Reaction was allowed to proceed overnight. Mixture was diluted with distilled water and aqueous fraction was extracted three times with ethyl acetate. Organic fraction was washed with brine solution, dried over  $\text{MgSO}_4$  and evaporated to a red solid. Purification through silica gel chromatography (1:1  $\text{CH}_2\text{Cl}_2$ :ethyl acetate) lead to isolation of a red solid with a metallic like sheen in 95% yield.

<sup>1</sup>**H-NMR** ( $\text{CDCl}_3$ , 400 MHz):  $\delta$  9.69 (bs, 1H), 6.80 (s, 1H), 4.61 (d, 2H), 2.82 (s, 3H), 2.59 (s, 3H), 1.89 (sept, 1H), 0.92 (d, 6H).

**HRMS** (ESI-TOF) calcd for  $\text{C}_{18}\text{H}_{18}\text{N}_2\text{O}_4\text{Br}$  ( $\text{M}+\text{H}$ )<sup>+</sup>: 405.0450, found 405.0440.



*N*-chlorosuccinimide (3.6 mg, 0.03 mmol.) was added to a solution of **IB-DNQ** (8.0 mg, 0.025 mmol) in DMF (1 mL, 0.025 M). Flask was placed in an oil bath at 70°C and allowed to proceed overnight. Flask was cooled to room temperature before diluted with distilled water and aqueous

fraction was extracted three times with CH<sub>2</sub>Cl<sub>2</sub>. Organic fraction was dried over MgSO<sub>4</sub> and evaporated to a orange-red oil. Purification through silica gel chromatography (1:1 CH<sub>2</sub>Cl<sub>2</sub>:ethyl acetate) led to isolation of four red solid products: di-chlorinated compound (rf=0.61, 41% yield), two monochlorinated compounds (rf = 0.52, 14% yield; rf = 0.44, 24% yield) and starting material (21% yield).

### Monochlorinated

<sup>1</sup>H-NMR (CDCl<sub>3</sub>, 400 MHz): δ 9.69 (bs, 1H), 6.79 (s, 1H), 4.62 (d, 2H), 2.78 (s, 3H), 2.60 (s, 3H), 1.89 (sept, 1H), 0.92 (d, 6H).

HRMS (ESI-TOF) calcd for C<sub>18</sub>H<sub>18</sub>N<sub>2</sub>O<sub>4</sub>Cl (M+H)<sup>+</sup>:361.0955, found 361.0955.

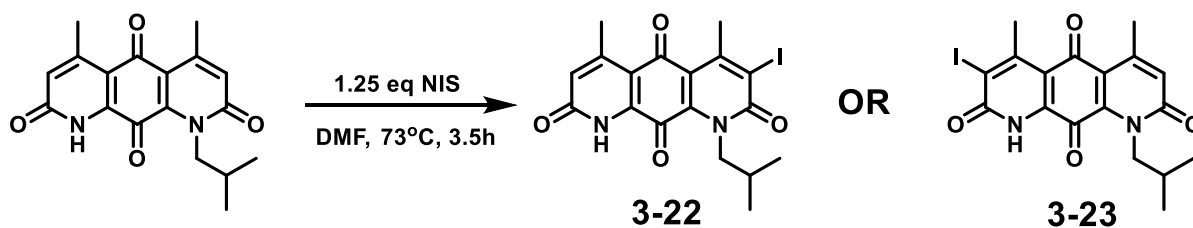
<sup>1</sup>H-NMR (CDCl<sub>3</sub>, 400 MHz): δ 6.80 (s, 1H), 4.63 (d, 2H), 2.78 (s, 3H), 2.60 (s, 3H), 1.88 (sept, 1H), 0.93 (d, 6H).

HRMS (ESI-TOF) calcd for C<sub>18</sub>H<sub>18</sub>N<sub>2</sub>O<sub>4</sub>Cl (M+H)<sup>+</sup>:361.0955, found 361.0961.

### Dichlorinated

<sup>1</sup>H-NMR (CDCl<sub>3</sub>, 400 MHz): δ 9.46 (bs, 1H), 4.58 (d, 2H), 2.71 (s, 6H), 1.89 (sept, 1H), 0.74 (d, 6H).

HRMS (ESI-TOF) calcd for C<sub>18</sub>H<sub>17</sub>N<sub>2</sub>O<sub>4</sub>Cl<sub>2</sub> (M+H)<sup>+</sup>:395.0955, found 395.1.

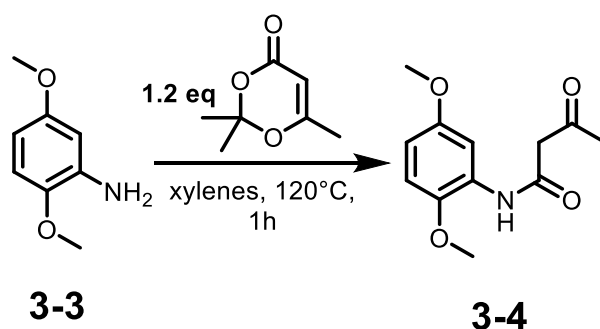


*N*-iodosuccinimide (5.6, 0.025 mmol) was added to a solution of **IB-DNQ** (6.3 mg, 0.02 mmol) in DMF (0.02 M). Flask was placed in an oil bath at 73°C and allowed to stir for 3.5h. Distilled water (1.25 mL) was added to flask and stirred at room temperature for 1h during which time a red precipitate had formed. Solid was filtered and rinsed with hexanes followed by ether. Solid

was dissolved in CH<sub>2</sub>Cl<sub>2</sub> dried with MgSO<sub>4</sub>, and concentrated to a dark red solid. Purification through silica gel chromatography (1:1 CH<sub>2</sub>Cl<sub>2</sub>:ethyl acetate) led to isolation of a red solid product in 44% yield.

**<sup>1</sup>H-NMR** (CDCl<sub>3</sub>, 400 MHz): δ 9.60 (bs, 1H), 6.80 (s, 1H), 4.63 (d, 2H), 2.88 (s, 3H), 2.59 (s, 3H), 1.88 (sept, 1H), 0.93 (d, 6H).

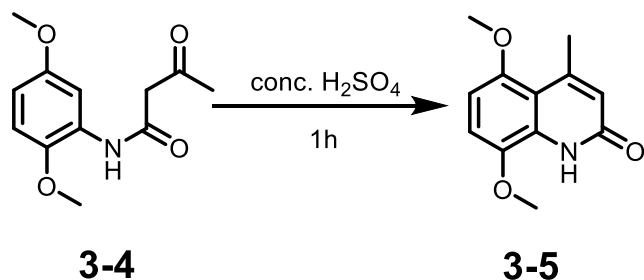
**HRMS** (ESI-TOF) calcd for C<sub>18</sub>H<sub>18</sub>N<sub>2</sub>O<sub>4</sub>I (M+H)<sup>+</sup>: 453.0311, found 453.0308.



In an Erlenmeyer flask containing a stir bar, added 2,5-dimethoxyaniline, **3-3**, (5.0 g, 32.4 mmol), xylenes (20 mL, 1.5 M), and 2,2,6-trimethyl-4H-1,3-dioxin-4-one (5.15 mL, 39.4 mmol). Flask was placed in an oil bath at 120°C. Mixture was stirred for 2.25h after which the flask was removed from heat and allowed to cool. Concentrated to half volume and loaded onto silica gel for chromatographic purification (1:1 hexanes:ethyl acetate). Further purified product with column chromatography using increasing amounts of ethyl acetate (3:1 to 2:1 to 1:1 hexanes:ethyl acetate to 100% ethyl acetate). Product was evaporated to a yellow solid, **3-4**, (6.42 g, 27.1 mmol) in 84% yield.

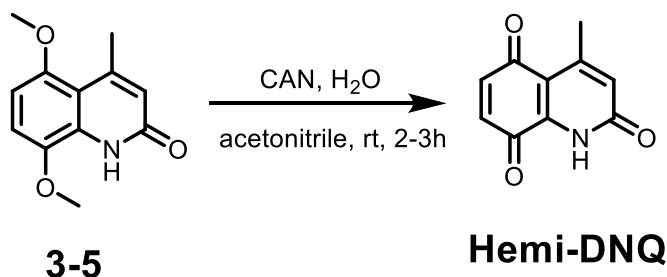
**<sup>1</sup>H-NMR** (CDCl<sub>3</sub>, 500 MHz): δ 9.26 (bs, 1H), 8.07 (s, 1H), 6.79 (d, 2H), 6.59 (d, 2H), 3.86 (s, 3H), 3.77 (s, 3H), 3.59 (s, 2H), 2.32 (s, 3H).

**HRMS** (ESI-TOF) calcd for C<sub>12</sub>H<sub>16</sub>NO<sub>4</sub> (M+H)<sup>+</sup>: 238.1079, found 238.1076



To a flask with a stir bar containing **3-4** (5.0 g, 21.1 mmol) was added concentrated H<sub>2</sub>SO<sub>4</sub> (24 mL). Mixture was stirred for 1h and then poured into a flask in an ice-water bath containing crushed ice. Flask was washed with distilled water and added to the flask. Concentrated NH<sub>4</sub>OH (60 mL) was added dropwise over 20 min to neutralize solution. Over course of neutralization a brown precipitate formed. A brown solid was collected via vacuum filtration to produce **3-5** (3.68g, 16.8 mmol) in 80% yield.

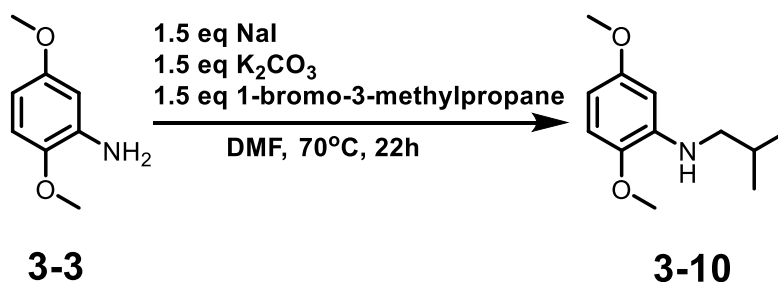
<sup>1</sup>H-NMR (CDCl<sub>3</sub>, 400 MHz): δ 9.09 (s, 1H), 6.86 (d, 1H), 6.50 (d, 1H), 6.37 (s, 1H), 3.90 (s, 3H), 3.82 (s, 3H), 2.60 (s, 3H).



In a flask with a stir bar, **3-5** (509 mg, 2.3 mmol) was dissolved in acetonitrile (60 mL). A solution of cerium (IV) ammonium nitrate (CAN) was prepared separately by dissolving CAN (2.71 g, 4.9 mmol) in distilled water (30 mL). CAN solution was added to flask via pipette. Upon addition of CAN, solution changed from yellow to dark red to light red after completion of the addition. Mixture was allowed to stir for 3h before diluting with distilled water (50 mL). Mixture was extracted with chloroform three times and combined organic fractions were dried over MgSO<sub>4</sub> and rotovapped to an orange to orange-red solid. **Hemi-DNQ** (382 mg, 2.0 mmol) was

obtained as a crude solid in 87% yield. Further attempts to purify the compound by silica gel chromatography resulted in decomposition of the product.

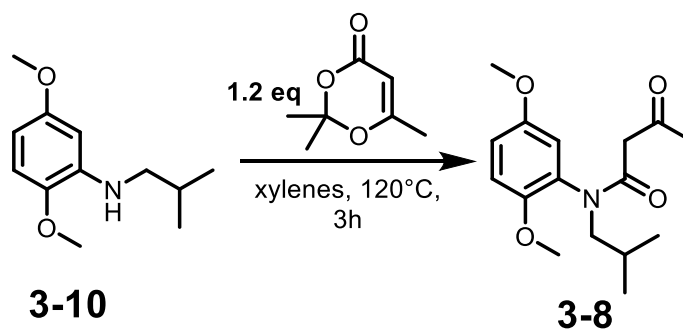
$^1\text{H-NMR}$  ( $\text{CD}_3\text{OD}$ , 400 MHz):  $\delta$  6.89 (d, 1H), 6.83 (d, 1H), 6.56 (s, 1H), 2.55 (s, 3H).



To flask with stir bar added 2,5-dimethoxyaniline (1.5 g, 9.7 mmol), sodium iodide (2.20 g, 14.7 mmol) and  $\text{K}_2\text{CO}_3$  (2.03 g, 14.7 mmol). Added DMF (10.5 mL, 1M) to flask and then placed in oil bath at  $70^\circ\text{C}$ . Then added and 1-bromo-3-methylpropane (1.6 mL, 14.7 mmol) to flask and allowed to stir for 22h. Flask was cooled and diluted with distilled water (25 mL) before extracting with ethyl acetate three times. Organic fractions were dried over  $\text{MgSO}_4$  and evaporated to a clear oil. Product was purified through column chromatography (9:1 hexanes:ethyl acetate) to produce **3-10** (1.02g, 4.9 mmol) in 50% yield.

$^1\text{H-NMR}$  ( $\text{CDCl}_3$ , 500 MHz):  $\delta$  6.75 (d, 1H), 6.40 (d, 1H), 6.25 (s, 1H), 3.88 (s, 3H), 3.86 (s, 3H), 3.06 (d, 2H), 2.05 (sept, 1H), 1.12 (d, 6H).

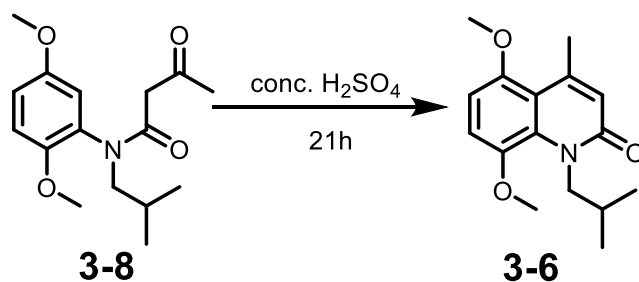
**HRMS** (ESI-TOF) calcd for  $\text{C}_{12}\text{H}_{20}\text{NO}_2(\text{M})^+$ : 210.1494, found 210.1496.



**3-10** (507 mg, 2.42 mmol) and xylenes (1.5 mL) were added to a flask and placed in an oil bath at 120°C. 2,2,6-trimethyl-4*H*-1,3-dioxin-4-one (0.38 mL, 2.9 mmol) addition to the mixture, turned the solution color brown. After 3h of stirring flask was taken out of bath and cooled to room temperature. Mixture was loaded onto silica gel column and product was eluted in 3:1 hexanes:ethyl acetate. Product **3-10** (693 mg, 2.36 mmol) was isolated as a yellow oil in 97% yield.

**<sup>1</sup>H-NMR** (CDCl<sub>3</sub>, 500 MHz): δ 6.80 (m, 1H), 6.62 (d, 1H), 6.60 (d, 1H), 3.65 (s, 3H), 3.60 (s, 3H), 3.40 (ddd, 2H), 3.08 (d, 2H), 2.02 (s, 3H), 1.65 (sept, 1H), 0.81 (d, 6H).

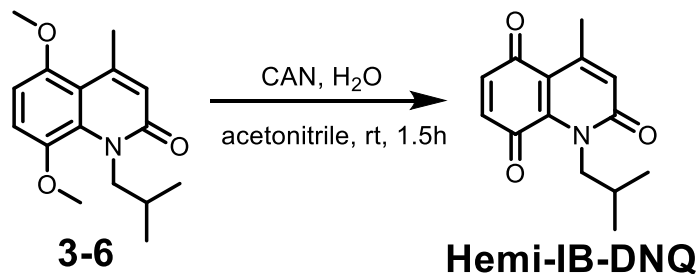
**HRMS** (ESI-TOF) calcd for C<sub>16</sub>H<sub>24</sub>NO<sub>4</sub> (M+H)<sup>+</sup>: 294.1705, found 294.1710.



In a small flask with a stir bar, **3-8** (133 mg, 0.45 mmol) was added with concentrated H<sub>2</sub>SO<sub>4</sub> (0.52 mL). After 21h solution was poured into an Erlenmeyer flask containing crushed ice in an ice-water bath. Concentrated NH<sub>4</sub>OH (1.28 mL) was added dropwise to ice to neutralize the acid. Once all ice had melted, the mixture was filtered to collect yellow precipitate. The yellow solid was dissolved in ethyl acetate and diluted with an equal volume of distilled water, separated, dried over MgSO<sub>4</sub> and evaporated. Residue was dissolved in CH<sub>2</sub>Cl<sub>2</sub> and purified using silica gel chromatography (1:1 hexanes:ethyl acetate) to obtain **3-6** (85.8 mg, ) as a yellow oil in 69% yield.

**<sup>1</sup>H-NMR** (CDCl<sub>3</sub>, 500 MHz): δ 7.00 (d, 1H), 6.66 (d, 1H), 6.53 (s, 1H), 4.63 (d, 2H), 3.84 (s, 3H) 3.83 (s, 3H) 2.61 (s, 3H), 1.88 (sept, 1H), 0.77 (d, 6H).

**HRMS** (ESI-TOF) calcd for  $C_{16}H_{22}NO_3$  ( $M+H$ )<sup>+</sup>: 276.1600, found 276.1593

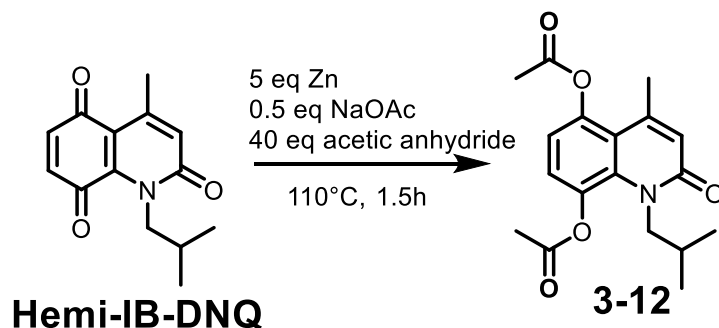


In a flask with a stir bar, **3-6** (87 mg, 0.32 mmol) was dissolved in acetonitrile (1.7 mL). A solution of cerium (IV) ammonium nitrate (CAN) was prepared separately by dissolving CAN (348 mg, 0.63 mmol) in distilled water (0.23 mL). CAN solution was added to flask via pipette and immediately solution became dark red. Mixture was allowed to stir for 1.5h before diluting with distilled water (10 mL). Mixture was extracted with chloroform three times and combined organic fractions were dried over  $MgSO_4$  and rotovapped to an orange/orange-red oil. Oil was dissolved in  $CH_2Cl_2$  and purified by silica gel chromatography (1:1 hexanes:ethyl acetate).

**Hemi-IB-DNQ** (35.9 mg, 0.15 mmol) was obtained as a red solid in 47% yield.

<sup>1</sup>H-NMR ( $CDCl_3$ , 500 MHz):  $\delta$  6.78 (d, 1H), 6.76 (d, 1H), 6.67 (s, 1H), 4.59 (d, 2H), 2.56 (s, 3H), 1.87 (sept, 1H), 0.91 (d, 6H).

**HRMS** (ESI-TOF) calcd for  $C_{14}H_{16}NO_3$  ( $M+H$ )<sup>+</sup>: 246.1130, found 246.1133.



To a flask containing Hemi-IB-DNQ (30.3 mg, 0.09 mmol) and a stir bar, sodium acetate (7.3 mg, 0.09 mmol) and zinc dust (40.8 mg, 0.62 mmol) were added. Flask was evacuated and back

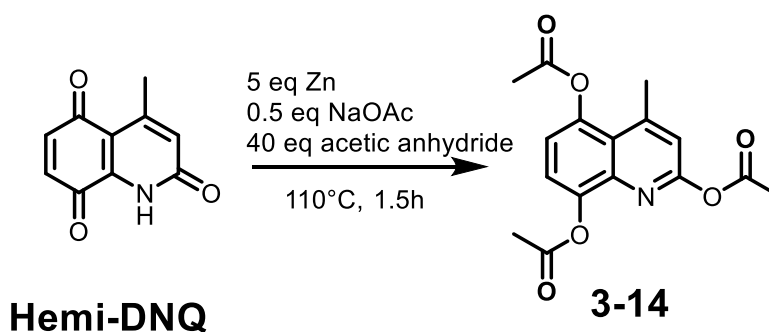


filled with argon three times. Acetic anhydride (0.49 mL, 5.2 mmol) was added, and flask was placed in an oil bath at 110°C. Solution immediately turned gray. Stirring proceeded for 1.5h and mixture was filtered and washed with ethyl acetate. Solution was slightly yellow and was rotovapped to a white solid producing **3-12** (30.2 mg, 0.09 mmol) in 74% yield.

**<sup>1</sup>H-NMR** (CDCl<sub>3</sub>, 500 MHz): δ 7.15 (d, 1H), 6.89 (d, 1H), 6.50 (s, 1H), 4.35 (d, 2H), 2.49 (s, 3H), 2.36 (s, 3H), 2.34 (s, 3H), 1.94 (sept, 1H), 0.76 (d, 6H).

**<sup>13</sup>C-NMR** (CDCl<sub>3</sub>, 125 MHz): δ 169.3, 168.9, 163.1, 146.4, 144.4, 136.1, 133.9, 125.8, 124.3, 118.3, 117.8, 51.4, 29.9, 27.8, 24.1, 21.5, 19.9.

**HRMS** (ESI-TOF) calcd for C<sub>18</sub>H<sub>22</sub>NO<sub>5</sub> (M+H)<sup>+</sup>: 332.1498, found 332.1496.

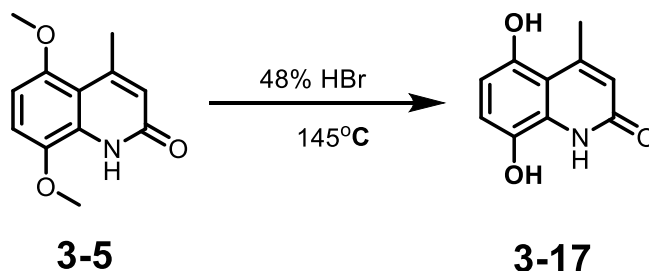


Zinc dust (228 mg, mmol) and sodium acetate (29.4 mg, mmol) were added to flask containing Hemi-DNQ (130 mg, 0.69 mmol) and stir bar. Flask was evacuated and backfilled with nitrogen three times and acetic anhydride (2.6 mL, 27.5 mmol) was added. The resulting orange solution was placed in an 110°C oil bath and stirred for 75 min. Reaction was filtered and flask was rinsed with ethyl acetate. Solution was filtered to a yellow oil then dissolved in CH<sub>2</sub>Cl<sub>2</sub> and diluted with an equivalent volume of distilled water. Organic fraction was extracted twice with CH<sub>2</sub>Cl<sub>2</sub>, organic fraction was dried over MgSO<sub>4</sub> and rotovapped to a yellow oil. Product **3-14** (10 mg, 0.03 mmol) was isolated as a white solid following silica gel chromatography (ethyl acetate).

**<sup>1</sup>H-NMR** (CDCl<sub>3</sub>, 500 MHz): δ 7.41 (d, 1H), 7.19 (d, 1H), 7.04 (s, 1H), 2.78 (s, 3H), 2.45 (s, 3H), 2.40 (s, 3H), 2.36 (s, 3H).

**<sup>13</sup>C-NMR** (CDCl<sub>3</sub>, 125 MHz): δ 169.8, 169.6, 168.9, 156.5, 148.1, 145.3, 144.9, 141.3, 122.6, 121.8, 120.1, 118.9, 31.2, 23.3, 21.8, 21.2.

**HRMS** (ESI-TOF) calcd for C<sup>16</sup>H<sup>16</sup>NO<sup>6</sup> (M+H)<sup>+</sup>: 318.0978, found 318.0979.



To a flask containing a stir bar and **3-5** (167 mg, 0.76 mmol), concentrated HBr was added (1.8 mL). An air condenser was fitted to the flask and the flask was placed in an oil bath at 145°C. The solution was heated for 24h and then poured into distilled water (20 mL) to form a precipitate. Precipitate was collected through vacuum filtration to produce **3-17** (115 mg, 0.60 mmol) as a light brown solid in 79% yield.

**<sup>1</sup>H-NMR** (CDCl<sub>3</sub>, 400 MHz): δ 9.68 (s, 1H), 9.45 (s, 2H), 6.72 (d, 1H), 6.37 (d, 2H), 6.12 (s, 1H), 3.32 (s, 3H).

**HRMS** (ESI-TOF) calcd for C<sub>10</sub>H<sub>10</sub>NO<sub>3</sub> (M+H)<sup>+</sup>: 192.0661, found 192.0661.

### Dose-dependent in vitro IB-DNQ cytotoxicity assay

Cells were seeded at 5000 cells per well in 96 well plates and allowed to attach. Media containing varying concentrations (0.003-100μM) of IB-DNQ, Hemi-DNQ or Hemi-IB-DNQ was made and cells were exposed for 2-h. Treatment media was removed and replaced with drug-free media and cells were allowed to grow for 48 h. To investigate the inhibitory effects of

dicoumarol on NQO1 activity, cells were treated with vehicle (DMSO) or with a combination of 25  $\mu$ M dicoumarol with Hemi-DNQ, Hemi-IB-DNQ or IB-DNQ for 2-h. Viability was assessed using the sulforhodamine B (SRB) assay.<sup>33</sup> Percent death was plotted against concentration and fitted to a logistic dose response curve.

### **Animal dosing and sample collection**

Four, healthy, intact, female domestic shorthair cats weighing 4-5 kg were used for all pharmacokinetic and toxicologic studies. IB-DNQ, P-DNQ, NP-DNQ and IP-DNQ were dissolved into HP $\beta$ CD and sterile water was administered intravenously (2.0 mg/kg IV). Cats received a minimum of three doses of each DNQ derivative with a minimum washout period of 2 weeks between dosing. Sample collection times for all methods of administration were 0, 10, 20, 30, 40, 60, 120, 240, 480 min and 24 h post administration. Cats were monitored peri- and post-derivative administration to document clinical symptoms. Upon completion of DNQ derivative administrations, the cats were monitored for an additional 9 months for assessment of delayed toxicity. All experiments with healthy research cats were approved by the University of Illinois Animal Care and Use Committee.

### **Plasma IB-DNQ quantification method**

Plasma samples were analyzed with the 5500 QTRAP LC/MS/MS system (Sciex, Framingham, MA) in Metabolomics Lab of Roy J. Carver Biotechnology Center, University of Illinois at Urbana-Champaign. Software Analyst 1.6.2 was used for data acquisition and analysis. The 1200 series HPLC system (Agilent Technologies, Santa Clara, CA) includes a degasser, an autosampler, and a binary pump. Multiple reaction monitoring (MRM) was used for

quantification of IB-DNQ, P-DNQ, IP-DNQ and NP-DNQ with DNQ as the internal standard. The detection limit was 1.0 ng/mL.

### **Pharmacokinetic profile of IB-DNQ**

Pharmacokinetic analyses were performed using a non-linear regression program (Winnonlin, version 5.1) (Pharsight Corporation, Cary, NC). The area under the curve (AUC), terminal half-life ( $t_{1/2 \beta}$ ), volume of distribution at steady state ( $V_{d_{ss}}$ ), total clearance (Cl), maximum drug concentration ( $C_{max}$ ) and time at which  $C_{max}$  was achieved ( $T_{max}$ ) were determined.

### **Computational Modeling**

DNQ and derivatives were built and a 10Å water layer was built around the molecule. The derivative structure was energy minimized using MOE with a MMFF94x forcefield using gas phase calculations and a cutoff of 0.01. Charges were fixed using an MMFF94 forcefield. The NQO1 structure was downloaded from the PDB (1DXO). One of the homodimers was extracted and protonated. Derivatives were then modeled into the protein active site, using the site of duroquinone to identify the active site. Derivatives were docked using the Dock program in MOE, using Triangle Matching for placement of the molecules and London dG for rescoring of the placement. Using Lig X, the top configuration was protonated and energy was minimized. Images of this minimized conformation were taken for comparison between derivatives. Similarly the NADPH cytochrome P450 reductase structure was downloaded from the PDB (3QFR), a single homodimer was extracted and protonated, and derivatives were modeled into the presumed protein active site, using the placement of the cofactors to identify the active site.

Derivatives were docked and the top configuration was taken for analysis between derivatives as described for NQO1.

### **ROS Generation Assays**

Cells (JHU029, MDA-MB-231 NQO1 $\pm$ ) were treated with DNQ derivatives (1, 5, 10, 25  $\mu$ M) for 3h. After 3h compound was washed out and replaced with media containing 5  $\mu$ M MitoSOX red (ThermoFisher, Waltham, MA). After 10 min cells were washed and trypsinized. Cell suspensions were then analyzed via flow cytometry using the appropriate wavelengths for MitoSOX red. Samples were compared to the DMSO treated control sample and reported as fold-change compared to DMSO control.

### **3.5. References**

- (1) Zawilska, J.B.; Wojcieszak, J.; Olejniczak, A.B. Prodrugs: a challenge for the drug development. *Pharmacol. Rep.* **2013**, *64*, 1-14.
- (2) Huttunen, K.M.; Raunio, H.; Rautio, J. Prodrugs – from serendipity to rational design. *Pharmacol. Rev.* **2011**, *63*, 750-771.
- (3) Huttunen, K.M.; Rautio, J. Prodrugs – an efficient way to breach delivery and targeting barriers. *Curr. Top. Med. Chem.* **2011**, *11*, 2265-2287.
- (4) Stella, V.J.; Borhardt, R.T.; Hageman, M.; Oliyai, R.; Maag, H.; Tilley, J. (Eds.). Prodrugs: Challenges and Rewards. (AAPS Press/Springer **2007**).
- (5) Testa, B.; Mayer, J.B. Hydrolysis in drug and prodrug metabolism: chemistry, biochemistry and enzymology. (Wiley-VCH. **2003**)

- (6) Ettmayer, P.; Amidon, G.L.; Clement, B.; Testa, B. Lessons learned from marketed and investigational prodrugs. *J. Med. Chem.* **2004**, *47*(10), 2393-2404.
- (7) Testa, B. Prodrug research: futile or fertile. *Biochem. Pharmacol.* **2004**, *68*(11), 2097-2106.
- (8) Parkinson, E.I.; Bair, J.S.; Cismesia, M.; Hergenrother, P.J. Efficient NQO1 substrates are potent and selective anticancer agents. *ACS Chem. Biol.* **2013**, *8*, 2173-2183.
- (9) Bair, J.S. The Development of Deoxyxyboquinone as a Personalized Anticancer Compound, University of Illinois at Urbana-Champaign, 2012.
- (10) Parkinson, E.I. Deoxyxyboquinones as NQO1-targeted Anticancer Compounds and Deoxyxybomycins as Potent and Selective Antibiotics, University of Illinois at Urbana-Champaign, 2015.
- (11) Heimbach, T.; Oh, D.M.; Li, L.Y.; Forsberg, M.; Savolainen, J.; Leppaene, J.; Matsunaga, Y.; Flynn, G.; Fleisher, D. Absorption rate limit considerations for oral phosphate prodrugs. *Pharm. Res.* **2003**, *20*(6), 848-856.
- (12) Yang, Y.H.; Aloysius, H.; Inoyama, D.; Chen, Y.; Hu, L.Q. Enzyme-mediated hydrolytic activation of prodrugs. *Acta Pharm. Sin. B* **2011**, *1*(3), 143-159.
- (13) Stella, V.J.; Nti-Addae, K.W. Prodrug strategies to overcome poor water solubility. *Adv. Drug Deliv. Rev.* **2007**, *59*(7), 677-694.
- (14) Heimbach, T.; Oh, D.M.; Li, L.Y.; Rodriguez-Hornedo, N.; Garcia, G.; Fleisher, D. Enzyme-mediated precipitation of parent drugs from their phosphate prodrugs. *Int. J. Pharm.* **2003**, *261*, 81-92.

- (15) Heimbach, T.; Fleisher, D.; Kaddoumi, A. in Prodrugs: Challenges and Rewards. Part 1 eds. Stella, V.; Borchardt, R.; Hageman, M.; Oliyai, R.; Maag, H.; Tilley, J.(Springer New York) 155-212.
- (16) McComb, R.; Bowers, G.; Posen, S. Alkaline Phosphatase (Plenum Press, New York and London, 1979).
- (17) Rautio J.; Kumpulainen, H.; Heimbach, T.; Oliyai, R.; Oh, D.; Jarvinen, T.; Savolainen, J. Prodrugs: design and clinical applications. *Nat. Rev.* **2008**, 7, 255-270.
- (18) Huang, X.; Dong, Y.; Bey, E.A.; Kilgore, J.A.; Bair, J.S.; Li, L.S.; Patel, M.; Parkinson, E.I.; Wang, Y.; Williams, N.S.; Gao, J.; Hergenrother, P.J.; Boothman, D.A. An NQO1 substrate with potent anticancer activity that selectively kills by PARP1-induced programmed necrosis. *Cancer Res.* **2012**, 72(12), 3038-3047.
- (19) Ecobichon, D. Relative amounts of hepatic and renal carboxylesterase in mammalian species. *Res. Commun. Chem. Pathol. Pharmacol.* **1972**, 3, 629-636.
- (20) Liederer, B.M.; Borchardt, R.T. Enzymes involved in the bioconversion of ester-based prodrugs. *J. Pharm. Sci.* **2006**, 95, 1177-1195.
- (21) Ma, X.; Huang, X.; Moore, Z.; Huang, G.; Kilgore, J.A.; Wang, Y.; Hammer, S.; Williams, N.S.; Boothman, D.A.; Gao, J. Esterase-activatable beta-lapachone prodrug micelles for NQO1-targeted lung cancer therapy. *J. Control. Release* **2015**, 200, 201-211.
- (22) Ma, X.; Huang, X.; Huang, G.; Li, L.S.; Wang, Y.; Luo, X.; Boothman, D.A.; Gao, J. Prodrug strategy to achieve lyophilizable, high drug loading micelle formulations through diester derivatives of beta-lapachone. *Adv. Healthcare Mater.* **2014**, 3, 1210-1216.

- (23) Zhou, Y.; Dong, Y.; Huang, G.; Wang, Y.; Huang, X.; Zhang, F.; Boothman, D.A.; Gao, J.; Lang, W. Lysosome-oriented, dual-stage pH-responsive polymeric micelles for beta-lapachone delivery. *J. Mater. Chem.* **2016**, *4*, 7429-7440.
- (24) Sweeny, D.J.; Li, W.; Clough, J.; Bhamidipati, S.; Rajinder, S. Metabolism of fostamatinib, the oral methylene phosphate prodrug of the spleen tyrosine kinase inhibitor R406 in humans: contribution of hepatic and gut bacterial processes to the overall biotransformation. *Drug Metab. Dispos.* **2010**, *38*, 1166-1176.
- (25) Heck, H.D.; Casanova, M.; Starr, T.B. Formaldehyde toxicity – new understanding. *Crit. Rev. Toxicol.* **1990**, *20*, 397-426.
- (26) Mantyla, A.; Garnier, T.; Rautio, J.; Nevalainen, T.; Vepsalainen, J.; Koskinen, A.; Croft, S.L.; Jarvinen, T. Synthesis, in vitro evaluation, and antileishmanial activity of water-soluble prodrugs of buparvaquone. *J. Med. Chem.* **2004**, *47*, 188-195.
- (27) Krise, J.P.; Zygmunt, J.; Georg, G.I.; Stella, V.J. Novel prodrug approach for tertiary amines: synthesis and preliminary evaluation of N-phosphonooxymethyl prodrugs. *J. Med. Chem.* **1999**, *42*, 3094-3100.
- (28) Ueda, Y.; Matiskella, J.D.; Golik, J.; Connolly, T.P.; Hudyma, T.W.; Venkatesh, S.; Dali, M.; Kang, S.H.; Barbour, N.; Tejawani, R.; Varia, S.; Knipe, J.; Zheng, M.; Mathew, M.; Mosure, K.; Clark, J.; Lamb, L.; Medin, I.; Gao, Q.; Huang, S.; Chen, C.P.; Bronson, J.J. Phosphonooxymethyl prodrugs of the broad spectrum antifungal azole, ravuconazole: synthesis and biological properties. *Bioorg. Med. Chem. Lett.* **2003**, *13*, 3669-3672.
- (29) Avendano, C.; de la Cuesta, E.; Gesto, C. A comparative study of synthetic approaches to 1-methyl-2,5,8(1H)-quinolinetriene and 4-methyl-2,5,8(1H)-quinolinetriene. *Synthesis* **1991**, *9*, 727-730.



- (30) Gesto, C.; de la Cuesta, K.; Avendano, C. An efficient synthesis of 8-methoxy- and 8-hydroxy-1-methylcarbostyryl. *Synth. Commun.* **1990**, *20*(1), 35-39.
- (31) Bair, J.S.; Palchaudhuri, R.; Hergenrother, P.J. Chemistry and biology of deoxyxyboquinone, a potent inducer of cancer cell death. *J. Am. Chem. Soc.* **2010**, *132*(15), 5469-5478.
- (32) Uliana, M.P.; Vieira, Y.W.; Donatoni, M.C.; Correa, A.G.; Brocksom, U.; Brocksom, T.J. Oxidation of mono-phenols to para-benzoquinones: a comparative study. *J. Braz. Chem. Soc.* **2008**, *19*(8), 1484-1489.
- (33) Vichai, V.; Kirtikara, K. Sulforhodamine B colorimetric assay for cytotoxicity screening. *Nat. Protoc.* **2006**, *1*, 1112-1116.